1992

A study of the reactivity of reduced molybdenum ethoxides: Synthesis and characterization of MoO(OH) and some novel molybdenum ethoxide cluster molecules

Judith S. Hollingshead
Iowa State University

Order Number 9223931

A study of the reactivity of reduced molybdenum ethoxides: Synthesis and characterization of MoO(OH) and some novel molybdenum ethoxide cluster molecules

Hollingshead, Judith Shutek, Ph.D.

Iowa State University, 1992

U·M·I
300 N. Zeeb Rd.
Ann Arbor, MI 48106

A study of the reactivity of reduced molybdenum ethoxides. Synthesis and characterization of MoO(OH) and some novel molybdenum ethoxide cluster molecules

by

Judith S. Hollingshead

A Dissertation Submitted to the
Graduate Faculty in Partial Fulfillment of the
Requirements for the Degree of
DOCTOR OF PHILOSOPHY

Department: Chemistry
Major: Inorganic chemistry

Approved:

Signature was redacted for privacy.

In Charge of Major Work//

Signature was redacted for privacy.

For the Major Department

Signature was redacted for privacy.

For the Graduate College

Iowa State University
Ames, Iowa

1992

TABLE OF CONTENTS

LIST OF FIGURES

LIST OF TABLES

GENERAL INTRODUCTION

Low temperature routes to synthesizing transition metal ceramics represent a non-traditional way to producing these materials. However, the popularity of low temperature synthetic methods is growing owing to the advantages they present [1-4]. Typically, the ceramic materials isolated by these routes are of higher surface area and higher purity than those isolated from traditional solid state methods. Furthermore, because of the low temperatures that can be used in the processing, new, less thermodynamically stable ceramics (metastable phases) may be accessable. However, traditional solid state synthetic techniques use high temperatures (typically greater than 600°C) and, thus, cannot readily produce metastable materials.

A low temperature route to metal oxides that is commonly employed is known as the sol-gel method. In this method, a metal alkoxide or similar labile compound is hydrolyzed at room temperature to produce the hydroxide or hydrous oxide. This material can then, ideally, be thermally decomposed at relatively low temperatures to produce the oxide.

Owing to their facile hydrolysis properties, molybdenum alkoxides represent an ideal group of materials for use in the sol-gel method for producing lower valent oxides. Previous work in this area has shown that the hydrolysis of molybdenum(III) isopropoxide can be complicated by concurrent oxidation of the molybdenum [5]. However, the properties that govern the oxidation have not been thoroughly investigated. It may be possible to control aspects of the reaction that will lead smoothly to an unoxidized product.

The hydrolysis properties of molybdenum alkoxides and subsequent thermal decomposition of the hydrolysis products are the main topics addressed in the first section (Part 1) of this dissertation. It has been determined that molybdenum(III) ethoxide can be

hydrolyzed with no concurrent oxidation of the metal, and the product of this hydrolysis reaction can be converted to the new oxide material, MoO(OH).

Related to this area is the surprising discovery of the novel cluster, $Mo_6O(OEt)_{18}$. This material forms during the hydrolysis of $Mo(OEt)_3$ when excess water (2 to 4 molar) is used. The second section of this dissertation (Part 2) will discuss the synthesis and structure of this material. Also included in this section are attempts to isolate $Mo_6O(OEt)_{18}$ using other oxidizing agents (antimony pentoxide, nitrous oxide, iodosobenzene, and trimethylamine-N-oxide) as reactants with molybdenum(III) ethoxide. Partial characterization of some new molybdenum ethoxide clusters that have been isolated from these reactions is also presented.

The synthesis and study of many molybdenum alkoxides have been reported [6]. However, the synthetic route to these species gives rather low yields due to the difficulty in isolating the pure starting material, $Mo_2(NMe_2)_6$ [7]. A yield of 20-30% is typical for a large scale synthetic reaction of $Mo_2(NMe_2)_6$. The research presented in the final section (Part 3) describes a new synthetic route to molybdenum ethoxide. The material isolated from this method has also been used to isolate the new cluster species, $Mo_4(OEt)_{14}(HOEt)_2$.

Explanation of Dissertation Format

The alternate thesis format is used for this dissertation. It consists of three parts, each is formatted for publication in a technical journal. The references cited in the general introduction can be found at the end of the dissertation. In addition, references for each part can be found listed independently at the end of each section.

PART 1. A STUDY OF THE HYDROLYSIS AND SUBSEQUENT THERMAL DECOMPOSITION OF PRODUCTS DERIVED FROM REDUCED MOLYBDENUM ALKOXIDES

INTRODUCTION

Low temperature routes, such as the sol-gel method, the "precursor" method, and the "solid-solution precursor" method, have proven to be successful methods for the preparation of ceramic materials [1-6]. The most widely used solid state synthetic technique is known as the ceramic method. In this method, mixtures of solid reactants are heated at elevated temperatures (typically greater than 600°C). These high temperatures are needed to overcome the large diffusion distances (up to 10,000 Å) of the reacting species. Furthermore, this method typically does not yield a single-phase product. Low temperature routes can reduce the diffusion distance to as small as ~10 Å and thus, allow significantly lower temperatures to be employed. Because of the high temperatures needed in the ceramic method, many oxides cannot be isolated due to their low thermodynamic stability. This is especially true for those compounds that are known to be thermodynamically unstable (metastable phases).

The precursor methods, in which a monophasic material contains the desired elements in the right proportion, have been used to isolate metastable metal oxides. An example of a metastable compound isolated by this method is $Ca_2Fe_{2-x}Mn_xO_5$ [2]. This compound is synthesized starting with the solid solution precursor compound $Ca_2Fe_{2-x}Mn_x(CO_3)_4$. When this precursor is thermally decomposed and then reduced in hydrogen, the metastable oxide is formed. This compound will readily transform into the brownmillerite-type structure upon heating at ~900°C. Furthermore, all attempts to isolate $Ca_2Fe_{2-x}Mn_xO_5$ via the ceramic method, by using a mixture of the binary oxides in the appropriate stoichiometry, have failed.

Some other examples of new metal oxides isolated from their corresponding carbonate precursors are $Ca_2Co_2O_5$, $CaCo_2O_4$, and Ca_2FeCoO_5 [3]. In addition, mixed metal hydroxides of the type, $Ln_{1-x}M_x(OH)_3$ where Ln = La or Nd; M = Al, Cr, Fe, Co, Ni, and $Ln_{1-x-y}M'_xM''_y(OH)_3$ where M' = Ni and M" = Co or Cu have been used as precursors to the corresponding oxides [4]. An example of two novel oxides prepared via hydroxide precursors are $LaNi_{1-x}Cu_xO_3$ where x = 0.25 or 0.50. Cyanide and nitrate precursors have also been used to isolate perovskite-type oxides, as in the case of $La_{1-x}Ln_xCoO_3$ (Ln = La, Ce, Pr, and Nd) and $La_{1-x}Co_xO_3$ from their corresponding cyanides, or the case of $BaPbO_3$ and $BaSrPbO_4$ from their corresponding nitrates [4]. Finally, other "metal-organic" type precursors, such as metal oxalates and citrates, have been used to synthesize metastable oxides. Szabo [5] and Sallavuard [6] have been able to synthesize metastable hexagonal $SmAlO_3$ and $LnGaO_3$ (Ln = Ce, Pr, Nd) via the decomposition of the corresponding mixed metal citrates.

The sol-gel method, another route to preparing ceramic metal oxides, which typically involves hydrolysis and polymerization of ionic species in aqueous media, has been employed to isolate metal oxides from non-aqueous solutions of metal alkoxides [1]. Two oxides isolated via this route are MY_2O_5 where M = Hf or Zr. These oxides were isolated by hydrolyzing a benzene solution of the appropriate alkoxides and subsequently processing the products to produce the pure oxides.

In this section, low temperature routes to the isolation of reduced Mo oxide species are explored. The most commonly known reduced molybdenum oxide is MoO_2, which contains Mo in the +4 oxidation state. More reduced binary oxides, such as Mo_2O_3,

have not been isolated. These types of oxides are metastable and readily decompose into Mo and MoO_2 when subjected to high temperatures. Thus, the ceramic method will not easily afford any reduced binary molybdenum oxide phase. The following work describes the study of the hydrolysis of molybdenum(III) alkoxides, and the thermal processing of the precursor species isolated from these reactions.

EXPERIMENTAL

General considerations. All starting materials that were used in this work are oxygen and water-sensitive. Therefore, all experimental procedures were performed by using Schlenk techniques, an inert atmosphere dry box and a glass vacuum line. All solvents were dried prior to use. Chlorobenzene and toluene were dried by using phosphorus pentoxide under refluxing conditions. Tetrahydrofuran was stirred with sodium and benzophenone to remove water and peroxides. Ethanol and tert-butanol were dried by addition of sodium metal. All solvents and reactant water were deoxygenated under vacuum by the triple freeze-thaw method. Finally, dried solvents were vacuum-distilled onto activated 3 Å molecular sieves in specially-made round-bottom flasks. Solvents were either transferred by vacuum distillation from solvent flasks or by syringe under a flow of argon gas.

Synthesis of $MoCl_3$. The synthesis of molybdenum(III) chloride was performed by the procedure outlined by Chisholm et. al. [7] from the reaction between molybdenum (V) chloride and molybdenum hexacarbonyl.

(1) $$3MoCl_5 + 2Mo(CO)_6 \Rightarrow 5MoCl_3 + 12CO$$

The reaction was carried out in refluxing chlorobenzene for 9 hours. The final product showed retention of only a small amount of chlorobenzene, based on the FT-IR spectrum, and was amorphous to x-rays.

A large scale preparation of $MoCl_3$ was performed in an inert atmosphere by the following procedure. Molybdenum hexacarbonyl (39.13 g, 0.148 mol) was partially dissolved in 400 mL of chlorobenzene in a two-neck, 1000 mL round-bottom flask fitted

with a side-arm addition tube. Molybdenum pentachloride (60.77 g, 0.222 mol) was slowly added to the solution through the addition tube while the reaction mixture was vigorously stirred. Upon addition of the $MoCl_5$, the colorless solution became brown and evolved carbon monoxide gas. After the $MoCl_5$ was completely added, the mixture was heated to reflux until CO gas was no longer evolved (approximately 24 hours). After the solvent was vacuum-distilled into a cold-trap cooled with liquid nitrogen, a free flowing red-brown powder was recovered. The preparation gave essentially a 100% yield of product.

Synthesis of $LiN(CH_3)_2$. The large-scale synthesis of $LiNMe_2$ was based on the reaction of one mole of butyl lithium with excess dimethylamine gas. Butyl lithium in hexane (1 mol) was transferred by the cannula technique into a taped 1000 mL round-bottom flask under inert atmosphere. The butyl lithium solution was put through the freeze-thaw cycle twice to remove any residual gases. An excess (15%) of dimethylamine gas was condensed onto the frozen butyl lithium solution. This was accomplished by first condensing the gas into a graduated flask that was attached to the vacuum line through a ground-glass joint and needle-valve adapter using an isopropanol/liquid nitrogen slush bath. When the appropriate volume of gas (~80 mL) was condensed into the flask, it was then transferred from the graduated flask onto the butyl lithium using a liquid nitrogen bath. The liquid nitrogen bath was replaced with an isopropanol/liquid nitrogen (-89°C) slush bath, and the reaction was allowed to proceed overnight. A white, flocculent material was formed upon completion of the reaction. The reaction mixture was then warmed to room temperature while the reaction vessel was

opened to a Hg bubbler to allow the excess dimethylamine and butane to bubble off. The hexane was then distilled into the cold-trap. Subsequently, the $LiNMe_2$ was used within a day to avoid decomposition and reduction of yields. A quantitative yield of $LiNMe_2$ was assumed for the following production of $Mo_2(NMe_2)_6$.

Synthesis of $Mo_2[N(CH_3)_2]_6$. The preparation of $Mo_2(NMe_2)_6$ was based on the method outlined by Chisholm et. al. [7] as given in the following reaction:

(2) $$2MoCl_3 + 6LiNMe_2 \Rightarrow Mo_2(NMe_2)_6 + 6LiCl$$

where the reaction was carried out in tetrahydrofuran at 0°C.

In the large scale preparation, tetrahydrofuran (500 mL) was vacuum-distilled onto the freshly prepared $LiNMe_2$ in a 1000 mL flask to which a three-way adapter, side-arm addition tube, and water-cooled condenser were attached. The solution was then cooled to 0°C with a NaCl/ice bath. $MoCl_3$ (67.9 g, 0.336 mol) was slowly added to the solution via the addition tube. The solution turned from yellow to brown with the addition of the $MoCl_3$. Once all the $MoCl_3$ was added, the reaction was allowed to warm to room temperature. After stirring overnight, the solvent was vacuum-distilled into a cold-trap. The brown product was then heated gently (60°C) under dynamic vacuum to ensure its dryness. During this drying process, a small amount of purple monomer, $Mo(NMe_2)_4$, sublimed into the cold-trap. The crude product (110 g) was scraped from the flask in the dry box.

The crude product was purified by sublimation at 125°C. This was accomplished by loading a portion of well-ground crude product into a 100 mL round-bottom flask which was fitted with a 30 cm glass tube with ground-glass joints at each end. At the

other end of the tube, a ground-glass joint and needle-valve adapter was attached so that the apparatus could be connected to the vacuum line. The length of the tube and flask was set up horizontally so that it was parallel to the manifolds of the vacuum line. Heating tape was wrapped around the flask so that it was completely covered. The temperature of the heating tape was regulated using a thermocouple and a temperature controller.

The crude product was initially heated to approximately 80°C for 2 to 3 hours to sublime away the remaining monomer, $Mo(NMe_2)_4$, into the cold-trap. The temperature was then raised to 125°C to sublime the yellow $Mo_2(NMe_2)_6$ into the attached tube. A 20% to 30% yield of product was isolated.

Synthesis of $[Mo(OC_2H_5)_3]_4$. This alkoxide was prepared from $Mo_2(NMe_2)_6$ by the following reaction [8]:

(3) $$2Mo_2(NMe_2)_6 + 12EtOH \Rightarrow [Mo(OEt)_3]_4 + 12HNMe_2$$

$Mo_2(NMe_2)_6$ (3.00 g, 0.00657 mol) was dissolved in toluene (30 mL) in a 100 mL round-bottom reaction flask. Under argon-flow, an excess of ethanol (40 %) was added by syringe to the yellow solution which immediately turned brown. The reaction mixture was stirred for 1 to 2 hours. The toluene was then distilled into a cold-trap which left an oily material in the flask. The flask was then heated to 80°C under dynamic vacuum overnight to remove remaining volatile materials. The black molybdenum ethoxide was scraped from the flask in essentially quantitative yield and was not purified further. IR (Nujol mull) cm^{-1}: 1350w, 1261m, 1097s, 1057s, 906m, 789m, 613m, 552w, 507m, 460s, 440s, 383s.

Synthesis of $Mo_2(OC(CH_3)_3)_6$. This molybenum alkoxide was prepared according to the following reaction [8]:

(4) $$Mo_2(NMe_2)_6 + 6Bu^tOH \Rightarrow Mo_2(OBu^t)_6 + 6HNMe_2$$

$Mo_2(NMe_2)_6$ (3.03 g, 0.00664 mol) was dissolved in hexane (40 mL) in a 100 mL round-bottom flask. Under an argon-flow, an excess of tert-butanol (40%) was added by syringe to the yellow solution which turned dark red immediately. The reaction mixture was stirred at room temperature for 1 hour. The solvent was vacuum-distilled into a cold-trap leaving a dark red solid. The solid was scraped from the flask and used with no further purification.

Hydrolysis reactions. All hydrolysis reactions were carried out in dry toluene under inert gas at room temperature for approximately 1 hour. These conditions were deemed to be the optimum for yield and quality of product. The appropriate molybdenum alkoxide was loaded in the drybox into a 250 mL round-bottom flask fitted with a ground-glass joint and Teflon needle-valve adapter. Toluene was added by vacuum distillation, and the alkoxide was completely dissolved. Deoxygenated water then was added to the solution by syringe under a flow of inert gas. When the reaction was complete (about 1 hour), the reaction mixture was filtered, and the solid product was extracted with the solvent distilled from the filtrate in order to insure that all soluble impurities were removed. The product was then dried under dynamic vacuum for 24 hours.

Hydrolysis of $Mo_2(OC(CH_3)_3)_6$. $Mo_2(OBu^t)_6$ (2.60 g, 0.00412 mol) was dissolved in 40 mL of toluene. Deoxygenated water (0.445 g, 0.0247 mol) was

transferred by syringe into the solution under a flow of argon. A brown non-crystalline solid precipitated from the reaction mixture almost immediately. After 1 hour, the mixture was filtered to recover the product. The solid that was isolated from this reaction was dried in vacuo for 24 hours leaving a brown finely divided powder in quantitative yield. The product was amorphous to x-rays. IR (Nujol mull) cm^{-1}: 1086w, 1018w, 972w, 480w. Analytical. Found: Mo, 63.2, Mo average oxidation state, 4.7.

Hydrolysis of $[Mo(OC_2H_5)_3]_4$. $[Mo(OEt)_3]_4$ (5.0 g, 0.54 mmol) was dissolved in 100 mL of toluene. Deoxygenated water (1.17 mL, 6.49 mmol) was transferred to the solution under an argon-flow via syringe. A dark brown solid precipitated from the reaction mixture almost immediately after the addition of water. The reaction was complete in about 1 hour, and the solid product was isolated by filtration. A dark brown solid and a clear filtrate were recovered. After the product had been dried in vacuo for 24 hours, a finely divided brown powder was obtained in a quantitative yield. This solid did not exhibit an x-ray diffraction pattern. IR (Nujol mull) cm^{-1}: 1261w, 1094w, 1043m, 897w, 557vw, 482m. Analytical. Calc. for $Mo_2O_6C_2H_{10}$: Mo, 59.6; O, 29.8; C, 7.5; H, 3.1. Found: Mo, 58.2; C, 8.7; H, 3.0; O(by difference), 30.1.

Thermal decomposition reactions. Thermal decomposition reactions were carried out by one of two procedures, either under dynamic vacuum or in a flowing gas. When decomposition was carried out in vacuum, the solid was loaded into a dry Pyrex tube fitted with a ground-glass joint and Teflon needle-valve adapter. The vessel was evacuated to a pressure of 10^{-4} torr and allowed to remain under dynamic vacuum throughout the reaction. The tube was placed in a portable furnace and heated to the

desired temperature. Typically, heating ramps of approximately 50°C per 30 minutes were used. Extreme care was taken during these reactions to eliminate any place where oxygen could leak into the system.

When decomposition reactions were carried out in a flowing gas, a specially-made tube was employed. This tube was 32 inches in length, and had a 24/40 joint at one end and a glass stopcock at the other. The solid, that was to be decomposed, was loaded into a pre-dried ceramic boat in the drybox. The boat was then slid into the specially-made Pyrex tube which was then fitted with a ground-glass joint and Teflon needle-valve adapter. The tube was placed in a furnace, and hydrogen gas was allowed to flow over the boat throughout the reaction. Typical temperature ramps for these reactions were from 50 to 100°C per 15 minutes. When the reaction was finished, the tube was removed from the furnace and evacuated while it was hot. It remained under dynamic vacuum until it cooled to room temperature.

Thermal decomposition of $Mo_2(OH)_5(OEt)$ in vacuo. $Mo_2(OH)_5(OEt)$ was loaded into a reaction tube as described above. The reaction tube was evacuated to a pressure of less than 10^{-4} torr. The tube was placed in a portable tube furnace, and the temperature was raised over 3 days to 240°C. It remained at this level for 1 day. The brown solid turned black and was still amorphous to x-rays. Analytical. Found: Mo, 69.0; Mo average oxidation state, 3.4.

Thermal decomposition of $Mo_2(OH)_5(OEt)$ in flowing hydrogen. $Mo_2(OH)_5(OEt)$ was loaded into the ceramic boat and specially-made Pyrex tube as described previously. The tube was placed in a furnace, and hydrogen gas was allowed to

flow through the reaction tube throughout the thermal treatment process. The tube was initially heated to 130°C for 5 hours, then cooled and evacuated to less than 10^{-4} torr. IR (Nujol mull) cm^{-1}: 1150w, 1032m, 891vw, 498m.

Thermal treatment of this sample was continued in flowing hydrogen at higher temperatures. The specially-made reaction tube, loaded with the sample, was heated in a tube furnace to 250°C. After 48 hours, the reaction vessel was removed from the furnace and evacuated while cooling to room temperature. IR (Nujol mull) cm^{-1}: 650m, 500w. Analytical. Calc. for MoO_2H: Mo, 74.4; O, 24.8; H, 0.8. Found: Mo, 74.3; H, 0.6; O(by difference), 23.9. Mo average oxidation state: 3.0.

Thermal decomposition of $Mo_2(OH)_5(OEt)$ in $Ar/H_2(6.0\%)$. This experimental procedure was carried out under conditions identical to the decomposition reaction done in pure hydrogen except a mixed gas $Ar/H_2(6.0\%)$ was employed. The final temperature of the reaction , 300°C, was maintained for 48 hours. The tube was then removed from the furnace and evacuated while cooling to room temperature. Analytical. Found: Mo, 73.3. Mo average oxidation state, 3.7.

Thermal decomposition of MoO(OH) <u>in vacuo</u>. MoO(OH) was loaded into a dry Pyrex tube fitted with a ground-glass joint and Teflon needle-valve adapter. The reaction tube was connected to the vacuum line through the adapter and evacuated to a pressure of less than 10^{-4} torr. The tube was placed in a portable furnace and heated to 200°C. It was at this temperature that volatile products began evolving. Once this evolution ceased and high vacuum was recovered, the temperature was further increased to 300°C. After 24 hours, the reaction tube was removed from the furnace and allowed to

cool to room temperature. Analytical. Found: Mo, 77.2; Mo average oxidation state, 3.34.

Thermal reaction of MoO(OH) with Li_2CO_3 or Na_2CO_3. MoO(OH) (0.30 g, 0.0023 mol) and Li_2CO_3 (0.087 g, 0.0012 mol) were ground together and loaded into a dry quartz tube fitted with a ground-glass joint and Teflon needle-valve adapter. The reaction tube was evacuated and remained under dynamic vacuum throughout the heating process. The temperature was raised to 600°C and was maintained at this level for 2 days. The tube was then cooled to room temperature. The solid recovered from the reaction was annealed at 900°C in a sealed Cu tube for 2 days. X-ray powder diffraction lines, d-spacings Å: 5.209(6)s, 2.607(2)w, 2.445(1)ms, 2.092(1)ms, 1.9385(8)w, 1.6590(6)mw, 1.5327(5)mw, 1.4330(4)mw, 1.3814(4)mw, 1.2338(3)w.

Thermal reaction of MoO(OH) with Na_2CO_3 was carried out as described in the above procedure. The solid recovered from this reaction was annealed in a Cu tube at 500°C for 4 days. X-ray powder diffraction lines, d-spacings Å: 5.99(1)s, 5.26(1)m, 3.218(3)m, 2.996(3)mw, 2.746(2)m.

Thermal reaction of MoO(OH) with Na. MoO(OH) (0.33 g, 0.0026 mol) and freshly cut Na metal (0.062 g, 0.0026 mol) were loaded into a copper tube which had been sealed at one end. The tube was attached to a needle-valve adapter through a piece of vacuum tube which fit tightly around the Cu tube and the adapter. The tube was evacuated to a pressure of less than 10^{-4} torr. The Cu tube was sealed using a cold-weld pinch-off device at a length of approximately 5 cm. This tube was then placed into a quartz reaction tube which was fitted with a ground-glass joint and Teflon needle-valve

adapter. The quartz reaction tube was evacuated to a pressure of less than 10^{-4} torr. This tube was then sealed at the Teflon valve and placed in a furnace. The temperature was raised to 550°C and maintained at this level for 5 days. The reaction vessel was then removed from the furnace and cooled to room temperature. The sealed Cu tube was removed from the quartz tube and opened in a drybox. A gray polycrystalline material was recovered. X-ray powder diffraction lines, d-spacings Å: 5.238(8)s, 3.217(2)m, 2.746(2)m, 2.223(1)vs, 2.098(1)m, 1.858(1)m, 1.752(1)m, 1.608(1)w, 1.5705(5)m, 1.2811(3)ms.

Thermal reaction of MoO(OH) with $NaNH_2$. MoO(OH) (0.17 g, 0.0013 mol) and $NaNH_2$ (0.051 g, 0.0013 mol) were ground together and loaded into a dry Pyrex tube fitted with a ground-glass joint and Teflon needle-valve adapter. The reaction tube was evacuated to a pressure of less than 10^{-4} torr and then heated to 200°C at a temperature ramp of 50° per hour. After 24 hours, the reaction tube was removed from the furnace and cooled to room temperature. The black solid recovered by this procedure was amorphous to x-rays. In an attempt to crystallize the product, it was further annealed at 400°C in a sealed Cu tube for 3 days. X-ray diffraction lines, d-spacings Å: 5.27(1)m, 3.217(4)w, 2.744(3)w, 2.115(2)vw, 1.751(1)vw.

Elemental analysis. Elemental molybdenum was determined by precipitation of the 8-hydroxyquinolate, $MoO_2(ONC_9H_6)_2$ [9]. Samples were placed in capped vials in the drybox. Once the capped vials were removed from the drybox, they were quickly transferred to aqueous potassium hydroxide solutions (2 pellets of KOH in ~50 mL of water). The sample weights were determined by the difference in the weights of the vials.

Conversion of the molybdenum to MoO_4^{2-} was accomplished by adding hydrogen peroxide and gently heating the sample solutions. Once the molybdenum had been completely converted to MoO_4^{2-}, the solutions were neutralized to a pH = 4 to 6 with a dilute sulfuric acid solution (~1 M) and then buffered with acetic acid/ammonium acetate buffer. The analyte was precipitated by addition of 8-hydroxyquinoline solution. The solid was filtered through tared filter frits, washed with hot water, and dried at 140°C to constant weight. Analyses for C, H, and N were performed by Oneida Research Services, Inc. in Whitesboro, New York.

Oxidation state analysis of molybdenum by Ce(IV) titration. The 0.10 M solution of ceric ammonium nitrate in 1.0 M sulfuric acid was prepared and standardized according to established procedures [10]. The 0.10 M ferrous ammonium sulfate solution in 0.18 M sulfuric acid was made as reported by Banks and O'Laughlin [11] and was accurately standardized before each use.

Because samples of the molybdenum alkoxides and oxides were reactive to air and moisture, they had to be rigorously protected from oxidation prior to the addition of Ce(IV) solution for an accurate oxidation state determination. Samples, loaded into vials and sealed in the drybox, were removed, weighed, then returned to the drybox where they were transferred to beakers which were subsequently covered with a latex glove secured with a rubber band. Once the covered beakers were removed from the drybox, a measured volume of standard Ce(IV) solution was added via a buret through a small hole placed in the top of the latex. Sample solutions were exposed to air only after the solid sample had totally dissolved in the cerium solution. Once the solutions could be exposed

to air, an aliquot of freshly-standardized Fe(II) solution was added to each beaker to react with the excess Ce(IV). Titration of the excess Fe(II) was then performed with the standard Ce(IV) solution. The endpoint was determined potentiometrically using a calomel reference electrode and a Pt indicating electrode.

Physical methods. X-ray powder patterns were recorded on an Enraf-Nonius Delft (END) FR-552 Guinier camera. All diffraction lines were indexed with reference to NBS powdered silicon as an internal standard. Samples were ground and mounted by two different methods in the drybox. In one method, the sample was placed between pieces of cellophane tape to protect it from air and water. To limit sample exposure to air, the samples were sealed in a jar of argon during the transportation to the camera. The sample was quickly transferred to the sample holder on the camera, and the chamber was then placed under vacuum. X-ray exposure times of 4 to 6 hours were typical for samples mounted in this manner. In an alternate method, the sample was placed in a 0.5 mm diameter thin-walled capillary. The sample was protected from oxygen and water by sealing the end of the capillary with grease in the drybox and then sealing the capillary with a flame after its removal from the drybox. X-ray exposure times of 24 to 48 hours were needed for samples mounted in this manner because the capillary only holds a small amount of material.

Infrared spectra were recorded using an IBM IR/90 Fourier-transform infrared spectrometer. Samples were prepared in a Nujol mull and pressed between CsI plates. Samples were transported to the spectrometer in sealed argon-filled jars. Mid-IR (4000-400 cm^{1-}) and far-IR (600-200 cm^{1-}) spectra were recorded separately.

X-ray photoelectron spectra were obtained on freshly ground powders using an AEI ES 200 B photoelectron spectrometer. Non-monochromatic Al Kα (1486.6eV) x-rays were used to irradiate the sample. Binding energies of all peaks were referenced to the C(1s) peak (BE = 285.0 eV) of the adventitious carbon in the system. The data were resolved into constituent peaks using the APES program developed in this group [12,13].

Magnetic susceptibiltiy measurements were carried out on a SQUID (superconducting quantum interference device) susceptometer. Samples were ground and placed in specially-designed quartz tubes (2mm o.d., 1mm i.d.). Measurements were taken over a temperature range of 2 to 350K, at a magnetic field of 1 Tesla. The magnetic data were fitted to the Curie-Weiss law with the RLSRMS program (Recursive Least-Squares Refinement of Magnetic Susceptibility Data) [14]. The fit was based on the determination of C and θ by regression. These values were then placed back into the Curie-Weiss equation. χ_0 was determined by the difference between the observed susceptibility and that which was calculated by the Curie-Weiss equation. All χ_0 values were then averaged to give the final value.

A GC-Mass spectrum was obtained for the gases evolved during the vacuum decomposition of $Mo(OH)_5(OEt)$ on a Finnigan 4000 GC Mass Spectrometer. The solid sample was decomposed as described in the experimental section. The volatile materials that were evolved during the process were collected in a 100 mL flask using a liquid nitrogen bath. The gases were then transferred to a septum vial using a needle valve that connected the vial to the vacuum line. An air-tight syringe was used to draw a sample of gas from the vial. The gases were then injected into the GC where they were initially

frozen in a U-tube before entering the column. The U-tube was then slowly warmed (final temperature: 100°C) to allow the gases to bleed into the column. This procedure gave better resolution of the eluted peaks.

RESULTS AND DISCUSSION

Because of the work that was done previously using $Mo_2(NMe_2)_6$ as the starting material for hydrolysis, and the subsequent problems with removal of the amido ligand, we decided to look further at using molybdenum alkoxides as starting materials. Previously, a study of the hydrolysis of $Mo_2(OPr^i)_6$ was completed [15], and it was shown that during the reaction a significant amount of oxidation of the molybdenum occurred. In an attempt to inhibit this oxidation, a bulkier alkoxide ligand was used. Molybdenum(III) tert-butoxide was hydrolyzed in toluene at room temperature according to the proposed reaction:

(5) $$Mo_2(OBu^t)_6 + 6H_2O \Rightarrow 2"Mo(OH)_3" + 6Bu^tOH$$

The reaction produced an amorphous brown material quantitatively. However, analyses on the product indicated that the molybdenum was oxidized by the water from its initial oxidation state of +3. This result suggests that the bulkier tert-butoxide ligand was actually facilitating the oxidation of the molybdenum. This phenomenon can possibly be explained by the greater stability of the butyl radical eliminated from the ligand. Tert-butoxide can form more stable butyl radicals when its C-O bond is broken than the iso-propoxide ligand. Thus, $Mo_2(OBu^t)_6$ upon hydrolysis, would be expected to form a more oxidized product than $Mo_2(OPr^i)_6$. From this argument, it was supposed that a less bulky alkoxide of molybdenum would lead to an unoxidized hydrolysis product i.e. molybdenum remaining in the +3 state.

Molybdenum(III) ethoxide was chosen because the synthesis is straight-forward, and the material is highly soluble in hydrocarbon solvents. Molybdenum(III) methoxide

was also considered as a possible starting material. However, it is very insoluble in hydrocarbon solvents, and thus, is believed to be a polymeric material. Molybdenum(III) ethoxide has not been structurally characterized, but it is believed to be a tetramer from mass spectrometry studies [4].

The stoichiometry of the hydrolysis reaction was carried out according to the following equation:

(6) $$[Mo(OEt)_3]_4 + 12H_2O \Rightarrow "4Mo(OH)_3" + 12HOEt$$

Analysis of the insoluble product of this reaction indicated that indeed the molybdenum was not oxidized and remained in its initial +3 state. An empirical formula for the product corresponds closely to $Mo_2(OH)_5(OEt)$. It thus appears that this material precipitated from solution before complete hydrolysis of the ethoxide ligands was effected.

The infrared (mid and far) spectra of $Mo_2(OH)_5(OEt)$ are shown in Figure 1-1. The mid-IR spectrum shows bands at 1261, 1094, 1043 and 897 cm^{-1}. These bands are also seen in the mid-IR spectrum of molybdenum(III) ethoxide and can be attributed to the alkoxide ligand. This is direct evidence that some ethoxide ligand remains in this material. The far-IR spectrum shows only 2 very broad bands at 557 and 482 cm^{-1} with two weak shoulders at ~400 and 350 cm^{-1}. These bands can be assigned to Mo-O stretching vibrations. All of the bands are significantly broadened because of the amorphous nature of the solid. It is noted that no band due to the O-H stretching vibration can be detected in the spectrum. However, if significant H-bonding occurs in

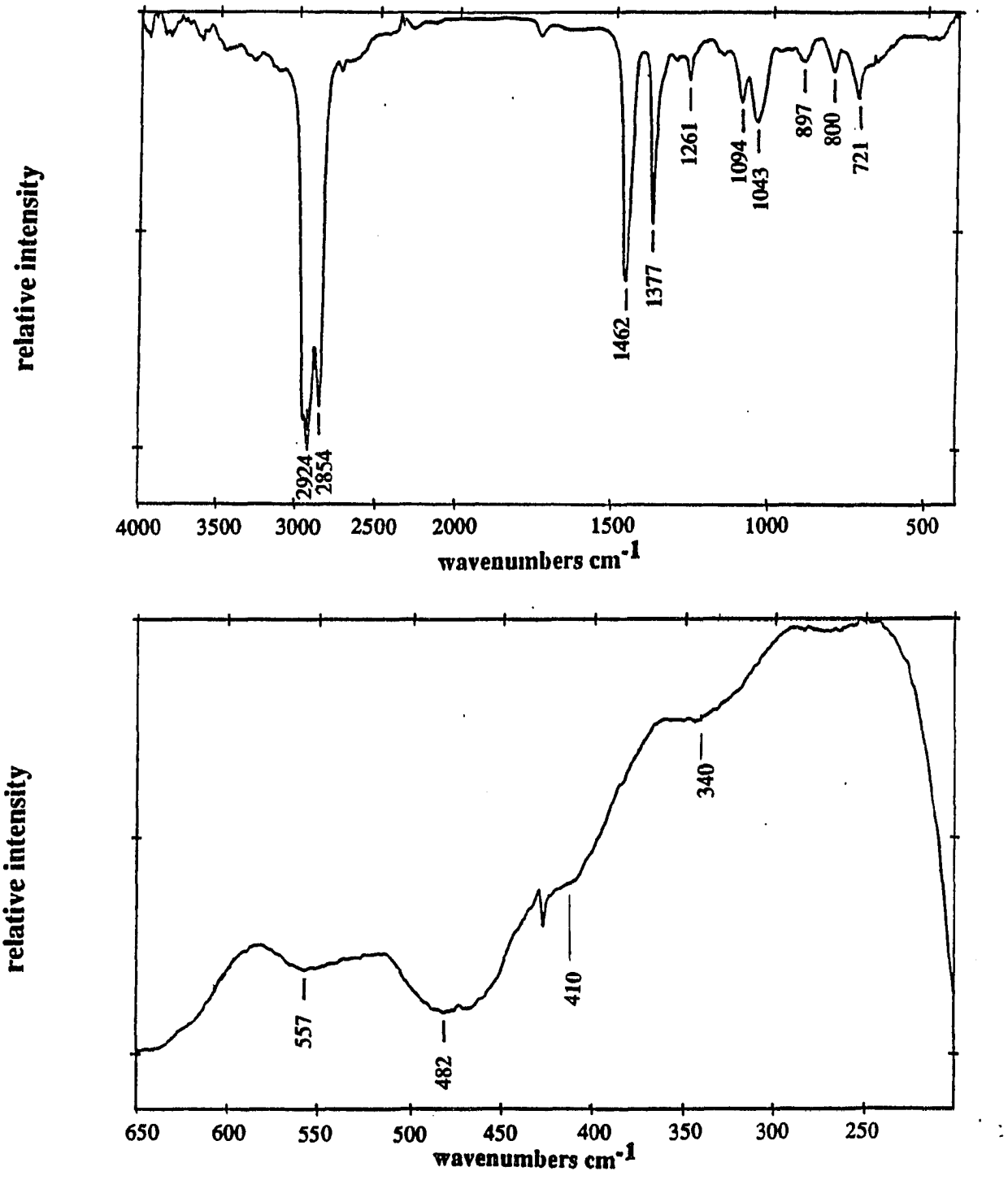

Figure 1-1. Fourier-transform (mid and far) infrared spectra of $Mo_2(OH)_5(OEt)$ (Nujol mull)

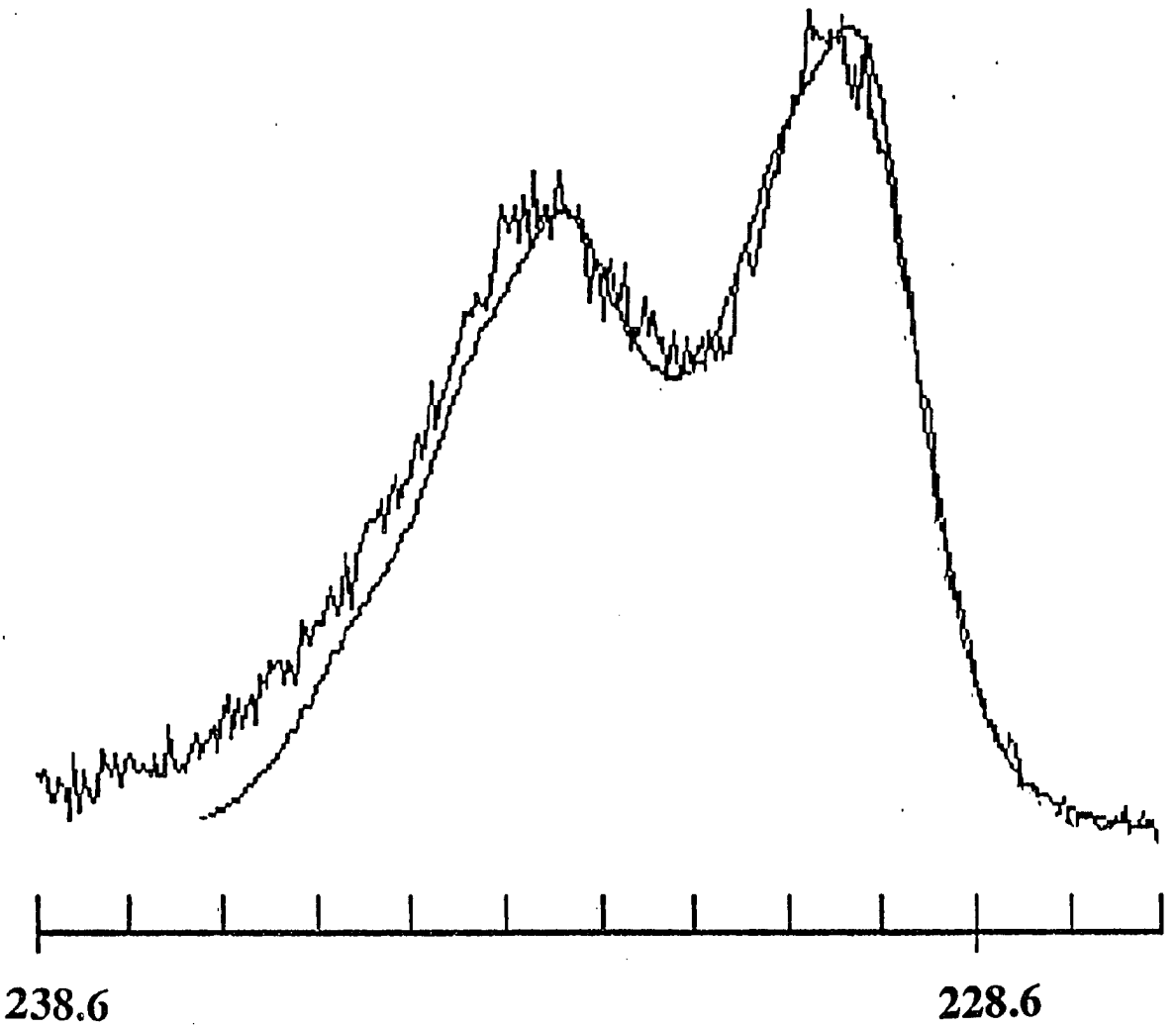

Figure 1-2. Mo 3d XPS spectrum of $Mo_2(OH)_5(OEt)$. Binding energies are referenced to C 1s band at 285.0 eV

this material, as is suspected, the bands arising from O-H stretching modes would be broadened and possibly not easily seen.

The x-ray photoelectron spectrum (XPS) of $Mo_2(OH)_5(OEt)$ is shown in Figure 1-2. It is evident from the spectrum that more than one kind of molybdenum is present. However, the major constituent of the observed peak is at a Mo $3d_{5/2}$ binding energy of 230.4 eV. If this value is compared to that of other known Mo compounds, it appears that the Mo is near the oxidation state of +3. MoO_2 gives a Mo $3d_{5/2}$ peak at 231.0 eV [16]. This oxide contains Mo in the oxidation state +4. Thus, one would expect its Mo $3d_{5/2}$ binding energy to be slightly higher than for a species with a +3 oxidation state. More appropriately, the Mo $3d_{5/2}$ binding energy of $Mo_2(OH)_5(OEt)$ can be compared to that of $MoCl_3$ which exhibits a Mo $3d_{5/2}$ binding energy of 229.0 eV [16]. Both compounds possess Mo in the +3 oxidation state and thus should exhibit similar Mo $3d_{5/2}$ binding energy values. The difference between the two values can be explained by the electronegativity difference of the two ligands which gives rise to different effective charges on the molybdenum atoms. Because oxygen is a more electronegative element than chlorine, when it is bound to molybdenum, it leaves a higher effective charge on the metal atom. Thus, a higher Mo $3d_{5/2}$ binding energy value would be expected for $Mo_2(OH)_5(OEt)$ than for $MoCl_3$. The correlation between binding energies and oxidation state in these systems must be approached with some caution, however, because of the potential problems in surface contaminants, which may play a more important role when highly amorphous, reactive materials are studied, and lack of reference of the binding energies to a common internal standard.

Magnetic susceptibility data for this material were taken as described in the experimental section. The χ (molar susceptibility)-vs.-T(K) plot is shown in Figure 1-3. The data were fitted to the Curie-Weiss law as described by equation 7.

(7) $$\chi = C/(T-\theta) + \chi_o$$

The Curie-Weiss law defines χ as the molar susceptibility, C as the Curie constant, T as the absolute temperature, θ as the correction for interatomic interactions, and χ_o as the sum of the diamagnetic susceptibility (χ_D) and the temperature-independent paramagnetic susceptibility (χ_{TIP}).

The Curie constant is related to the magnetic moment, μ, by equation 8.

(8) $$C = (N(\mu_B)^2\mu^2)/(3k)$$

In this equation, N is Avogadro's number (6.02×10^{23}), μ_B is the Bohr magneton (BM = 9.27×10^{-21} erg/gauss), and k is the Boltzman constant (1.381×10^{-16} erg/deg).

From the fitting of the data for $Mo_2(OH)_5(OEt)$, a Curie constant of 0.0257(9) and a θ value of -2.4 K were calculated. The magnetic moment was determined to be 0.45 μ_B. This value is well below what one would expect for 1 unpaired electron (1.73 μ_B). This small magnetic moment indicates that the majority of the sample is diamagnetic, and the small signal observed can be attributed to paramagnetic impurities in the sample or localized paramagnetic centers or defects present in the structure of the material. Furthermore, this result suggests that the Mo(III) atoms present in the sample must be metal-metal bonded to account for the diamagnetic behavior.

χ_o determined from the RLSRMS program was found to be 0.42×10^{-4} emu/mole.

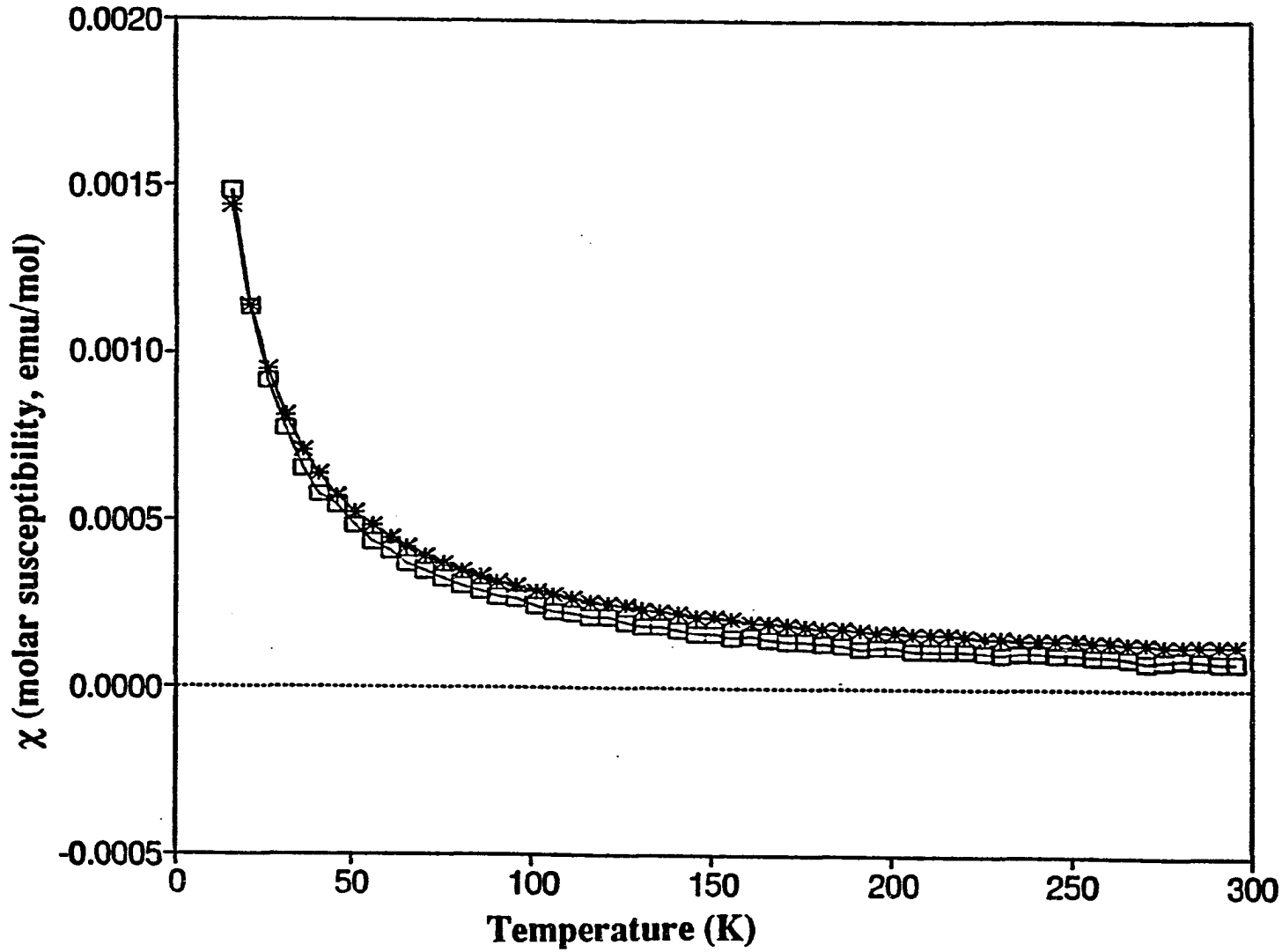

Figure 1-3. A plot of molar magnetic susceptibility (χ) versus temperature (K) obtained at 1 Tesla of $Mo_2(OH)_5(OEt)$. Open squares represent observed data and astericks represent a least-squares fit of the data to the Curie-Weiss law

When T becomes large, the first term of the Curie-Weiss law approaches zero because the magnetic moment is small. Thus, the observed susceptibility at higher temperatures is due primarily to χ_o.

Thermal decomposition reactions. Thermal decomposition of a suitable precursor should be the final step in the low temperature route to the oxide. Various methods can be used, but the most logical is thermal decomposition under dynamic vacuum so that the volatile species evolved, such as water, do not react with the oxide formed.

When thermal decomposition of $Mo_2(OH)_5(OEt)$ in vacuo was completed, the material changed from brown to black and was still amorphous to x-rays. Analyses on the product of the thermal decomposition reaction indicated that it was not converted to Mo_2O_3; rather, a partially oxidized product was obtained. This result indicates that a simple loss of water and ethanol is not occurring. The ethoxide ligand is most likely disproportionating in such a manner that the C-O bond is breaking and leaving a partially oxidized Mo atom. It has been shown that pyrolysis of $Zr(OR)_4$ (where R = t-Bu, or i-Pr) leads to the formation of olefins [1]. These olefins are formed when the C-O bond of the alkoxide ligand is broken. However, with Zr alkoxides, the C-O bond breakage is accompanied by a hydrogen transfer from the leaving olefin to the remaining oxygen to produce a mixed alkoxide-hydroxide compound. This proposed intermediate then rearranges by hydrogen transfer to form a zirconium oxide-alcohol adduct. The alcohol is readily lost at the decomposition temperature to form the oxide. Thus, no concurrent oxidation of the metal is observed upon pyrolysis.

In an attempt to better understand the decomposition process in vacuum, a GC-mass spectrum was obtained on the volatile materials that were given off during this process. Final analysis of the volatile materials evolved during thermal decomposition showed that the major constituents of the gas were ethene and ethane. This indicated that the C-O bond of the coordinated ethoxide ligand is easily broken during thermolysis. Other minor products, 1-propene, propane, and butane, were also noted in the spectrum suggesting that the formation of radicals from the breaking of the C-O bond is occurring.

In an attempt to counter the oxidation of the molybdenum and concurrent subsequent hydrocarbon radical formation that occurs during thermolysis in vacuum, thermal decomposition of $Mo_2(OH)_5(OEt)$ was carried out in flowing hydrogen gas. Initially, the thermal decomposition was carried out at 130°C. A black amorphous solid was recovered. The mid-IR spectrum of the material obtained from this reaction is shown in Figure 1-4. A peak at 1032 cm^{-1} is evidence that some ethoxide ligand is still present in the material. However, this peak is weakened in intensity as compared to peaks in the mid-IR of $Mo_2(OH)_5(OEt)$.

When the same reaction is carried out at 250°C, the mid-IR spectrum of the product showed essentially no bands between 900 and 1200 cm^{-1} (see Figure 1-5). The far-IR spectrum shows only 2 broad bands at ~500 and 650 cm^{-1} which can be attributed to Mo-O stretching modes. As with the precursor material, no bands arising from O-H stretching modes can be seen in the region of 3000-3500 cm^{-1}. Again, this is probably due to hydrogen-bonding in this material and the amorphous nature of the solid.

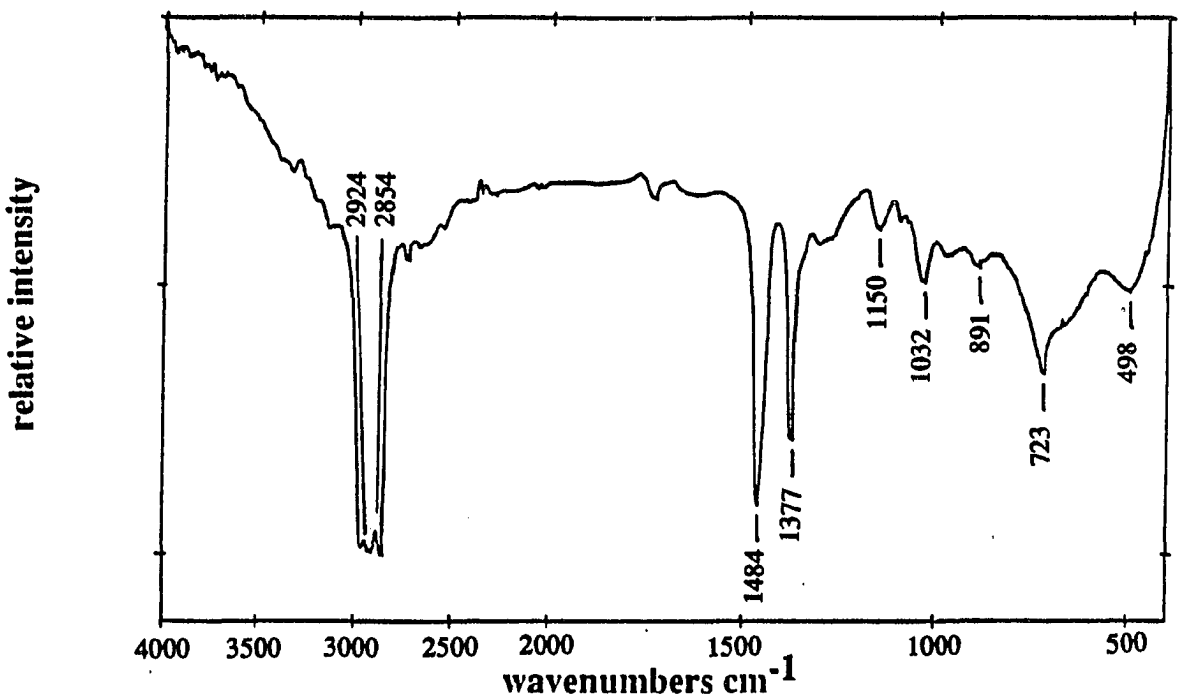

Figure 1-4. Fourier-transform mid-infrared spectrum of the product of the thermal decomposition of $Mo_2(OH)_5(OEt)$ in flowing hydrogen at 130°C (Nujol mull)

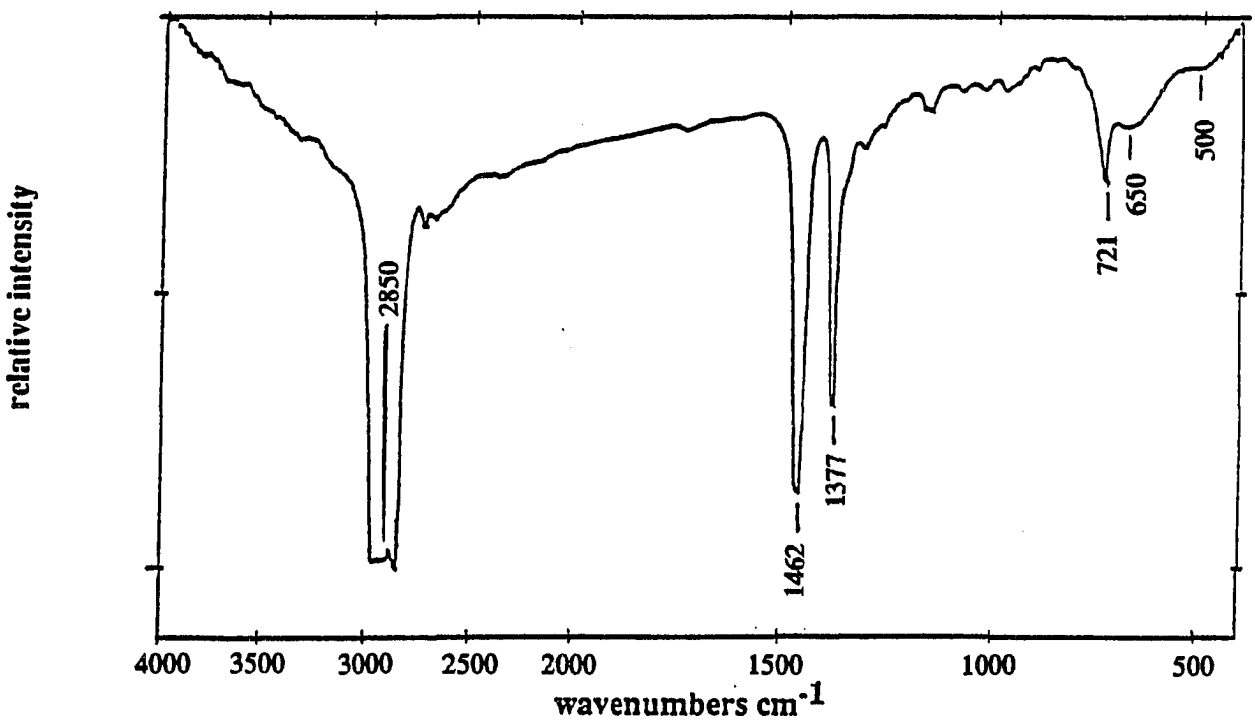

Figure 1-5. Fourier-transform mid-infrared spectrum of MoO(OH) (Nujol mull)

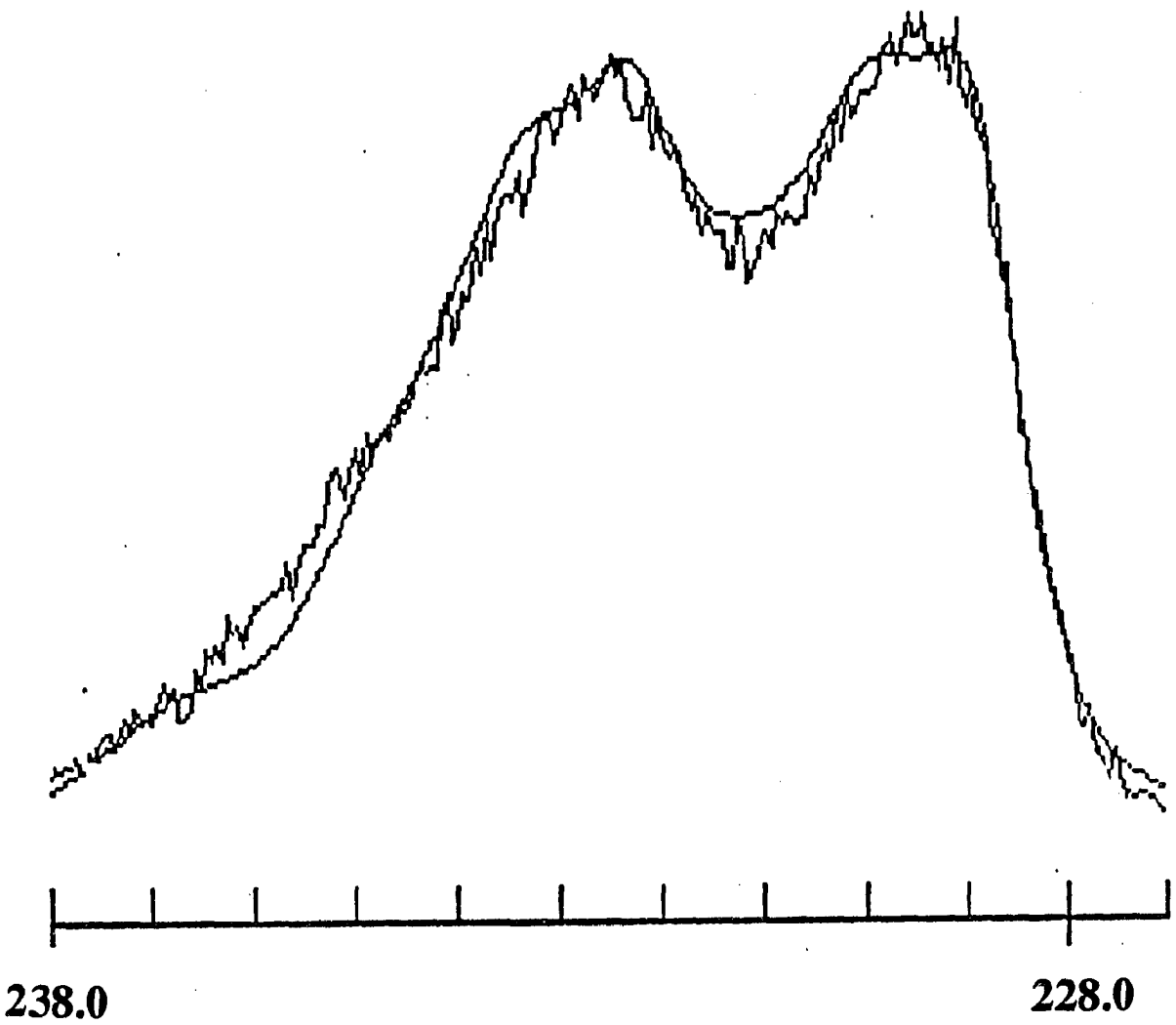

Figure 1-6. Mo 3d XPS spectrum of MoO(OH). Binding energies are referenced to C 1s band at 285.0 eV

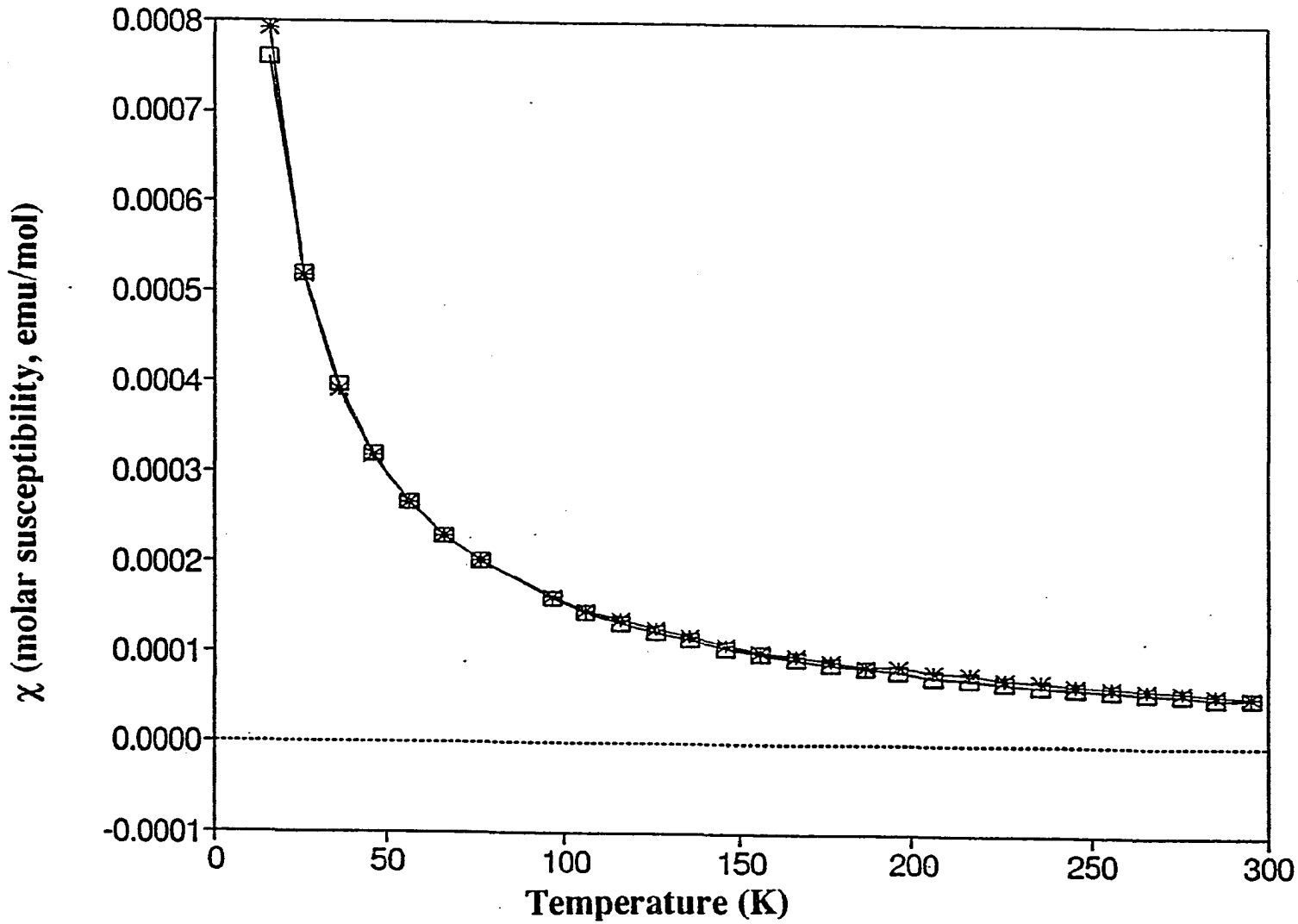

Figure 1-7. A plot of molar magnetic susceptibility (χ) versus temperature (K) obtained at 1 Tesla of MoO(OH). Open squares represent observed data and astericks represent a least-squares fit of the data to the Curie-Weiss law

Elemental and Mo oxidation state analyses of this material suggest that the empirical formula is MoO(OH).

The x-ray photoelectron spectrum of MoO(OH) is shown in Figure 1-6. The Mo 3d peaks can be resolved into components that indicate more than one kind of molybdenum is present. However, the major component exhibits a Mo $3d_{5/2}$ binding energy of 230.2 eV, a value slightly lower (by 0.2 eV) than that for the precursor, $Mo_2(OH)_5(OEt)$. This suggests that the material contains predominantly Mo(III) and did not disproportionate into a mixture of Mo and MoO_2. If the material was a mixture of Mo and MoO_2, two resolved peaks should be evident in the XPS spectrum with Mo $3d_{5/2}$ binding energies of 228.0 and 231.0 eV, respectively [16].

The magnetic susceptibility data for MoO(OH) are shown in Figure 1-7. The plot of χ (molar susceptibility)-vs.-T(K) gives a curve which can be fit to the Curie-Weiss Law. The Curie constant and θ value were determined to be 0.0169(5) and -6.0 K, respectively. From the Curie constant, a magnetic moment equal to 0.37 μ_B was calculated using equation 7. This moment is sufficiently small that it may be attributed to some paramagnetic impurity present in the sample or the presence of localized paramagnetic centers or defects in the structure of the material. This result indicates that a metal-metal bonded framework like that present in the precursor, $Mo_2(OH)_5(OEt)$, is still present in the material derived from thermal treatment in hydrogen.

The χ_o value was determined to be -0.43×10^{-5} emu/mole. Because the magnetic moment is low, the sum of the paramagnetic and diamagnetic susceptibility, χ_o, must be

making a dominant contribution to the observed susceptibility especially at higher temperatures.

In an attempt to bypass this molybdenum-oxide-hydroxide material and directly produce the oxide, Mo_2O_3, thermal decomposition of the precursor, $Mo_2(OH)_5(OEt)$, was carried out in a reduced partial pressure of hydrogen. The reaction was done under identical conditions to the decomposition reaction in pure hydrogen except a mixed gas [$Ar/H_2(6.0\%)$] and a temperature of 300°C were employed. The isolated product of this thermal reaction appeared black and was pyrophoric when exposed to air. Analyses on the product of this reaction indicated that a partially oxidized material was formed. After a sample of this material was annealed at 500°C for 7 days, the powder pattern showed faint lines that can be attributed to molybdenum dioxide. Thus it appears, from the analyses completed on this material, that Mo_2O_3 is not being formed. Furthermore, the average oxidation state of the molybdenum suggests that the partial pressure of hydrogen gas is not high enough to inhibit the oxidation of molybdenum during the course of the decomposition reaction.

The thermal decomposition of the precursor material, $Mo_2(OH)_5(OEt)$, has afforded the new reduced molybdenum oxide MoO(OH). However, $Mo_2(OH)_5(OEt)$ does not appear to decompose easily to the pure oxide, Mo_2O_3. The thermodynamically stable oxide, MoO_2, is always present as a significant impurity in the final products.

Thermal decomposition of MoO(OH). It seemed reasonable to presume that the species isolated from the thermal decomposition of $Mo_2(OH)_5(OEt)$ in hydrogen gas at

250°C, MoO(OH), could be simply an intermediate to the formation of Mo_2O_3. The continued thermal decomposition at higher temperatures could follow reaction 9.

(9) $$2MoO(OH) \Rightarrow Mo_2O_3 + H_2O$$

When the thermal decomposition of MoO(OH) was completed as described in the experimental section, a black pyrophoric product was isolated. Analyses completed on the product of this reaction suggest that, again, a partially oxidized species was formed. Furthermore, when this material was annealed at 400°C for an additional 24 hours, the x-ray powder pattern showed d-spacing lines that match those of MoO_2. These results indicate that the thermal treatment produces a mixture of MoO_2 and Mo_2O_3. If the product of this reaction was a 50/50 mixture of MoO_2 and Mo_2O_3, one would expect 77.5% Mo and an average Mo oxidation state of 3.33 in agreement with the observed data. This suggests that the above reaction conditions produce Mo_2O_3, but simultaneous decomposition to molybdenum dioxide also occurs.

In this decomposition route, the MoO(OH) must evolve hydrogen gas to produce MoO_2 as shown in the reaction:

(10) $$MoO(OH) \Rightarrow MoO_2 + 1/2H_2$$

This would account for the increase in pressure registered during heating of the sample at 200°C. If water was the only material evolved during the reaction, a significant increase in pressure should not be observed because the water vapor would collect in the cold-trap. However, if hydrogen gas were evolved, it would not condense at liquid nitrogen temperatures, and an increase in pressure would be noted in the system.

Decomposition of MoO(OH) under various other conditions was also attemped. When the material was decomposed in flowing argon at 350°C, the x-ray powder pattern of the product suggested molybdenum dioxide was again formed. Decomposition at higher temperatures (300-325°C) in pure hydrogen gas resulted in the formation of Mo metal. These observations indicate that the smooth decomposition of MoO(OH) to Mo_2O_3 may be prevented by the competing reaction to produce MoO_2 and H_2.

Isolation of reduced ternary molybdenum oxides from MoO(OH). As noted above, it does not seem likely that single phase Mo_2O_3 can be produced easily from MoO(OH). However, it may be possible to produce reduced ternary molybdenum oxides starting with this material. Because MoO(OH) is finely divided and highly reactive, it should readily react with added compounds or elements to form ternary phases.

The reduced ternary molybdenum oxide, $LiMoO_2$, has been previously synthesized via traditional high temperature solid state means [17]. The reaction proceeds as given in the following reaction.

(11) $$Mo(s) + Li_2MoO_4(l) \Rightarrow LiMoO_2(s)$$

The reaction was carried out in a sealed Cu tube for 3 weeks at 900°C in the presence of excess Li_2MoO_4. By this route, pure material cannot be isolated because excess lithium molybdate is impregnated into the final product. In theory, it should be possible to wash the lithium molybdate away with water. However, it has been shown that even after extensive washing, 10-20% lithium molybdate is still present in the sample. Extensive washing with H_2O also causes some oxidation of the $LiMoO_2$ to $Li_{1-x}MoO_2$.

Furthermore, significantly long reaction times (3 weeks) are needed to ensure that all of the Mo metal has reacted with the excess lithium molybdate.

Because of these difficulties, the following reaction, starting with MoO(OH), was proposed to produce $LiMoO_2$:

(12) $Li_2CO_3(s) + 2MoO(OH)(s) \Rightarrow 2LiMoO_2(s) + CO_2(g) + H_2O(g)$

When this reaction was carried out in dynamic vacuum at 600°C for 2 days, single phase $LiMoO_2$ was formed. The x-ray powder pattern of the material isolated from this reaction showed slightly broader lines than those found for material prepared by the high temperature method. However, after annealing this material for 2 days at 900°C, the lines sharpened considerably and were comparable to those for the material isolated from the reaction of Mo and excess lithium molybdate at 900°C. X-ray powder diffraction data for the material isolated from the low temperature route and then annealed at 900°C are given in Table 1-1. All of the lines observed from the material isolated by the low temperature method are within 3σ of those isolated via the high temperature route. No lines due to Mo, MoO_2 or Li_2MoO_4 were observed in the powder pattern of the annealed sample. Furthermore, under these reaction conditions, significantly shorter reaction times are needed and much lower temperatures can be used to isolate $LiMoO_2$.

The analogous reaction between Na_2CO_3 and MoO(OH) to produce $NaMoO_2$ [18] was also attempted. When this reaction was carried out under the same conditions as in the use of Li_2CO_3, the x-ray powder pattern showed the presence of both Na_2MoO_4 as evidenced by lines at d-spacings (Å) of 5.26(1), 3.22(3), and 2.746(2) and a phase in the Na_xMoO_2 system as evidenced by d-spacing lines (Å) at 5.99(1), and 2.996(3). It was

Table 1-1. X-ray powder pattern data (d-spacings, Å) for $LiMoO_2$-L[a] and $LiMoO_2$-H[c]

h k l	$LiMoO_2$-L[a]	intensity[b]	$LiMoO_2$-H[c]	intensity[b]
0 0 3	5.209(6)	s	5.168(6)	s
0 0 6	2.607(2)	w	2.579(1)	w
1 0 1	2.445(1)	ms	2.450(1)	ms
0 1 2	2.358(1)	m	2.363(1)	m
1 0 4	2.092(1)	ms	2.0893(9)	ms
0 1 5	1.9385(8)	w	1.9371(7)	w
1 0 7	1.6590(6)	mw	1.6509(5)	mw
0 1 8	1.5327(5)	mw	1.5265(4)	mw
1 1 0	1.4330(4)	mw	1.4343(4)	mw
1 1 3	1.3814(4)	mw	1.3826(3)	mw
1 1 6			1.2525(2)	vw
0 2 1	1.2338(3)	w	1.2359(2)	w
0 1 11			1.2231(2)	vw

a. Values observed from Guinier x-ray powder pattern of sample prepared from MoO(OH) and Li_2CO_3 at 600°C and then annealed at 900°C.

b. Relative intensities indicated by s, strong; m, medium; w, weak; and vw, very weak.

c. Values observed from Guinier x-ray powder pattern of sample prepared from Mo and Li_2MoO_4 at 900°C [17].

further found that the crystallinity of the Na_xMoO_2 phase could be improved by annealing the product of this reaction with the mineralizing agent, I_2, in a sealed Cu tube at 750°C for 2 weeks. The x-ray diffraction pattern matched that of the Na_xMoO_2 phase where x = 0.66 [17]. It may be that the stability of the sodium carbonate, as compared to lithium carbonate, interferes with the smooth reaction to form $NaMoO_2$.

Other starting materials were used in an attempt to form $NaMoO_2$. Initially, Na metal was used according to the following reaction:

(13) $\quad Na(l) + MoO(OH)(s) \Rightarrow NaMoO_2(s) + 1/2H_2(g)$

This reaction was carried out in a sealed copper tube at 400°C for 3 days. The product that was recovered appeared gray and polycrystalline in nature. The x-ray powder pattern of the material showed only lines that can be attributed to Mo metal and Na_2MoO_4. No phase related to the Na_xMoO_2 series was observed in the powder pattern.

Another attempt was made with sodium amide, $NaNH_2$ as the reactant. The reaction to produce $NaMoO_2$ was expected to proceed as follows:

(14) $\quad NaNH_2(s) + MoO(OH)(s) \Rightarrow NaMoO_2(s) + NH_3(g)$

When this reaction was carried out in vacuo at 175°C for 24 hours, a black amorphous material was isolated. When the solid was annealed at 500°C for 2 to 3 days, the powder pattern showed only very low intensity lines that can be attributed to Na_2MoO_4. Initial reaction temperatures greater than 175°C provided the same result.

These results are significant because they suggest that MoO(OH) may be a good starting material for producing reduced ternary molybdenum oxides at lower temperatures

than those that have traditionally been used. Thus, it is possible that less thermodynamically stable ternary molybdenum oxides may be isolated by this route.

CONCLUSIONS

In this section, it has been shown that molybdenum(III) ethoxide can be hydrolyzed successfully with no concurrent oxidation of the molybdenum. The product obtained, however, is not a totally hydroxylated species, but rather, the mixed hydroxide-ethoxide compound, $Mo_2(OH)_5(OEt)$. This species appears to exhibit metal-metal bonding, as one might expect from a compound with a molybdenum d^3 electron population. $Mo_2(OH)_5(OEt)$ does decompose thermally in vacuo to produce a mixture of materials with one easily identifiable constituent, MoO_2. This result suggests that the ethoxide ligand remaining in the hydrolysis product complicates the thermal decomposition.

When thermal decomposition of $Mo_2(OH)_5(OEt)$ is carried out in flowing hydrogen gas, a different result is realized. A new material, MoO(OH), is isolated.

It has been shown that MoO(OH) decomposes in vacuo by two routes: one, to produce the target molybdenum oxide, Mo_2O_3 and water; and the other, to produce MoO_2 with the evolution of hydrogen gas. The data suggest that these two decomposition routes occur simultaneously in a ratio of approximately one to one. Attempts to control reaction conditions so as to reduce the production of MoO_2 during decomposition have been unsuccessful. The decomposition of MoO(OH) to MoO_2 appears to be an extremely facile process.

The highly reactive nature of MoO(OH) suggests that it may be a good starting material for the production of reduced ternary molybdenum oxides. This work has shown that MoO(OH) can be used to synthesize $LiMoO_2$ and a member of the Na_xMoO_2 (x =

0.66) series. These ternary molybdenum oxides were isolated at significantly lower temperatures than those commonly used in the past. The high surface area and reactive nature of MoO(OH) appear to facilitate these reactions at lower temperatures. These properties suggest that new ternary molybdenum oxides may be accessable via the use of MoO(OH) as a reactant.

Overall, this work indicates that the sol-gel method is a viable route to producing new reduced molybdenum oxides and mixed oxide-hydroxides. Further work in this area is needed to fully discover the potential of group VI alkoxides as possible routes to new oxide materials.

REFERENCES

1. Mazdiyasni, K.S. Cer. Int. 1982, 8, 42.
2. Vidyasagar, K.; Ganaphthi, L.; Gopalakrishnan, J.; Rao, C.N.R. J. Chem. Soc. Chem. Commun. 1986, 449.
3. Vidyasagar, K.; Gopalakrishnan, J.; Rao, C.N.R. Inorg. Chem. 1984, 23, 1206.
4. Vidyasagar, K.; Gopalakrishnan, J.; Rao, C.N.R. J. Solid State Chem. 1985, 58, 29.
5. Szabo, G. Ph.D. Thesis, Laboratoire de Chimie Minerale III, Universite Claude Bernard, Lyon, France, 1967.
6. Sallavuard, G. Ph.D. Thesis, Laboratoire de Chimie Minerale III, Universite Claude Bernard, Lyon, France, 1971.
7. Chisholm, M.H.; Haitko, D.A.; Murillo, C.A. In: Inorganic Synthesis, Volume XXI J.P. Fackler, Jr., Ed; John Wiley and Sons, Inc.: New York, 1982; pp. 51-56.
8. Chisholm, M.H.; Cotton, F.A.; Murillo, C.A.,; Reichart, W.W. Inorg. Chem. 1977, 16, 1801.
9. Elwell, W.R.; Wood, D.F. Analytical Chemistry of Molybdenum and Tungsten; Pergamon Press: New York; 1971.
10. Diehl, H.; Smith, G.F. Quantitative Analysis; John Wiley and Sons, Inc.: New York, 1952; pp. 270-275.
11. Banks, C.V.; O'Laughlin, J.W. Anal. Chem. 1956, 28, 1338.
12. Luly, M.H. "APES, A Fortran Program to Analyze Photoelectron Spectra" U.S.D.O.E. Report IS-4694; Iowa State University/Ames Lab, Ames, IA; 1979.

13. Beers B. "APES, Revision 4.3" Iowa State University/Ames Lab, Ames, IA; March 1983.

14. Syvinski, W.M. "RLSRMS (Recursive Least-Square Refinement for Magnetic Susceptibility Data)" Iowa State University, Ames, IA; 1991.

15. Tyszkiewicz, M.T. M.S. Dissertation, Iowa State University, Ames, IA, 1987.

16. Grim, S.O.; Matienzo, L.J. Inorg. Chem. 1975, 14, 1014.

17. Aleandri, L.E. Ph.D. Dissertation, Iowa State University, Ames, IA, 1987.

18. Ringenbach, C.; Kessler, H.; Hatterer, A. C. R. Acad. Sc. Paris, Ser. E 1969, 269, 1394.

PART 2. SYNTHESIS AND CHARACTERIZATION OF $Mo_6O(OEt)_{18} \bullet 4.8H_2O$ AND SOME OTHER MOLYBDENUM ETHOXIDE CLUSTER MOLECULES

INTRODUCTION

The use of alternate route methods to produce high purity ceramic materials have been very successful over the last decade. The sol-gel method has been used to synthesize metal oxides at considerably lower temperatures than those that have typically been used in the past [1]. By this route, metal alkoxides are hydrolyzed, and the hydroxide or hydrous oxide products are processed to form the pure oxide. Recently, we have employed this method in an attempt to isolate reduced molybdenum oxides (Part 1). Surprisingly, it is by this method that we have been able to isolate the novel oxygen-centered cluster, $Mo_6O(OEt)_{18}$.

This compound is unique because it is the first example of an interstitially-centered octahedral cluster for a group VI element. Other centered cluster species of scandium [2], yttrium [3], zirconium [4], many lanthanide elements [5] and niobium [6] are known. However, these clusters are stabilized by the interstitial atom and thus, could not exist without it. For hexanuclear clusters of molybdenum, it has been shown that these types of clusters are stable without the centering atom. The isolation of reduced molybdenum oxides such as $BaMo_5O_8$ [7] and $NaMo_4O_6$ [8], which contain discrete oligomeric cluster units and infinite metal-metal bonded chains made up of uncentered molybdenum octahedra proves this fact.

Other similar clusters have been isolated by analogous routes. Recently, the novel molecular species, $O[Fe(OCH_2)_3CCH_3]_6$, which is an oxygen-centered octahedron of Fe(III) atoms, has been reported [9]. This molecule was synthesized from the hydrolysis of the iron(III) alkoxide. In addition, ammonolysis, which is analogous to hydrolysis, has

produced the novel nitrogen-centered zirconium octahedral cluster, $[(tritox)Zr]_6(\eta^6\text{-}N)(\eta^3\text{-}NH)_6(\eta^2\text{-}NH_2)_3$ where "tritox" represents the $^tBu_3CO^-$ ligand [10].

In addition, the isolation of $Mo_6O(OEt)_{18}$ is very unique and surprising because it is the first example of a molybdenum or tungsten alkoxide compound produced in the presence of water.

EXPERIMENTAL

General considerations. All starting materials used in this work are oxygen and water-sensitive. Therefore, all experimental procedures were performed by using Schlenk techniques, inert atmosphere drybox and a glass vacuum line. All solvents were dried prior to use. Chlorobenzene and toluene were dried by using phosphorus pentoxide under refluxing conditions. Tetrahydrofuran was stirred with sodium and benzophenone to remove water and peroxides. Ethanol was dried by addition of sodium metal. All solvents and reactant water were deoxygenated under vacuum by the triple freeze-thaw method. Finally, dried solvents were vacuum-distilled onto activated 3 Å molecular sieves in specially-made round-bottom flasks. Solvents were either transferred by vacuum distillation from solvent flasks or by syringe under a flow of argon gas.

Starting materials. The synthetic procedures for isolating the starting materials that were used in this part, $MoCl_3$, $LiNMe_2$, $Mo_2(NMe_2)_6$, and $[Mo(OEt)_3]_4$, are described in detail in the experimental section of Part 1 of this thesis.

Synthesis of $Mo_6O(OC_2H_5)_{18} \bullet 4.8H_2O$, 1. In a typical reaction, molybdenum(III) ethoxide (5.00 g, 5.41 mmol) was loaded into a 250 mL round-bottom Schlenk flask in a drybox. Toluene (~100 mL) was added by distillation, and the alkoxide was completely dissolved. Deoxygenated water (1.17 mL, 64.8 mmol) was transferred to the solution under a flow of inert gas by syringe. A non-crystalline solid precipitated within minutes of the water addition. When the reaction was complete (about 1 hour), the solid was filtered and extracted with the solvent distilled from the filtrate to ensure that soluble impurities were removed. This solid product was then dried

under dynamic vacuum for 24 hours. The brown filtrate was allowed to stand under argon at room temperature. Within 2 to 3 days, dark brown crystals of 1 deposited on the side of the flask. Ir (Nujol mull) cm^{-1} (solid precipitate of reaction): 1153w, 1092w, 1036m, 899w. Analytical (solid precipitate of reaction). Found. Mo, 59.4. Average Mo oxidation state, 3.2. Because the yield of 1 was so small, no analytical data can be cited.

$[Mo(OC_2H_5)_3]_4$ reacted with C_6H_5IO. Molybdenum(III) ethoxide (0.788 g, 0.852 mmol) and iodosobenzene (0.130 g, 0.590 mmol) were loaded into a 100 mL reaction flask in a drybox. Toluene was distilled onto the reactants, and the mixture was allowed to proceed at 50°C. After 24 hours, all reaction products were soluble in the toluene. However, no material crystallized from this solvent at room temperature or at 0°C after 3 months. When a reaction with the same stoichiometry was performed in neat ethanol under refluxing conditions for 1 day, all products were again soluble in the ethanol. However, no material crystallized from the ethanol at room temperature or at 0°C after 2 months.

$[Mo(OC_2H_5)_3]_4$ reacted with Sb_2O_5. A mixture of molybdenum(III) ethoxide (0.755 g, 0.817 mmol) and antimony(V) oxide, taken directly from the reagent bottle, (0.087 g, 0.27 mmol) was reacted in toluene under refluxing conditions for ~24 hours. The mixture was filtered, and a white solid (presumably Sb_2O_3) and brown filtrate were recovered. The solvent of the filtrate was distilled slowly into a cold-trap. The brown product that remained was redissolved in 10 mL of fresh toluene and refiltered. Single crystals of $Mo_6O_4(OH)_4(OEt)_{10}$ were recovered directly from this filtration. No additional product crystallized from the remaining filtrate (yield: ~10 mg).

$[Mo(OC_2H_5)_3]_4$ reacted with N_2O. Molybdenum(III) ethoxide (0.588 g, 0.636 mmol) was dissolved in 30 mL of toluene which was transferred into the flask by vacuum distillation. Nitrous oxide (0.424 mmol, 65.6 mm Hg) was metered into the vacuum line to the desired pressure that was measured by a monometer attached to the vacuum line. The volume of the line was determined to be 122(1) cm^3. The N_2O was then allowed to react with the solution of molybdenum(III) ethoxide. The vigorously stirred solution remained in contact with the oxidizing gas for 24 hours. All products of this reaction were soluble in the toluene. The solvent was distilled into the cold-trap, and 10 mL of ethanol was transferred onto the remaining product via syringe under a flow of argon. A non-crystalline powder precipitated from the ethanol solution within 24 hours. The reaction mixture was again filtered, and the brown filtrate was kept at 0°C. After about 2 months, a small amount of material crystallized from the solution. IR (Nujol mull) cm^{-1}: 1300m, 1261m, 1101s, 1059s br, 908m, 802w, 614m, 562s, 350w. ^1H NMR (toluene-d_8 at 15°C): δ 3.8-5.4 (multiplet), 1-2 (multiplet).

$[Mo(OC_2H_5)_3]_4$ reacted with $(CH_3)_3NO$. Molybdenum(III) ethoxide (1.19 g, 1.28 mmol) and Me_3NO (0.068 g, 0.907 mmol) were loaded into a 100 mL reaction flask in a drybox. Toluene (30 mL) was distilled onto the reactants, and the mixture was stirred for 72 hours at room temperature. The reaction mixture was then heated until the toluene was refluxing and kept at this temperature for 4 hours. All products of the reaction were soluble at this time. The brown solution was concentrated by distilling away approximately half the toluene into a cold-trap. Within 2 weeks at O°C, brown needle-shaped crystals had deposited from the solution (yield ~30 mg).

Crystallographic determinations. A summary of the x-ray crystal data is given for $Mo_6O(OEt)_{18}$, $Mo_6O_4(OH)_4(OEt)_{10}$, and $Mo_9O_4(OH)_6(OEt)_{22}$ in Tables 2-1 to 2-3, respectively. For $Mo_6O(OEt)_{18}$, data were collected on a crystal with dimensions 0.1 x 0.15 x 0.15 on an Enraf-Nonius CAD4 diffractometer with a scan mode of θ - 2θ at a range of 4 to 55 degrees in 2θ at -75(1)°C. Cell constants and an orientation matrix for data collection were determined from a least squares refinement of 25 centered reflections with $17.6 < 2\theta < 34.4$. This material crystallized in the hexagonal space group R$\bar{3}$m (based on systematic extinctions, -h+k+l = 3n for hkil, -h+l = 3n for hi$\bar{h}$0l, l = 3n for hh2$\bar{h}$l, and l = 3n for 000l) with a_H = 18.317(5)Å and c_H = 15.359(3)Å. Three standard reflections showed no variation in intensity during data collection. An azimuthal scan of a reflection having chi near 90° indicated that no absorption correction was necessary. A total of 1245 unique reflections were collected, of which 697 were considered observed, i.e. with $I > 3\sigma(I)$. A solution was found by using SHELXS-86 (direct methods) [13] and refinement was successful by using full matrix least square methods in the SDP-CAD4 programs [14]. The structure was refined to R = 0.0311 and R_w = 0.0391. All non-hydrogen atoms were located and refined anisotropically. The ethyl groups of the ethoxide ligands, except C3 (bound to O3), were found to be disordered with respect to a mirror plane or a two fold axis. C4, bound to C3, is disordered with respect to a mirror plane. Similarly, C5 and C6, which make up one ethyl group of an ethoxide ligand, are both disordered with respect to a mirror plane. Finally, C1 and C2, the ethyl group bound to O2, are disordered with respect to a 2-fold axis. The 3m symmetry of the cluster unit thus results from averaging over the disordered C atom positions. Satisfactory refinement

Table 2-1. Table of crystallographic data for $Mo_6O(OEt)_{18} \bullet 4.8H_2O$

Formula	$Mo_6O_{19}C_{36}H_{90}\bullet 4.8H_2O$	Formula weight	1492.82
a (Å)	18.317(5)	Space group	R$\bar{3}$m
c (Å)	15.359(3)	T (°C)	-75(1)
V (Å^3)	4463(3)	λ (Å)	0.71073
Z	3	d(calc)g/cm^3	1.666
μ MoKα (cm^{-1})	12.638	$R(F_o)^a$	0.0311
		$R_w(F_o^2)^b$	0.0391

a. $R = \Sigma||F_o| - |F_c||/\Sigma|F_o|$.

b. $R_w = [\Sigma\omega(|F_o| - |F_c|)^2/\Sigma\omega|F_o|^2]^{1/2}$; $\omega = 1/\sigma^2(|F_o|)$.

Table 2-2. Table of crystallographic data for $Mo_6O_4(OH)_4(OEt)_{10}$

Formula	$Mo_6O_{18}C_{20}H_{54}$	Formula weight	1158.28
a (Å)	12.215(3)	Space group	PT
b (Å)	12.215(3)	Z	1
c (Å)	11.572(7)	T (°C)	25
α (°)	108.4(1)	μ Mo Kα (cm^{-1})	13.7
β (°)	108.4(1)	d(calc)g/cm^3	1.429
γ (°)	110.5(1)	R (F_o)	0.056
V (Å^3)	1346(3)	R_w (F_o^2)	0.080
λ (Å)	0.71073		

a. $R = \Sigma||F_o| - |F_c||/\Sigma|F_o|$.

b. $R_w = [\Sigma\omega(|F_o| - |F_c|)^2/\Sigma\omega|F_o|^2]^{1/2}$; $\omega = 1/\sigma^2(|F_o|)$.

Table 2-3. Table of crystallographic data for $Mo_9O_4(OH)_6(OEt)_{22}$

Formula	$Mo_9O_{32}C_{44}H_{116}$	Formula weight	2021.0
a (Å)	23.03(1)	Space group	C2/c
b (Å)	11.550(6)	Z	6
c (Å)	38.01(3)	T (°C)	25
β (°)	111.64(6)	μ Mo Kα (cm^{-1})	17.843
V ($Å^3$)	9399(8)	d(calc)g/cm^3	2.142
λ (Å)	0.71073	R (F_o)	0.164
		R_w (F_o^2)	0.229

a. $R = \Sigma||F_o| - |F_c||/\Sigma|F_o|$.

b. $R_w = [\Sigma\omega(|F_o| - |F_c|)^2/\Sigma\omega|F_o|^2]^{1/2}$; $\omega = 1/\sigma^2(|F_o|)$.

was obtained with the occupation of each disordered C position set at 50%. Also, the solvent of crystallization evidenced by O5 was presumed to be water, since examination of the electron density map showed no peaks corresponding to C atoms of possible ethanol molecules.

For $Mo_6O_4(OH)_4(OEt)_{10}$, data were collected on an Enraf-Nonius CAD4 diffractometer at 25°C with a θ - 2θ scan mode at a range of 4 to 50 degrees in 2θ on a crystal with dimensions of 0.1 x 0.2 x 0.15. Cell constants and an orientation matrix were determined from a least squares refinement of 25 reflections with $17.6 < 2\theta < 31.4$. This material crystallized in the triclinic space group PT with a = 12.215(3), b = 12.215(3) and c = 11.572(7) Å, α = 108.4(1)°, β = 108.4(1)°, and γ = 110.5(1)°. Three standard reflections showed no variation in intensity during data collection. A θ-dependent numerical correction for absorption was applied to the data which gave correction factors of 0.702 and 1.142 [15]. The total number of unique reflections was 4438, of which 2060 were considered observed. A solution was found by using direct methods (SHELXS-86)[13] and verified by Patterson methods (SHELXS-86). The structure was refined by using CAD4-SDP programs (full matrix least square techniques)[14]. All molybdenum and oxygen atoms were refined anisotropically. All carbon atoms, bound to bridging oxygen atoms, and the methyl carbon atoms of the terminal ethoxide ligands were refined isotropically. However, thermal parameters of the methylene carbon atoms bound to the terminal oxygen atoms could not be refined. The structure refined to R = 0.057, and R_w = 0.080.

For $Mo_9O_4(OH)_6(OEt)_{22}$, data were collected at 25°C on a Rigaku AFC6R diffractometer using graphite-monochromatized Mo Kα radiation and a 12 KW rotating anode generator on a crystal with dimensions of 0.03 x 0.10 x 0.10 over a range of 0 to 50 degrees in 2θ. A scan mode of ω - 2θ was used. Cell constants and an orientation matrix were determined from the least squares refinement of 14 centered reflections with 12.9° < 2θ < 15.0°. This material crystallized in the monoclinic space group C2/c determined from a statistical analysis of intensity distributions with a = 23.03(1), b = 11.550(6), c = 38.01(3), β = 111.64(6)°. Three standard reflections showed no variation in intensity during data collection. The total number of unique reflections collected was 8772, of which 2640 were counted as observed. The low percentage of observable data was indicative of a poor data set and suggested that a good structure refinement might not be possible. The structure was solved by using direct methods (SHELXS-86) [13] and refined by full matrix least squares techniques (TEXSAN) [16]. The structure refined to R = 0.164, and R_w = 0.229. All nonhydrogen positions were located except one carbon atom which is presumed to be bonded to C22. The missing atom is probably highly disordered because no signficant peak could be detected in the final electron difference map, and it is not likely that a methoxide group is present in the material because no methanol was used in the reaction. The molybdenum atoms were refined anisotropically. All other atoms, except C1, C2, C10, and C11, were refined isotropically. These 4 carbon atoms were not refined (positional or thermal parameters) because a successful refinement could not be achieved when their parameters were allowed to vary. However,

when these atoms were removed from the refinement, significant electron density was observed at these positions in the electron-density difference map.

Elemental analysis. Elemental molybdenum was determined by precipitation of the 8-hydroxyquinolate, $MoO_2(ONC_9H_6)_2$ [17]. Samples were placed in capped vials in the drybox. After removing the vials from the drybox, they were weighed and the samples were quickly transferred to basic solutions (2 pellets of KOH dissolved in ~50 mL of water), and the amount of these samples was obtained after weighing the empty vials. Conversion of the molybdenum to MoO_4^{2-} was accomplished by adding hydrogen peroxide and gently warming the solutions. These solutions were then neutralized to a pH = 4 to 6 and buffered with acetic acid/ammonium acetate buffer. The analyte was precipitated by addition of 8-hydroxyquinoline solution. The solid was filtered through tared filters, washed with hot water, and dried at 140°C to constant weight. Analyses for C, H, and N were performed by Oneida Research Services, Inc. in Whitesboro, New York.

Oxidation state analysis of molybdenum by Ce(IV) titration. A 0.10 M solution of ceric ammonium nitrate in 1.0 M sulfuric acid was prepared and standardized according to established procedures [18]. The 0.10 M ferrous ammonium sulfate solution in 0.18 M sulfuric acid was made as reported by Banks and O'Laughlin [19]. Accurate standardization of the latter solution is essential prior to each use.

Because the reaction products were reactive to air and moisture, they had to be rigorously protected from oxidation prior to the addition of the Ce(IV) solution for an accurate oxidation state determination. Samples, loaded into vials and sealed in the dry

box, were removed, weighed, then returned to the drybox where they were transferred to beakers which were subsequently covered with latex secured with a rubber band. Once the beakers were removed from the drybox, a measured volume of the standard Ce(IV) solution was added via a buret through a small hole placed in the top of the latex. Samples were exposed to air only after they had totally dissolved in the Ce(IV) solution. An aliquot of freshly-standardized Fe(II) solution was added to each sample to react with the excess Ce(IV). Titration of the excess Fe(II) was then performed with the standard Ce(IV) solution. The endpoint was determined potentiometrically using a calomel reference electrode and a Pt indicating electrode.

Physical methods. Infrared spectra were recorded using an IBM IR/90 Fourier-transform infrared spectrometer. Samples were prepared in a Nujol mull and pressed between CsI plates. Samples were transported to the spectrometer in sealed argon-filled jars. Mid-IR (4000-400 cm^{1-}) and far-IR (600-200 cm^{1-}) spectra were recorded separately.

^{1}H NMR specta were recorded on either a Nicolet NT-300 or Bruker VM-300 instrument at 300 MHz. Samples were prepared by loading them into specially-made NMR tubes which were attached to Teflon needle-valve adapters. Deuterated solvents (benzene-d_6 or toluene-d_8) were transferred onto the samples by vacuum distillation, and the tubes were sealed by a flame to protect the samples from oxygen and water.

RESULTS AND DISCUSSION

As discussed in Part 1, when the stoichiometric amount of water (12 mol/mol of tetramer) was used to hydrolyze $[Mo(OEt)_3]_4$, the mixed hydroxide-ethoxide material, $Mo_2(OH)_5(OEt)$, was isolated. In an attempt to completely hydrolyze the ethoxide, an excess of water (slightly greater than 14 mol/mol of tetramer) was used in this hydrolysis reaction. The reaction proceeded with the formation of the brown precipitate, but now a brown filtrate was also observed.

In an attempt to determine if the brown precipitate that was isolated from this reaction was different from the material that was isolated when 12 moles of water were used in the hydrolysis of $[Mo(OEt)_3]_4$, molybdenum and oxidation state determinations were carried out. The average percent molybdenum was found to be 59.4%, and the average Mo oxidation state was 3.2. These results suggest that the excess water was not acting to hydrolyze the remaining ethoxide ligand, but rather, was partially oxidizing the material. Furthermore, the mid-IR spectrum still showed evidence of coordinated ethoxide ligand by the presence of 2 bands at 1094 and 1042 cm^{-1}.

Attempts to thermally decompose the hydrolysis product in dynamic vacuum gave similar results to that which was observed when $Mo_2(OH)_5(OEt)$ was pyrolyzed in vacuo. Analysis for molybdenum (72.9%) was well below the ideal result for Mo_2O_3, 80.0%, and the average Mo oxidation state increased from +3.2 to +3.6. These results were further evidence that ethoxide ligand remained in the material.

The more interesting material isolated from this reaction, an oxygen-centered molybdenum cluster, was crystallized from the filtrate at room temperature within 2-3 days as the hydrate with the formula $Mo_6O(OEt)_{18} \bullet 4.8H_2O$, 1.

Description of the structure of $Mo_6O(OEt)_{18}$. Tables of final atomic positions, anisotropic displacement parameters, bond distances and bond angles are given in Tables 2-2 to 2-5, respectively. Complete crystallographic data are given in Table A-1 in the appendix.

The molecular structure of **1**, as shown in Figure 2-1, indicates a distorted octahedral cluster of Mo atoms with an oxygen atom in the center. The octahedral Mo_6 cluster unit is ligated by twelve edge bridging OEt groups, and each Mo atom is also bonded to a terminal OEt ligand, as indicated by the formula $[Mo_6O(OEt)_{12}](OEt)_6$. The cluster unit is so severely distorted that two distinct triangular subunits can be recognized. The subunits can be thought of as two M_3X_{13} clusters joined together by sharing the central atom O1 and 6 inter-trimer bridging ethoxide ligands, formulated as $[Mo_3O_{1/2}(OEt)_{6/2}(OEt)_6]_2$. A measure of the distortion of the octahedral cluster unit is given by the deviation of the Mo-O1-Mo angle from 90°. In the distorted unit, this angle differs from 90° by 13.45°, i.e. the intra-trimer angle equals 76.55°. Also, if the Mo-O1 distance remained the same in the distorted and undistorted units, viz. 2.107 Å, a Mo-Mo bond distance of 2.98 Å would exist in the undistorted octahedral cluster. This distance is too long for a good Mo-Mo bonding interaction to occur. Thus, the cluster distorts so that six strong Mo-Mo bonds are formed at a distance of 2.6108 Å within the two

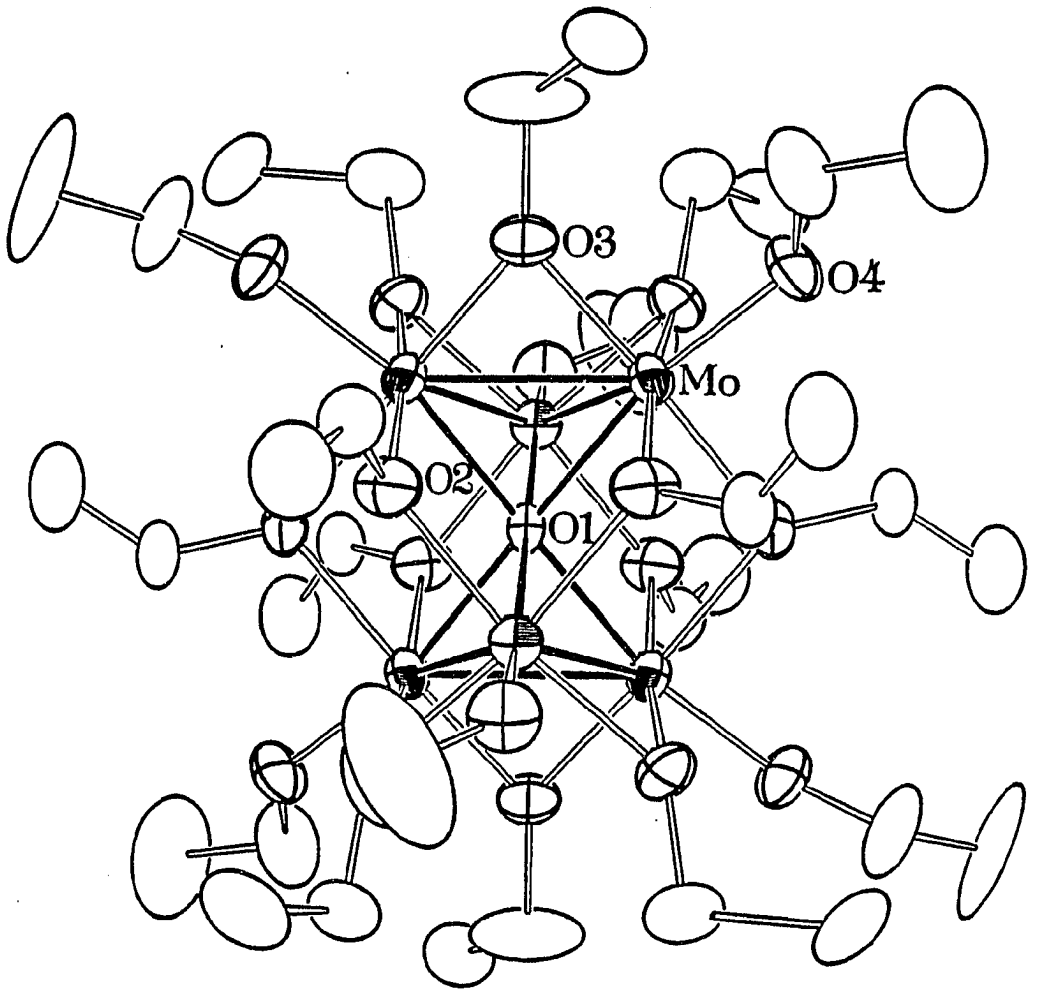

Figure 2-1. A view of the $Mo_6O(OEt)_{18}$ cluster unit approximately perpendicular to the crystallographic 3-fold axis (50% ellipsoids). Only one orientation of the disordered ethyl groups is shown for clarity

Table 2-4. Table of fractional atomic positions, number of positions, occupancy and isotropic thermal parameters for $Mo_6O(OEt)_{18} \bullet 4.8H_2O$

Atom	No. of Positions	K[a]	x	y	z	B
Mo	18 h	1	0.095	0.04750(2)	0.40412(4)	2.16(1)
O(1)	3 b	1	0.000	0.000	0.500	1.6(2)
O(2)	18 g	1	0.1417(3)	0.000	0.500	3.1(1)
O(3)	18 h	1	0.0556	0.0557(2)	0.3238(3)	3.00(8)
O(4)	18 h	1	0.2010	0.1007(2)	0.3401(3)	3.3(1)
O(5)	18 f	0.8	0.000	0.9199(7)	0.000	12.2(5)
C(1)	36 i	1	0.1980(6)	-0.0276(6)	0.4745(7)	3.0(2)
C(2)	36 i	1	0.2537(7)	-0.0361(7)	0.5203(9)	5.0(3)
C(3)	18 h	1	0.0635(3)	0.1266	0.2294(5)	6.1(3)
C(4)	36 i	1	0.0622(8)	-0.1548(8)	0.2217(7)	5.0(3)
C(5)	36 i	1	0.2436(7)	0.1826(8)	0.2981(9)	5.3(4)
C(6)	36 i	1	0.03354(9)	0.2133(9)	0.291(1)	9.7(5)

a. K is the occupancy number.

Table 2-5. Table of general anisotropic displacement parameters[a] expressed in U's for $Mo_6O(OEt)_{18} \cdot 4.8H_2O$

Name	U(1,1)	U(2,2)	U(3,3)	U(1,2)	U(1,3)	U(2,3)
Mo1	0.0206(3)	0.0287(2)	0.0301(2)	0	0.0031(3)	0
O1	0.016(3)	U(1,1)	0.030(5)	U(1,1)	0	0
O2	0.031(2)	0.056(4)	0.038(2)	U(2,2)	-0.002(1)	2U(1,3)
O3	0.045(1)	U(1,1)	0.032(2)	0.028(2)	0.005(1)	-U(1,3)
O4	0.027(3)	0.047(3)	0.046(3)	U(1,1)	0.013(2)	U(1,3)/2
O5	0.18(1)	0.21(1)	0.69(5)	U(1,1)	-0.005(7)	U(1,3)/2
C1	0.034(4)	0.039(4)	0.52(6)	0.027(2)	0.002(4)	0.001(4)
C2	0.054(5)	0.062(5)	0.090(9)	0.042(3)	-0.001(6)	-0.002(6)
C3	0.131(9)	0.033(5)	0.034(4)	U(2,2)	0.007(2)	2U(1,3)
C4	0.081(7)	0.053(6)	0.053(6)	0.031(5)	0.010(6)	-0.021(5)
C5	0.035950	0.053(7)	0.100(9)	0.013(5)	0.028(6)	0.028(7)
C6	0.039(7)	0.085(9)	0.21(2)	0.008(7)	0.04(1)	0.094(9)

a. The form of the anisotropic displacement parameter is: $\exp[-2\pi^2\{h^2a^2U(1,1) + k^2b^2U(2,2) + l^2c^2U(3,3) + 2hkabU(1,2) + 2hlacU(1,3) + 2klbcU(2,3)\}]$ where a, b, and c are reciprocal lattice constants.

Table 2-6. Table of bond distances in angstroms for $Mo_6O(OEt)_{18} \bullet 4.8H_2O$

Atom 1	Atom 2	Distance[a]	Atom 1	Atom 2	Distance[a]
Mo	Mo	2.6108(3)	O(2)	C(1)	1.41(1)
Mo	O(1)	2.1073(4)	O(3)	C(3)	1.470(9)
Mo	O(2)	2.098(3)	O(4)	C(5)	1.45(1)
Mo	O(3)	2.063(4)	C(1)	C(2)	1.49(2)
Mo	O(4)	1.948(3)	C(3)	C(4)	1.67(2)
C(5)	C(6)	1.49(2)			

a. Numbers in parentheses are estimated standard deviations in the least significant digits.

Table 2-7. Table of bond angles in degrees for $Mo_6O(OEt)_{18} \bullet 4.8H_2O$

Atom 1	Atom 2	Atom 3	Angle[a]	Atom 1	Atom 2	Atom 3	Angle[a]
Mo	Mo	Mo	60.0(1)	O(3)	Mo	O(4)	87.7(1)
Mo	Mo	O(1)	51.7(1)	Mo	O(1)	Mo	180.0(0)
Mo	Mo	O(2)	127.9(1)	Mo	O(1)	Mo	76.6(1)
Mo	Mo	O(2)	89.8(1)	Mo	O(1)	Mo	103.5(1)
Mo	Mo	O(3)	96.3(1)	Mo	O(2)	Mo	104.1(2)
Mo	Mo	O(3)	50.7(1)	Mo	O(2)	C(1)	118.4(4)
Mo	Mo	O(4)	138.4(1)	Mo	O(2)	C(1)	130.0(4)
O(1)	Mo	O(2)	76.2(1)	Mo	O(3)	Mo	78.5(1)
O(1)	Mo	O(3)	101.6(1)	Mo	O(3)	C(3)	132.1(3)
O(1)	Mo	O(4)	166.0(1)	Mo	O(4)	C(5)	128.6(6)
O(2)	Mo	O(3)	93.9(1)	O(2)	C(1)	C(2)	116.2(8)
O(2)	Mo	O(3)	170.3(1)	O(3)	C(3)	C(4)	102.2(5)
O(2)	Mo	O(4)	92.8(2)	O(4)	C(5)	C(6)	110.1(1)

a. Numbers in parentheses are estimated standard deviations in the least significant digit.

triangular subunits. The six inter-trimer Mo-Mo distances of 3.309 Å represent essentially nonbonding interactions.

Interstitially centered octahedral cluster species are well known for scandium [2], yttrium [3], zirconium [4], and the lanthanide elements [5]. A few examples are also known for niobium [6], viz. $[Nb_6HI_8]^{n+}$ (n=2 or 3) containing H as the centering element [19]. Until now, it has been considered that these centered cluster species are stabilized by addition of electrons from the valence orbitals of the centering element to the bonding metal-metal orbitals of the cluster unit [4]. Thus, with few exceptions, these clusters exist only when the centering atom is present. However, in the case of $Mo_6O(OEt)_{18}$, which has 16 electrons for Mo-Mo bonding, the central oxygen atom should not be required for stability. Addition of the 6 valence electrons from the central O atom gives a total of 22 electrons for the cluster unit. Presumably, these 6 additional electrons are placed at such low energies relative to the metal-metal orbitals that they may be considered only as weakly interacting with the Mo-Mo bonding orbitals.

Another approach to the bonding of this cluster unit is to consider the latter as if it were two "independent" M_3X_{13} units, each with 8 electrons available for Mo-Mo bonding. Of main significance is the Mo-Mo distance of 2.6108(3) Å, which is slightly greater than that of other 6, 7, or 8 electron M_3X_{13} clusters. For example, the 8 electron cases, $[Mo_3OCl_3(O_2CCH_3)_3(H_2O)_3]^{2+}$ [21] and $Zn_3Mo_3O_8$ [22], have d(Mo-Mo) of 2.550(5) and 2.580(2) Å, respectively. These distances are known to be influenced to some degree by interaction of the "capping" O atom with the Mo cluster orbitals of the triangular unit [23]. In the latter species, the Mo-O(cap) distances are 2.03(1) and 2.06(1)

Å, respectively, whereas in **1**, this distance is 2.1073(4) Å. The longer Mo-O1 distance is understandable because in **1** the O atom is 6 coordinate, and in the other examples, it is 3 coordinate.

Another significant difference between **1** and other M_3X_{13} clusters is the very short terminal Mo-O4 distance which is 1.948(3) Å. In the other known eight electron examples of the M_3X_{13} clusters, the corresponding distance is greater than 2.10 Å, viz. 2.13(1) Å in $[Mo_3OCl_3(O_2CCH_3)_3(H_2O)_3]^{2+}$, and 2.160(8) Å in $Zn_3Mo_3O_8$. This suggests that significant Mo-O pi interactions occur in the Mo-O terminal bonds of **1**, and this may in turn weaken the Mo-Mo bonding.

In another view, the structure of the cluster unit of **1** can be related to the isopolyanions $[M_6O_{19}]^{n-}$ (M=Mo or W, n=2; M=Nb or Ta, n=8) [24]. Essentially, **1** is a reduced ethoxy analogue of the oxo anion. Specifically, the $[Mo_6O_{19}]^{2-}$ anion consists of an undistorted octahedral arrangement of Mo atoms centered by one O atom, bridged on each edge by twelve O atoms and multiply bonded to six terminal O atoms. The isopolyanion is fully oxidized, and thus has no d-electrons available for Mo-Mo bonds. Electrons provided by the reduced oxidation state of molybdenum in the $Mo_6O(OEt)_{18}$ cluster, viz. Mo(3.33), are then utilized to form the Mo-Mo bonds of the distorted cluster.

Compound **1** is isolated in only very small but reproducible yields from the reaction of excess water with molybdenum(III) ethoxide. It seems reasonable to conclude that the water is acting as an oxygen donating species to form this material according to the following net reaction:

(4) $$6Mo(OEt)_3 + H_2O \Rightarrow Mo_6O(OEt)_{18} + H_2$$

Because this reaction is complicated by the competing hydrolysis reaction, it may be possible to use other oxygen atom-donating materials that are not plagued by competing reactions in order to successfully form 1 in higher yields.

Rational Synthesis of $Mo_6O(OEt)_{18}$. Because the yield of **1** is typically less than 1% when water is used as the sole oxidizing agent, other oxidizing agents were employed as reactants with molybdenum(III) ethoxide in an attempt to rationally synthesize $Mo_6O(OEt)_{18}$ in higher yields.

Iodosobenzene. Initially, iodosobenzene was chosen as the oxidizing agent because it is known to be a good oxygen atom-donating agent. The reaction was expected to go as follows:

(5) $$6Mo(OEt)_3 + C_6H_5IO \Rightarrow Mo_6O(OEt)_{18} + C_6H_5I$$

This reaction was carried out as described in the experimental section. However, no crystalline material was isolated from any of the reactions. This result probably indicates that the oxygen-centered cluster, **1**, is not being formed in this reaction. No specific attempts to characterize the soluble material were completed.

Antimony Pentoxide. This material was also considered as a good oxidizing agent to synthesize **1**. The stoichiometry of the reaction to form **1** was set up as follows:

(6) $$6Mo(OEt)_3 + 1/2Sb_2O_5 \Rightarrow Mo_6O(OEt)_{18} + 1/2Sb_2O_3$$

When this reaction was carried out as described in the experimental section, a small amount of single crystalline material, $Mo_6O_x(OH)_{8-x}(OEt)_{10}$, **2**, was isolated. The crystals were dark brown, opaque, and similar in shape to **1**. However, single crystal x-ray analysis of this material showed that it was not the oxygen-centered cluster.

Complete crystallographic data, fractional atomic positions, thermal parameters, bond distances, and bond angles are given in Tables A-7 to A-11, respectively, in the appendix.

2 is a nonoxygen-centered, regular octahedron of molybdenum atoms with oxo, hydroxo, and ethoxo ligands occupying all bridging positions in a completely random manner. The terminal positions appear to be occupied only by hydroxo and ethoxo ligands. The disorder of these ligands over the entire cluster makes it nearly impossible to determine the exact composition of the material. However, a general molecular composition, $Mo_6O_x(OH)_{8-x}(OEt)_{10}$, where x = 4, can be suggested based on bond order calculations and the derived formula from the structure determination. The number of ethoxide ligands was determined by setting the thermal parameters of each C atom and refining on the occupancy at the given position. The methylene carbon atoms, C16, C17, and C18, which are bound to the terminal oxygen atoms, could not be successfully refined. If the positional parameters were allowed to vary, the refined positions moved such that an elongated O-C bonding distance was realized. If the atoms were removed from the refinement, however, significant electron density was observed in those positions. Furthermore, the O-C(methyl) distance that was obtained when the methylene carbons were removed from the structure refinement (1.9 Å) was too long to be considered a bonding interaction and suggested that the methylene carbons should be present. In addition, the thermal parameters of all atoms of this structure were approximately 3 times larger than what is normally expected. This casts further doubt on the ability to determine the exact composition of the compound from the crystal structure in the present state of refinement.

However, the octahedron of molybdenum atoms is essentially regular with all Mo-Mo distances between 2.78 and 2.79 Å. From this distance an average bond order can be calculated. Assuming that a Mo-Mo single bond has a value of 2.61 Å, the average bond order for this cluster is 0.53 (i.e. total bond order equal to 6.35). From this value, the total number of metal cluster electrons (MCE) is determined to be approximately 13. Because this calculation is based on a value of 2.61 for an average Mo-Mo single bond, the value of 13 electron available for Mo-Mo bonding could be in error as much as 1 electron. This value does suggest that there is definitely less than 16 electrons available for metal-metal bonding. The MCE value most likely suggests that there are 14 electrons available for metal-metal bonding. If this is correct, it indicates that the compound has the formula $Mo_6O_4(OH)_4(OEt)_{10}$. This compound would be unique because it would be the first example of an uncentered hexanuclear molybdenum alkoxide cluster of the $M_6X_{12}Y_6$ type.

Because this material contains oxo and hydroxo ligands, it is reasonable to presume that the antimony pentoxide that was used to form this cluster had a significant amount of water hydrogen-bonded to its surface, and this water caused the formation of the cluster. When dried Sb_2O_5 was used in the reaction, no crystalline material could be isolated. This not only confirms the hypothesis that surface water caused the formation of 2 but also suggests that antimony(V) oxide is not effective as a reagent to form the oxygen-centered species, 1, as was hoped.

Nitrous oxide. This oxidizing agent was considered to be a good possibility for the formation of 1 because of its good oxygen atom-donating properties. Furthermore, the

only other product expected to be formed during the reaction would be nitrogen gas. Also, water should not be as significant a problem as was the case with antimony(V) oxide. The reaction was attempted with the following stoichiometry:

(7) $$6Mo(OEt)_3 + N_2O \Rightarrow Mo_6O(OEt)_{18} + N_2$$

When this reaction was completed as described in the experimental section, a small amount (approximately 30 mg) of solid, 3, was recovered.

The mid and far-IR of 3 are shown in Figure 2-2. All of the bands in the mid-IR region match almost identically the bands of the starting molybdenum(III) ethoxide. The far-IR, however, differs greatly from the starting material. 3 shows two strong bands at 614 and 562 cm^{-1} with another very weak band at ~340 cm^{-1}. The starting molybdenum(III) ethoxide spectrum shows many more bands in the far-IR.

A ^1H NMR spectrum of 3 in toluene-d_8 was also completed (Figure 2-3). The spectrum shows groups of resonances in 2 regions. The first set is a group of triplets between 1 and 2 ppm and can be attributed to methyl hydrogens of ethoxide ligands. The other set is a group of quartets between 3.8 and 5.5 ppm that can be attributed to methylene hydrogens of ethoxide ligands. The two groups of resonances suggest that the molecular structure of this material has relatively low symmetry because at least nine triplets can be observed in the region between 1 and 2 ppm. It also could be possible that 3 crystallized from the ethanol as a mixture of products which would account for the complicated spectrum that is observed. The spectrum suggests that this species is not 1 because one would not expect the highly symmetric oxygen-centered cluster to exhibit such a complicated ^1H NMR spectrum.

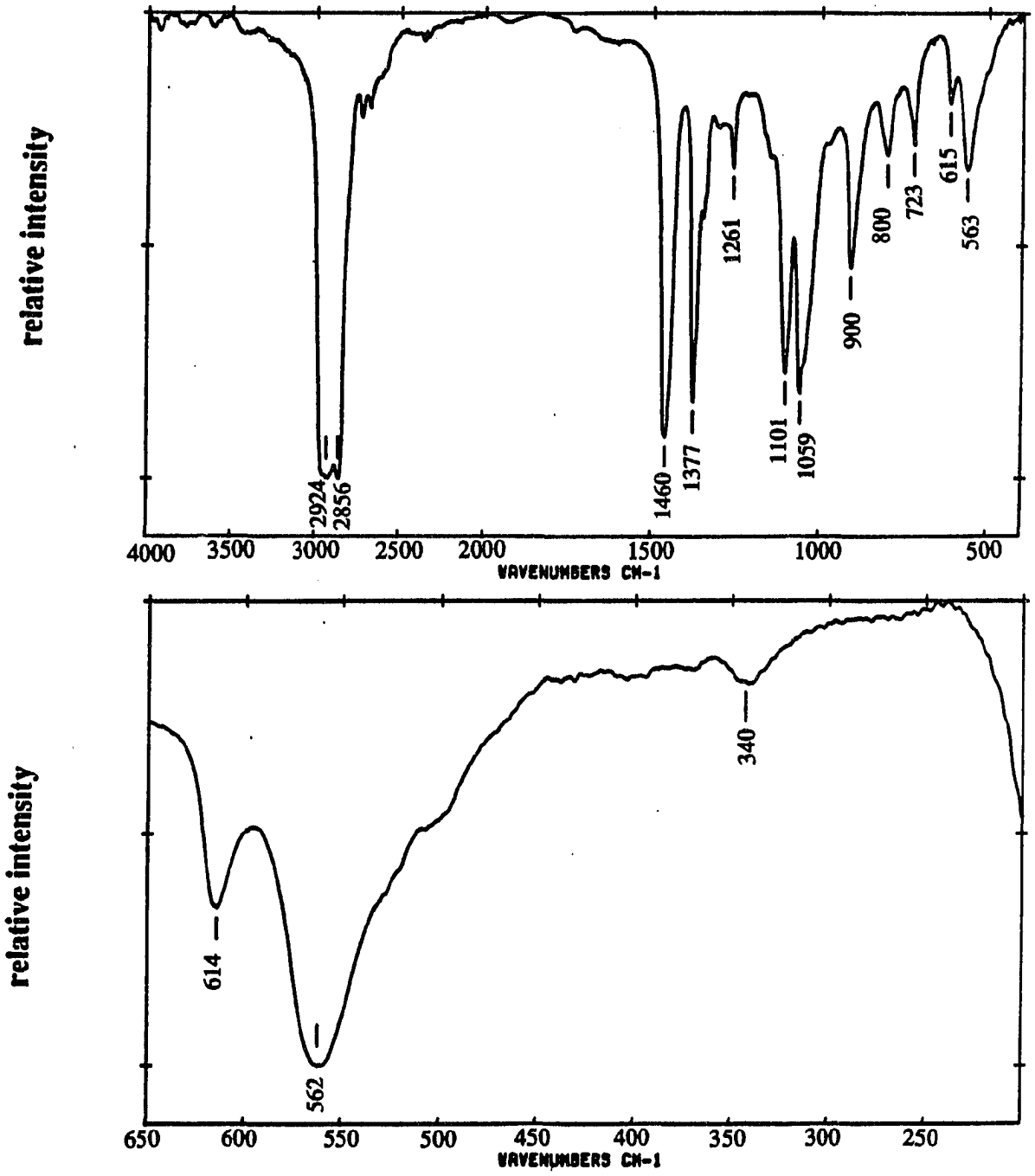

Figure 2-2. Fourier-transformed (mid and far) infrared spectra of the product of the reaction of $[Mo(OEt)_3]_4$ and N_2O (reaction 7) (nujol mull)

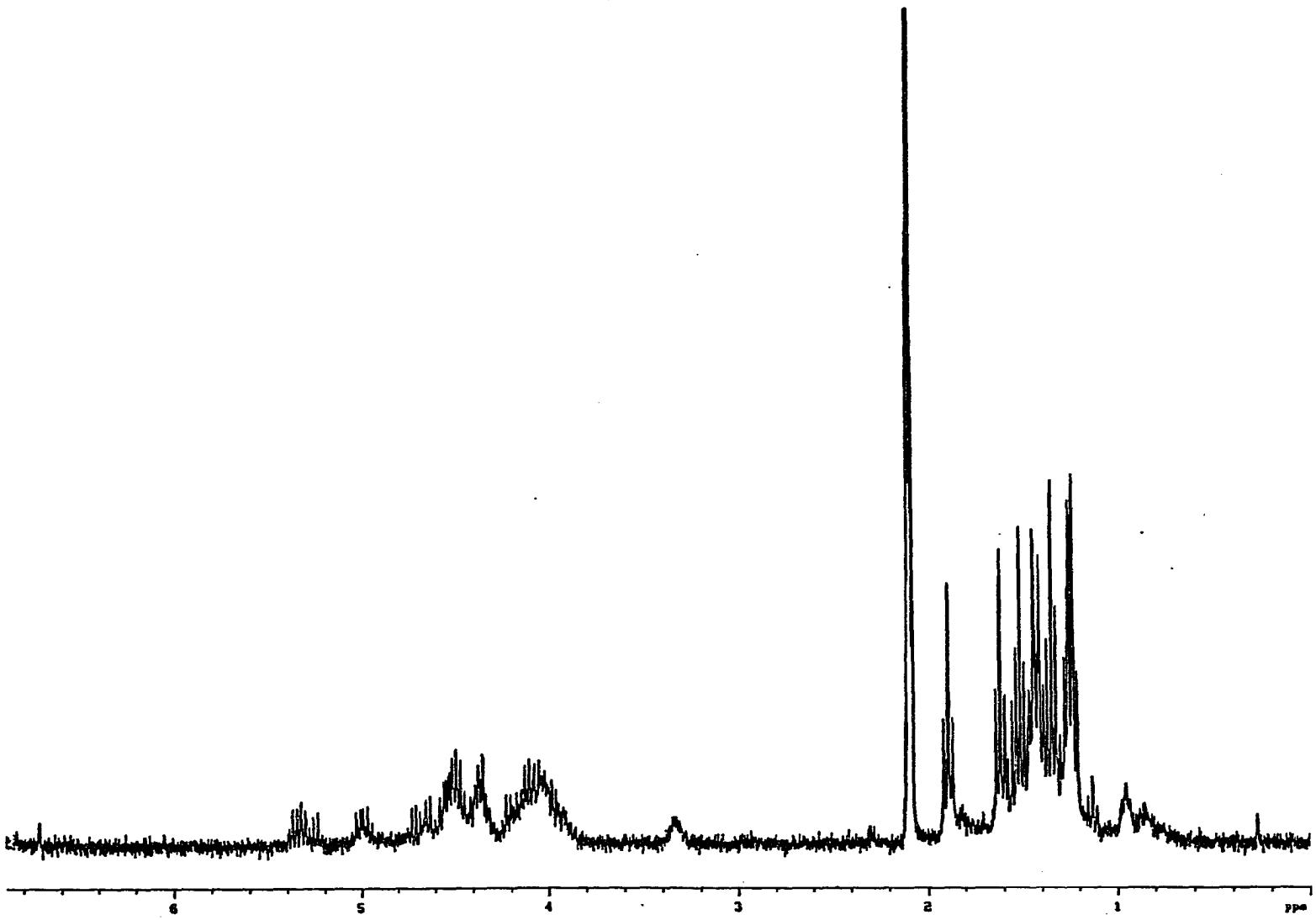

Figure 2-3. ^{1}Hydrogen nuclear magnetic resonance spectrum of the product of the reaction of $[Mo(OEt)_3]_4$ and N_2O (reaction 7) in toluene-d_8 at 15°C

Trimethylamine-N-oxide. This material is known to be a good oxygen atom-donating agent and was employed in the following reaction:

(8) $6Mo(OEt)_3 + Me_3NO \Rightarrow Mo_6O(OEt)_{18} + Me_3N$

Trimethylamine-N-oxide is normally isolated as the dihydrate. Thus, the water first had to be removed from the material before it could be used in this reaction. According to the literature, sublimation of this material is effective in removing the water of hydration [25]. For the given reaction, material that had been sublimed twice in vacuo was used to insure that no water was present. The reaction was carried out as described in the experimental section. Needle-shaped crystals, 4 were recovered in a low yield. Complete crystallographic data, fractional atomic positions, thermal parameters, bond distances, and bond angles are given in Tables A-3 to A-6, respectively, in the appendix.

Some general conclusions on 4 can be made from the structure. The derived molecular formula, $Mo_9O_4(OH)_6(OEt)_{22}$, can be thought of as consisting of two mixed hydroxo-ethoxo tetranuclear clusters connected by a molybdate type atom such that the formula could be rewritten as $[Mo_4(OH)_3(OEt)_{11}]$-$O_{2/2}$-MoO_2-$O_{2/2}$-$[Mo_4(OH)_3(OEt)_{11}]$. The two tetrameric metal-metal bonded species are crystallographically identical and possess nearly identical peripheral Mo-Mo distances ($d[Mo\text{-}Mo]_{ave}$ = 2.72(1) Å). Furthermore, the structure analysis showed the presence of hydroxide ligands indicating that the formation of this material was due to water, either from incomplete dehydration of the oxidizing agent or adventitious water or oxygen in the system. Attempts to isolate this material again have not been successful. It does not

appear that $Mo_6O(OEt)_{18}$ can be isolated via the use of trimethylamine-N-oxide because no other crystalline product could be isolated from the reaction.

The above results suggest that the oxygen-centered cluster isolated from the reaction of molybdenum(III) ethoxide and excess water (greater than 14 mol/mol of $[Mo(OEt)_3]_4$) cannot easily be made via the use of other oxidizing agents. Furthermore, the problem of water-contamination of the starting materials has proven to be a significant obstacle to isolating **1**.

CONCLUSIONS

The novel oxygen-centered cluster $Mo_6O(OEt)_{18}$, was surprisingly isolated from a reaction of molybdenum(III) ethoxide and excess water (greater than 14 moles per mole of $[Mo(OEt)_3]_4$). This material is very interesting because it is the first example of an oxygen-centered metal-metal bonded molybdenum octahedron.

If this material could be isolated in larger quantities, the study of its properties could be accomplished. However, rational syntheses using other oxidizing agents have not afforded this material to date. Conceivably, it should be possible to oxidize the cluster unit by 1 or 2 electrons to provide cluster species with 15 or 14 electrons for metal-metal bonding. In the case of a 1-electron oxidation, the extent of delocalization of the unpaired electron over the entire hexanuclear cluster unit, as opposed to one of the triangular subunits, would be of interest.

All attempts to isolate 1 using other oxidizing agents have been unsuccessful. Some attempts have afforded new mixed oxo-hydroxo-ethoxo clusters of molybdenum, but all clusters isolated are synthesized by water contamination of the starting materials or adventitious water or oxygen in the systems. Lack of reproducibility and small yields in the synthetic reactions have impeded the studies of these new species.

REFERENCES

1. Mazdiyasni, K.S. Cer. Int. **1982**, 8, 42.
2. Dudis, D.S.; Corbett, J.D.; Hwu, S.J. Inorg. Chem. **1986**, 25, 3434.
3. Ford, J.E.; Corbett, J.D.; Hwu, S.J. Inorg. Chem. **1983**, 22, 2789.
4. Smith, J.D.; Corbett, J.D. J. Amer. Chem. Soc. **1986**, 108, 1927. Ziebarth, R.P.; Corbett, J.D. J. Amer. Chem. Soc. **1989**, 111, 3272.
5. Simon, A.; Warkentin, E. Z. Anorg. Allg. Chem. **1983**, 497, 79.
6. Simon, A. Z. Anorg. Allg. Chem. **1967**, 355, 311.
7. McCarley, R.E. Polyhedron **1986**, 5, 51.
8. Chen, S.C. Ph.D. Dissertation, Iowa State University, Ames, IA, 1991.
9. Hegetschweiler, K.; Schmalle, H.; Streit, H.M.; Schneider, W. Inorg. Chem. **1991**, 29, 3625.
10. Wolczanski, P.T.; Holl, M.M.B. Submitted to J. Amer. Chem. Soc. (Sept. 1991).
11. Chisholm, M.H.; Haitko, D.A.; Murillo, C.A. In: Inorg. Synthesis, Volume XXI J.P. Fackler, Jr., Ed; John Wiley and Sons, Inc.: New York; 1982, pp. 51-56.
12. Chisholm, M.H.; Cotton, F.A.; Murillo, C.A.,; Reichart, W.W. Inorg. Chem. **1977**, 16, 1801.
13. Sheldrick, G.M. In: Crystallographic Computing 3, G.M. Sheldrick; C. Kruger; R. Goddard, Eds; Oxford University Press, 1985; pp. 175-189.
14. "SDP, Structure Analysis Computer Software Package" B.A. Frenz & Associates, Inc., College Station, Texas, 1985.
15. Walker, D.N.; Stuart, D. Acta. Crystallogr., **1983**, A39, 159.

16. "TEXSAN-TEXRAY Structure Analysis Computer Software Package" Molecular Structure Corporation, The Woodlands, TX, 1985.

17. Elwell, W.R.; Wood, D.F. In: Analytical Chemistry of the Molybdenum and Tungsten; Pergamon Press: New York, 1971.

18. Diehl, H.; Smith, G.F. In: Quantitative Analysis; John Wiley and Sons, Inc.: New York, 1952; pp. 270-275.

19. Banks, C.V.; O'Laughlin, J.W. Anal. Chem. **1956**, 28, 1338.

20. Also known, but less relevent to this finding, are the carbonyl cluster species containing C, P, and S centers. Vargas, M.D.; Nicholls, J.N. Adv. Inorg. Chem. and Rad. **1986**, 30, 123.

21. Bino, A.; Cotton, F.A.; Dori, Z. Inorg. Chem. **1979**, 33, L133.

22. Torardi, C.C.; McCarley, R.E. Inorg. Chem. **1985**, 24, 476.

23. Bursten, B.E.; Cotton, F.A.; Hall, M.B.; Najjar, R.C. Inorg. Chem. **1982**, 21, 302.

24. Lindquist, I.; Aronsson, B. Ark. Kemi. **1954**, 7, 49. Fuchs, J.; Jalr, K.F. Z. Naturforsch **1968**, 23b, 1380. Allcock, H.R.; Bissell, E.C.; Shawl, E.T. Inorg. Chem. **1973**, 12, 2963. Fuchs, J.; Freiwald, W.; Hartl, H. Acta. Cryst. **1978**, B34, 1764.

25. Monagle, J.J. J. Org. Chem., **1962**, 27, 3851.

PART 3. EXPLORATION OF AN ALTERNATE SYNTHETIC ROUTE TO REDUCED MOLYBDENUM ETHOXIDES. THE SYNTHESIS AND CHARACTERIZATION OF $Mo_4(OEt)_{14}(HOEt)_2$

INTRODUCTION

Metal alkoxides have been studied extensively over the last few decades [1], but it has only been within the last decade that cluster formation, i.e. molecular alkoxides of transition metals that exhibit metal-metal bonding, has become apparent in this class of materials with the discovery of the Mo-Mo bonded species, $Mo_2(OCH_2\text{-}^tBu)_6$ [2]. This compound adopts the ethane-like structure and does not contain bridging alkoxide ligands. Since the discovery of this compound, a variety of molybdenum and tungsten alkoxide clusters species have been synthesized and studied.

An analogy to these cluster species can be drawn with other known metal oxide materials. Molybdenum and tungsten alkoxide clusters have a metal oxide core that exhibit structures that can be found in some traditional solid state materials. For example, the tungsten oxide core of the alkoxide species $W_4(OEt)_{16}$ [3] contains the same unit that is observed in the solid state compound $Ba_{1.14}Mo_8O_{16}$ [4].

Alkoxides of molybdenum(III) typically have been synthesized by starting with the dimethylamine compound, $Mo_2(NMe_2)_6$, according to the following reaction [5]:

(1) $$Mo_2(NMe_2)_6 + 6ROH \Rightarrow Mo_2(OR)_6 + 6HNMe_2$$

These reactions are very facile, and high yields of products are usually obtained. However, the synthesis of the starting material, $Mo_2(NMe_2)_6$, has proven to be complicated and time consuming due to the fact that the material must be purified by a slow sublimation [5]. Furthermore, the isolated yield of material is low (20-30%).

In this section, a study of a new synthetic route to molybdenum ethoxide is reported. The molybdenum(II) species, $Mo_2Cl_4py_4$, **1**, [6] was used as a more

convenient starting material in an attempt to form molybdenum(III) ethoxide by the following reaction:

(2) $Mo_2Cl_4py_4 + 4NaOEt + 2EtOH \Rightarrow 2Mo(OEt)_3 + 4NaCl + 2H_2 + 4py$

1 was chosen because its synthesis, starting from the molybdenum acetate dimer, $Mo_2(OCCH_3)_4$, [7] is quite simple and facile, and the yield of product is typically greater than 80%. By starting with **1**, a more streamlined method for the synthesis of molybdenum(III) ethoxide may be realized. Furthermore, the method may prove to be general for the isolation of molybdenum alkoxides derived from other alcohols.

EXPERIMENTAL

General considerations. All starting materials used in this work were sensitive to oxygen and water. Therefore, all experimental procedures were performed by using Schlenk techniques, an inert atmosphere drybox and a glass vacuum line. All solvents were dried prior to use. Toluene and pyridine were dried by refluxing the respective solvent with either phosphorus pentoxide or calcium hydride. Ethanol was dried by the addition of sodium metal. All solvents were deoxygenated under vacuum by the triple freeze-thaw method. Finally, dried solvents were vacuum-distilled onto activated 3 Å molecular sieves in specially made round-bottom flasks. Solvents were transferred either by vacuum distillation from solvent storage flasks or by syringe under a flow of argon gas.

Synthesis of $Mo_2(O_2CCH_3)_4$. Dimolybdenum tetraacetate can be synthesized easily in glacial acetic acid from the following reaction [7]:

(3) $$2Mo(CO)_6 + 4CH_3CO_2H \Rightarrow Mo_2(O_2CCH_3)_4 + 12CO + 2H_2$$

The reaction was carried out in the presence of tetramethylethylenediamine, which causes a substantial increase in the yield of product. In a typical large scale preparation, $Mo(CO)_6$ (40.0 g, 0.152 mol) was loaded into a 500 mL reaction flask. N, N',N",N'"-tetramethylethylenediamine (24.8 g, 0.282 mol) was added to the solid. Glacial acetic acid (315 g, 5.24 mol) was then added slowly. Inert gas was bubbled through the acid solution for at least a 1/2 hour before the reaction was brought to reflux. This reaction must be monitored closely because the molybdenum carbonyl sublimes out of solution into the condenser where it can block the passage of evolved CO and, thus, cause a build-

up of pressure. The carbonyl must be periodically scraped from the sides of the reaction flask and condenser to avoid this hazard. As the reaction reached later stages, it could be left unattended and allowed to reflux for approximately 24 hours. When the reaction was complete, the yellow solid was filtered in air and washed with 200 mL of ethanol followed by 30 mL of diethyl ether. Finally, the molybdenum acetate compound was dried in vacuo with gentle heating (60°C) overnight.

Synthesis of $Mo_2Cl_4py_4$. This molybdenum-chloride complex, **1**, was synthesized according to the following reaction [6]:

(4) $Mo_2(OCCH_3)_4 + 4(CH_3)_3SiCl + 4py \Rightarrow Mo_2Cl_4py_4 + 4(CH_3)_3SiOCCH_3$

A typical large scale reaction was completed by loading the molybdenum acetate complex (4.00 g, 9.34 mmol) into a 250 mL reaction flask. Pyridine was transferred onto the solid by syringe under a stream of inert gas. An excess of trimethylsilylchloride (8.56 g, 78.8 mmol) was then added by syringe under an argon-flow. The mixture was allowed to react for approximately 20 hours at reflux. The red molybdenum chloride complex was then filtered and dried under dynamic vacuum for 24 hours. IR (Nujol mull) cm^{-1}: 1603s, 1485s, 1221m, 1150m, 1076m, 1043m, 1009m, 881w, 758s, 694s, 636s, 444w, 438w, 344s, 282s, 248m, 211w.

$Mo_2Cl_4py_4$ reacted with sodium ethoxide. The synthesis of $Mo_4(OC_2H_5)_{10}py$, **2**, was accomplished by the following procedure. $Mo_2Cl_4py_4$ (3.07 g, 4.72 mmol) and sodium ethoxide (1.28 g, 18.8 mmol) were loaded into a 250 mL reaction flask. Ethanol (~100 mL) was added to the reactants by syringe under a flow of argon. The reaction mixture was stirred for 20 hours and then filtered to remove the insoluble products

(NaCl). The brown filtrate afforded crystals within 1 week at 0°C. Recrystallization was done in toluene or ethanol. IR (Nujol mull) cm^{-1}: 1597w, 1150w, 1094s, 1049s, 897m, 758w, 625w, 570s, 554s, 507s, 442w, 424w, 402m, 384w. ^1H NMR (benzene-d_6 at 25°C): δ 0.45, 1.35, 1.75, 1.82 ppm (triplets, int. ratio 1:1:1:2); δ 3.8,4.28, 4.68, 4.76, 4.88 ppm (quartets, int. ratio 1:1:1:1;1); δ 6.65, 6.85, 9.1 ppm (broad multiplets). Analytical. Calc. for $Mo_4O_{10}NC_{25}H_{55}$. Mo, 42.0; C, 32.8; H, 6.0; N, 1.5; O, 17.7. Found. Mo, 41.9; C, 33.3; H, 5.9; N, 1.7; O (by difference), 17.2.

Isolation of 3 was accomplished by an alternate procedure whereby the same solvent and stoichiometry of reactants were used, but the mixture was stirred under refluxing conditions for 24 hours. The ethanol solvent was vacuum distilled into a cold-trap leaving an oil-like material in the flask. This product was redissolved in toluene, and the solution was filtered to remove insoluble sodium chloride. All other products were soluble in the toluene. The solvent was then distilled off again leaving an oily product in the flask. This oil was dried to a glass-like solid by gently heating (80°C) the material overnight. IR (Nujol mull) cm^{-1}: 1350s, 1306w, 1266s, 1150w, 1099vs, 1055s, 905s, 804m, 588vw, 561s, 427vw, 400w. ^1H NMR (benzene-d_6 at 25°C) δ 1.4 ppm (multiplet); δ 4.5 ppm (multiplet).

Synthesis of $Mo_4(OEt)_{14}(HOEt)_2$, 4. 3 (1.47 g) and C_6H_5IO (0.237 g, 1.08 mmol) were loaded into a 100 mL reaction flask in a drybox. Toluene was added by vacuum distillation, and the reaction mixture was warmed to 50°C. After 24 hours, all reaction products were soluble in the toluene. The solvent was distilled away leaving a brown oil-like material. This product was redissolved in ethanol. Immediately, a non-

crystalline solid precipitated from the ethanol solution. After about 4 days, the mixture was refiltered, and the brown filtrate was allowed to stand at room temperature. Within 2 weeks, 4 had crystallized from the solution.

Crystallographic determination. A summary of the x-ray crystal data for $Mo_4(OEt)_{14}(HOEt)_2$ is given in Table 3-1. Data were collected on a crystal with dimensions 0.10 x 0.10 x 0.15 on an Enraf-Nonius CAD4 diffractometer with a scan mode of θ - 2θ at a range of 4 to 45 degrees in 2θ at -75(1)°C. Cell constants and an orientation matrix for data collection were determined from a least squares refinement of 22 centered reflections with $16.7 < 2\theta < 31.9$. This material crystallized in the monoclinic space group $P2_1/n$ (based on systematic extinctions, h+l = 2n for h0l, k = 2n for 0k0 with a = 13.084(2), b = 9.712(1), c = 18.213(1) Å and $\beta = 90.44(1)°$. Three standard reflections showed no variation in intensity during data collection. A total of 3018 unique reflections were collected, of which 1942 were considered observed i.e. $I > 4\sigma(I)$. A solution was found by using SHELXS-86 (direct methods) [8] and refinement was successful by using full matrix least squares methods in the SDP-CAD4 programs [9]. The structure was refined to R = 0.026 and $R_w = 0.033$. All non-hydrogen atoms were refined anisotropically except C3 and C4. These carbon atoms, which make up one ethyl group bonded to O2, were determined to be disordered over 2 positions. Satisfactory refinement was obtained when an occupancy for each disordered atom was set at 50%. The hydrogen atoms were introduced at calculated atomic positions with C-H = 0.95 Å.

Table 3-1. Crystallographic data for $Mo_4(OEt)_{14}(HOEt)_2$

Formula	$Mo_4O_{16}C_{32}H_{82}$	Formula weight	1104.74
a (Å)	13.084(2)	Space group	$P2_1/n$
b (Å)	9.712(1)	Z	2
c (Å)	18.213(3)	T (°C)	-75(1)
β (°)	90.44(1)	μ Mo Kα (cm^{-1})	10.913
V ($Å^3$)	2314.2(5)	d(calc)g/cm^3	1.585
λ (Å)	0.71073	R (F_o)	0.026
		R_w (F_o^2)	0.033

a. $R = \Sigma||F_o| - |F_c||/\Sigma|F_o|$.

b. $R_w = [\Sigma\omega(|F_o| - |F_c|)^2/\Sigma\omega|F_o|^2]^{1/2}$; $\omega = 1/\sigma^2(|F_o|)$.

Elemental analysis. Elemental molybdenum was determined by precipitation of the 8-hydroxyquinolate, $MoO_2(ONC_9H_6)_2$ [10]. Samples were placed in capped vials in the drybox. The samples and vials were weighed, and the samples were transferred to basic solutions (2 KOH pellets in 50 mL of water), whereupon the weight of each sample was determined by the difference in the weight of the vials. Hydrogen peroxide was added to the sample solutions in order to completely decompose and oxidize the molybdenum to MoO_4^{2-}. These solutions were neutralized to a pH of 4 to 6, then buffered by addition of acetic acid/ammonium acetate solution. The analyte was precipitated by addition of 8-hydroxyquinoline solution. The solid was filtered through tared glass filters, washed with hot water, and dried at 140°C to constant weight. Analyses for C, H, and N were performed by Oneida Research Services, Inc. in Whitesboro, New York.

Oxidation state analysis of molybdenum by Ce(IV) titration. The 0.10 M solution of ceric ammonium nitrate in 1.0 M sulfuric acid was prepared and standardized according to established procedures [11]. The 0.10 M ferrous ammonium sulfate solution in 0.18 M sulfuric acid was made as reported by Banks and O'Laughlin [12]. It must be accurately standardized before each use.

Because these materials were reactive to air and moisture, they had to be rigorously protected from oxidation prior to the addition of the Ce(IV) solution for an accurate oxidation state determination. Samples, loaded into vials and sealed in the dry box, were removed, weighed, then returned to the drybox where they were transferred to beakers and subsequently covered with latex secured with a rubber band. Once the

beakers were removed from the drybox, the standard Ce(IV) solution was added via a buret through a small hole placed in the top of the latex. Samples were exposed to air only after they had totally dissolved in the Ce(IV) solution. An aliquot of freshly-standardized Fe(II) solution was added to each sample to react with the excess Ce(IV). Titration of the excess iron was then performed with the standard Ce(IV) solution. The endpoint was determined potentiometrically using a calomel reference electrode and a Pt indicating electrode.

Physical methods. Infrared spectra were recorded using an IBM IR/90 Fourier-transform infrared spectrometer. Samples were prepared by making a Nujol mull and pressing the mull between CsI plates. The samples then were transported to the spectrometer in sealed argon-filled jars. Mid-IR (4000-400 cm^{-1}) and far-IR (600-200 cm^{-1}) spectra were recorded separately.

^{1}H NMR was carried out on a Nicolet 300 MHz Spectrometer. Samples were dissolved in deuterated benzene by vacuum distilling the solvent onto the samples which had been loaded into specially made NMR tubes. The tubes were then sealed by a flame to protect the sample from oxygen and water.

RESULTS AND DISCUSSION

Because the established route to isolating molybdenum(III) ethoxide affords a low yield of product, a new route was explored by using $Mo_2Cl_4py_4$ and NaOEt with the stoichiometry of the reaction given in the following equation:

(5) $Mo_2Cl_4py_4 + 4NaOEt + 2EtOH \Rightarrow 2Mo(OEt)_3 + 4NaCl + 4py + H_2$

From this reaction, crystals with the empirical formula, $Mo_4(OEt)_{10}py$, 2, were isolated when the reaction was carried out at room temperature. The mid and far-IR spectra of unrecrystallized 2 are given in Figure 3-1. The mid-IR spectrum shows the presence of coordinated pyridine as evidenced by the bands at 1597 and 758 cm^{-1}. The bands at 1094, 1049, and 897 cm^{-1} are due to the ethoxide ligands present in the material. In the far-IR, all bands can be attributed to Mo-O or coordinated pyridine modes except the weak band at 328 cm^{-1}. This band arises from a small amount of the molybdenum-chloride complex, 1, present as an impurity in the unrecrystallized product.

A ^1H NMR spectrum of 2 (unrecrystallized) in C_6D_6 is shown on Figure 3-2. The spectrum shows the presence of coordinated pyridine evidenced by the resonances at 6.7, 6.9, and 9.0 ppm. The resonances associated with the ethoxide ligands are in the range of 0-5 ppm. The first set of resonances (0-2 ppm) can be attributed to the methyl hydrogens of the ethoxide ligands and the second set (3.5-5 ppm) are due to the methylene hydrogens of the ethoxide ligands. The first set shows 4 triplets in a ratio of 1:1:1:2. While the second set shows 5 equal intensity quartets. This spectrum can be explained by assuming that one pair of triplets has coincidentally fallen directly on top of one another creating the single triplet at 1.8 ppm with twice the intensity as the other triplets. This

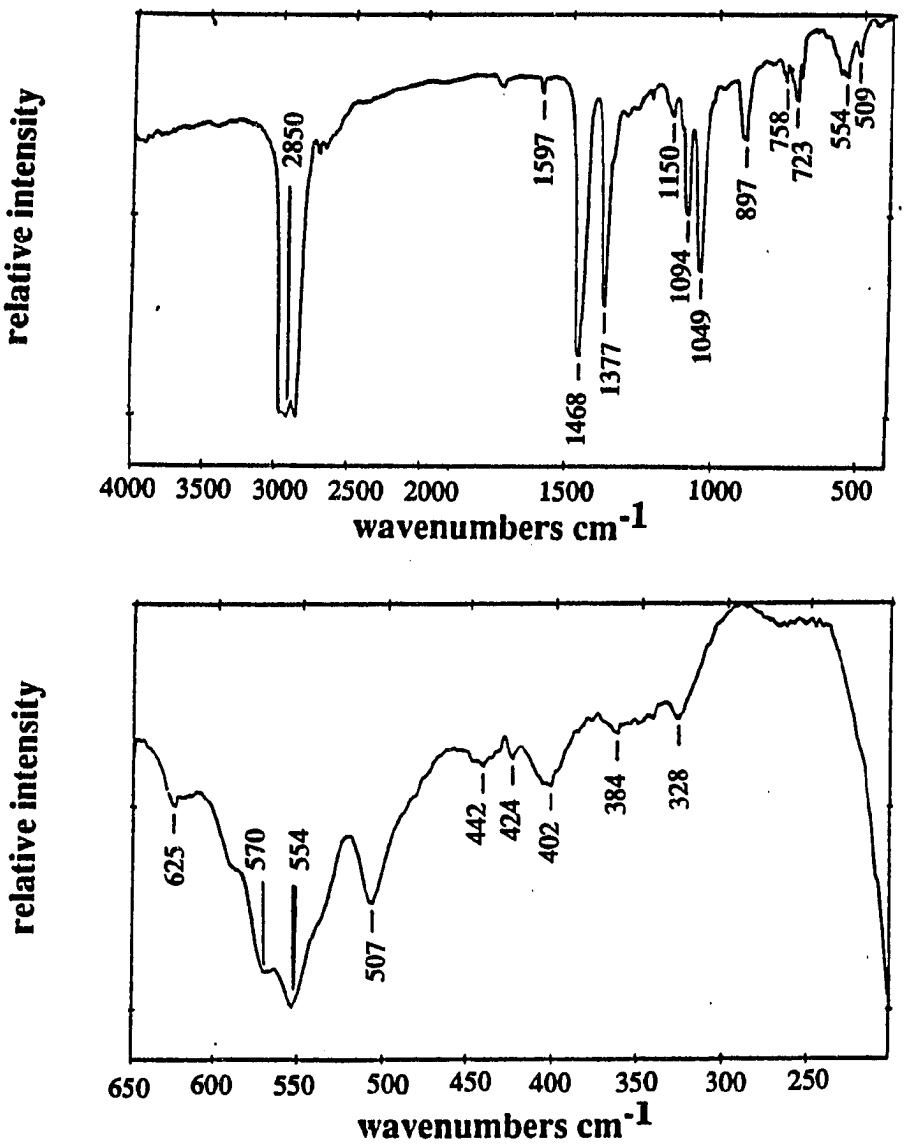

Figure 3-1. Fourier-transform (mid and far) infrared spectra of $Mo_4(OEt)_{10}py$, 2, (Nujol mull)

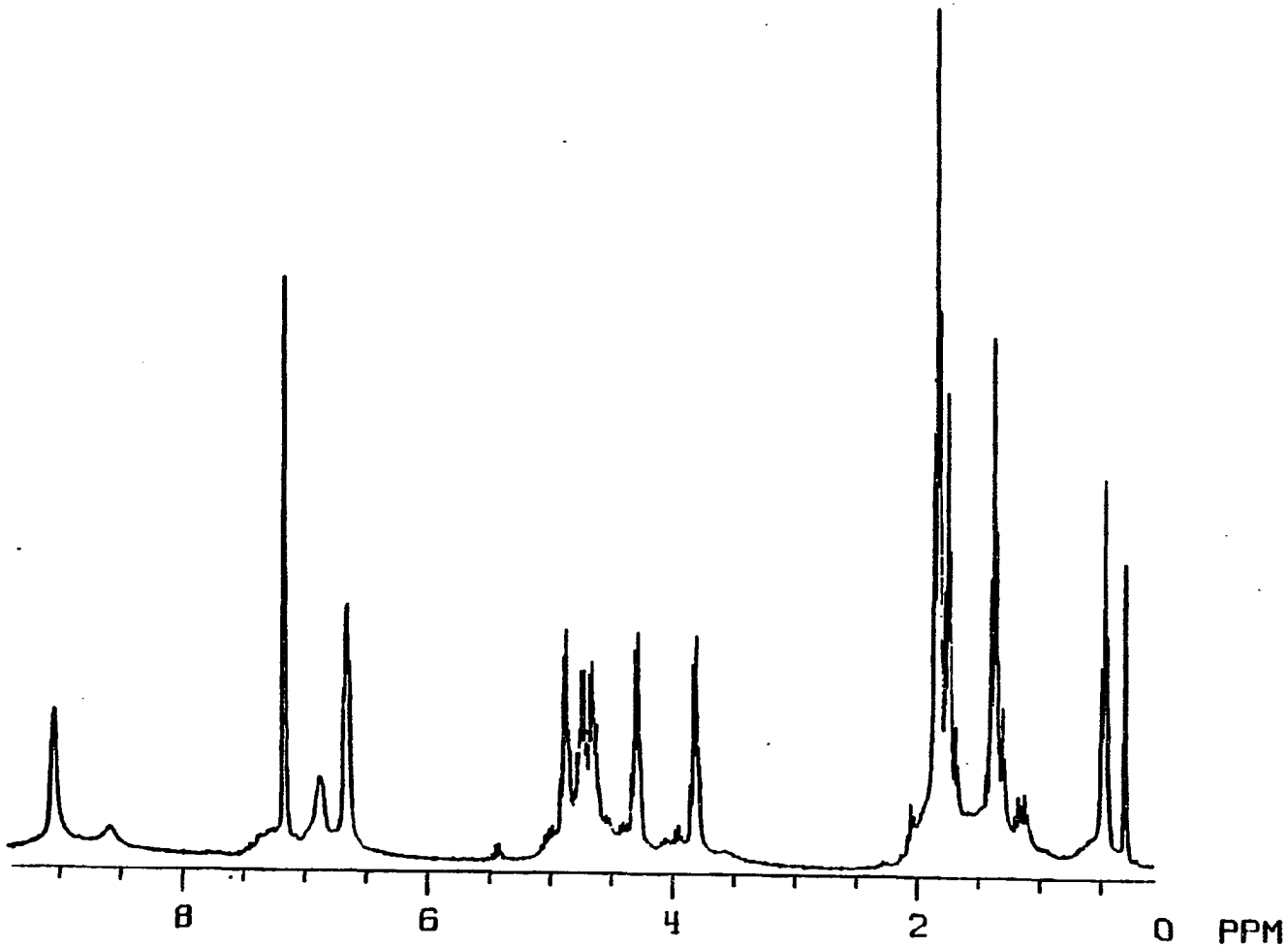

Figure 3-2. ^{1}Hydrogen nuclear magnetic resonance spectrum of $Mo_4(OEt)_{10}py$, **2**, (not recrystallized) in benzene-d_6 at 25°C

interpretation of the spectrum suggests that there are 5 pairs of inequivalent ethoxide ligands present in the molecular structure of 2.

Single crystal x-ray analysis of 2 has not been completed because all crystals that have been studied, thus far, by single crystal x-ray techniques were either highly twinned or very poorly diffracting. Substitution of the coordinated pyridine with 4-methylpyridine was completed, in an attempt to obtain crystals more suitable for x-ray analysis. However, only very small crystallites of the substituted material could be isolated.

2 is believed to be an intermediate species to the homoleptic molybdenum ethoxide because when this reaction was carried out at reflux, the final coordinated pyridine was removed, and a different product was formed.

Table 3-2 gives the far-IR bands of the soluble products isolated from this reaction at various reflux times. After one and a half hours at reflux, a significant number of bands are present. However, the bands at 625, 570, 553, 509, 441, 424, 405, and 327 wavenumbers can be attributed to 2. After 5 1/2 hours at reflux, 2 was converted completely to an ethoxylated species, as evidenced by the disappearance of the pyridine band at 625 cm^{-1}. After approximately 15 hours at reflux, the reaction was considered complete because no further change in the far-IR could be detected when longer reaction times were used. All of the bands in the far-IR can be attributed to Mo-O stretching modes. Due to the glass-like nature of the product, the bands exhibited in this spectrum are broad. For comparison, bands in the far-IR spectrum are given for $Mo(OEt)_3$ prepared by the established route via $Mo_2(NMe_2)_6$. As can be seen from the data, the

Table 3-2. Absorption frequencies (cm^{-1}) found in the far-infrared spectra of soluble materials isolated from reactions 1 and 2

A[a,e]	B[b,e]	C[c,e]	D[d,e]
625 w	-	-	613 s
570 s,sh	588 s	588 vw,sh	-
553 s	553 s,sh	561 s	552 w
509 m	-	-	507 m
441 w	451 vw,br	-	440 s
424 w	427 vw	427 w,sh	-
405 w	-	400 vw	383 s
358 w,br	358 vw,br	-	-
327 w	-	-	-
270 w,br	-	-	303 w,br

a. Soluble material of reaction 2 refluxed in ethanol for 1 1/2 hours.

b. Soluble material of reaction 2 refluxed in ethanol for 5 1/2 hours.

c. Soluble material from reaction 2 refluxed in ethanol for 1 day.

d. Soluble material from reaction 1, $[Mo(OEt)_3]_4$.

e. Relative intensities indicated by s, strong; m, medium; w, weak; vw, very weak; sh, shoulder; br, broad.

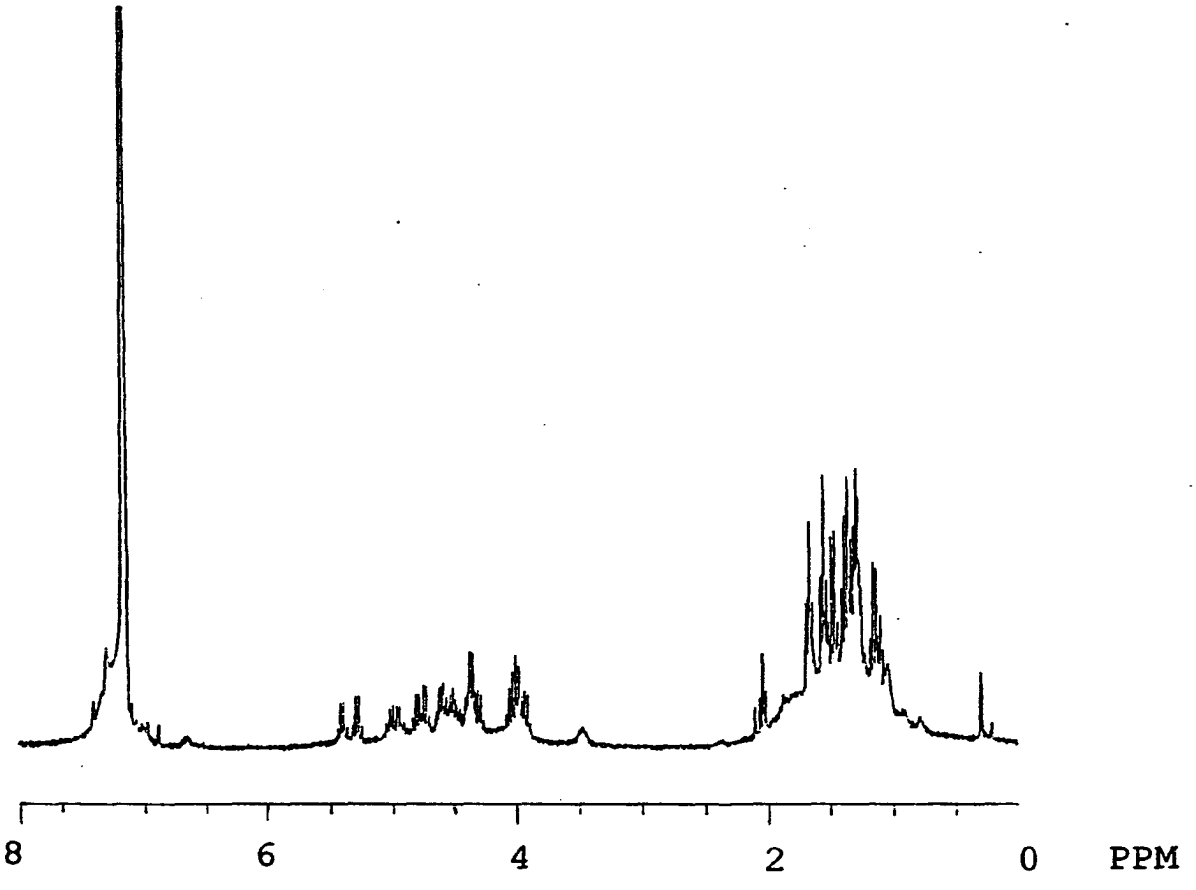

Figure 3-3. ^{1}Hydrogen nuclear magnetic resonance spectrum of 3 (the soluble product of reaction 2 refluxed in ethanol 1 day) in benzene-d_6 at 25°C

two ethoxides of molybdenum exhibit quite different spectra. Analyses completed on 3 indicated that the product is not $Mo(OEt)_3$, but rather, a more reduced compound. The average molybdenum oxidation state and percent molybdenum were determined to be 2.75 and 42.4%. This result may indicate that a compound with the formula $Mo_4(OEt)_{11}$ could be formed from this reaction.

The ^1H NMR spectrum of 3 in C_6D_6 is given in Figure 3-3. The spectrum shows 2 regions of multiplets for the methyl and methylene hydrogens of the ethoxide ligands. This spectrum indicates that 3 is a compound with very low symmetry or, more likely, a mixture of molybdenum ethoxide species. The NMR does indicate that no pyridine is coordinated to 3 by the absence of the 3 distinct pyridine resonances at 6.7, 6.9, and 9.1 ppm which agrees with the results obtained from the FT-IR experiment. From this data, a mixture of homoleptic ethoxide complexes is most probably being produced in this reaction.

Description of the structure of $Mo_4(OEt)_{14}(HOEt)_2$. 4, was isolated as described in the experimental section. Final positional parameters, and general displacement parameters are given in Tables 3-3 and 3-4, respectively. Tables 3-5 and 3-6 give selected bond distances and bond angles. Complete crystallographic data, bond distances, bond angles, and calculated hydrogen atom positions are given in Tables A-12 to A-15, respectively, in the appendix.

A view of 4 is shown in Figure 3-4. The cluster consists of 4 molybdenum atoms arranged in a planar rhomboidal fashion with nearly equal peripheral Mo-Mo distances of

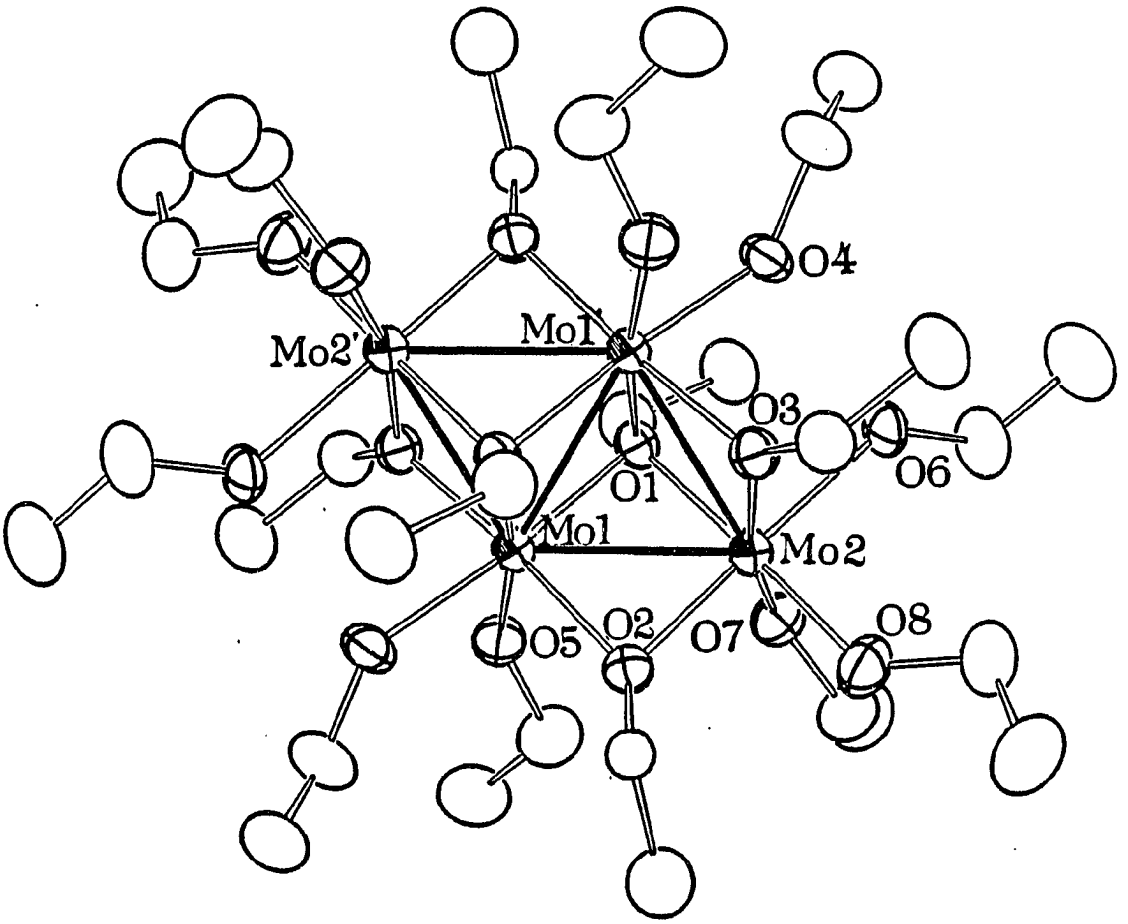

Figure 3-4. A view of $Mo_4(OEt)_{14}(HOEt)_2$, **4**, approximately perpendicular to the plane of the molybdenum atoms (50% ellipsoids)

Table 3-3. Table of fractional atomic positions, number of positions, occupancy and isotropic thermal parameters for $Mo_4(OEt)_{14}(HOEt)_2$

Atom	No. of Positions	K[a]	x	y	z	B[b]
Mo1	4 e	1	0.00997(3)	0.08131(5)	0.05923(2)	1.997(9)
Mo2	4 e	1	-0.17742(3)	-0.00574(5)	0.01977(2)	2.148(9)
O1	4 e	1	-0.0708(3)	0.1185(4)	-0.0389(2)	2.22(7)
O2	4 e	1	-0.1046(3)	-0.0098(4)	0.1175(2)	2.50(8)
O3	4 e	1	0.1231(3)	0.1916(4)	0.0084(2)	2.34(7)
O4	4 e	1	0.1042(3)	0.0581(4)	0.1527(2)	2.70(8)
O5	4 e	1	-0.0273(3)	0.2690(4)	0.0924(2)	2.84(8)
O6	4 e	1	-0.2543(3)	-0.0323(4)	-0.0813(2)	2.77(8)
O7	4 e	1	-0.2497(3)	0.1641(4)	0.0289(2)	3.12(9)
O8	4 e	1	-0.2839(3)	-0.1026(4)	0.0771(2)	3.42(9)
C1	4 e	1	-0.0747(4)	0.2517(6)	-0.0734(3)	3.2(1)
C2	4 e	1	-0.1541(5)	0.2625(7)	-0.1333(3)	3.8(1)
C3	4 e	0.5	-0.1137(7)	-0.103(1)	0.1778(5)	2.2(2)*

a. K is the occupancy number of the atomic position.

b. Starred atoms(*) were refined isotropically.

Table 3-3. (Continued)

Atom	No. of Positions	K[a]	x	y	z	B[b]
C3'	4 e	0.5	-0.138(1)	-0.024(1)	0.1947(7)	3.6(3)*
C4	4 e	0.5	-0.182(1)	-0.037(1)	0.2362(7)	4.3(3)*
C4'	4 e	0.5	-0.130(1)	-0.169(2)	0.2192(8)	5.7(4)*
C5	4 e	1	0.1520(4)	0.3339(6)	0.0053(3)	3.1(1)
C6	4 e	1	0.2099(5)	0.3790(7)	0.0729(4)	4.2(2)
C7	4 e	1	0.1020(5)	0.1364(8)	0.2193(3)	4.1(2)
C8	4 e	1	0.1279(5)	0.0445(8)	0.2844(3)	4.4(2)
C9	4 e	1	-0.1068(5)	0.3243(7)	0.1337(4)	4.3(2)
C10	4 e	1	-0.0733(6)	0.4478(8)	0.1746(4)	5.0(2)
C11	4 e	1	-0.3524(5)	0.0149(8)	-0.1046(4)	4.4(2)
C12	4 e	1	-0.3972(6)	-0.75(1)	-0.1613(4)	7.7(2)
C13	4 e	1	-0.3422(5)	0.1910(8)	0.0699(4)	4.3(2)
C14	4 e	1	-0.3820(5)	0.3307(8)	0.0462(4)	5.4(2)
C15	4 e	1	-0.3694(5)	-0.1763(7)	0.0561(4)	4.2(2)
C16	4 e	1	-0.4029(5)	-0.2681(9)	0.1162(4)	6.4(2)

Table 3-4. Table of general anisotropic displacement parameters[a] expressed in U's for $Mo_4(OEt)_{14}(HOEt)_2$

Name	U(1,1)	U(2,2)	U(3,3)	U(1,2)	U(1,3)	U(2,3)
Mo1	0.0246(2)	0.0280(2)	0.0232(2)	-0.0004(2)	-0.0018(2)	-0.0012(3)
Mo2	0.020(2)	0.0309(3)	0.0267(2)	-0.0007(3)	-0.0016(2)	-0.0014(3)
O1	0.029(2)	0.028(2)	0.027(2)	0.000(2)	-0.005(2)	0.001(2)
O2	0.032(2)	0.036(2)	0.027(2)	-0.004(2)	0.001(2)	0.001(2)
O3	0.030(2)	0.026(2)	0.032(2)	-0.004(2)	-0.000(2)	-0.002(2)
O4	0.038(2)	0.040(2)	0.025(2)	0.002(2)	-0.005(2)	-0.007(2)
O5	0.037(2)	0.033(2)	0.038(2)	0.002(2)	0.002(2)	-0.005(2)
O6	0.24(2)	0.044(2)	0.037(2)	0.007(2)	-0.010(2)	-0.005(2)
O7	0.033(2)	0.044(2)	0.041(2)	0.005(2)	0.002(2)	-0.004(2)
O8	0.034(2)	0.049(3)	0.047(2)	-0.009(2)	0.004(2)	0.005(2)
C1	0.045(3)	0.032(3)	0.043(3)	0.004(3)	-0.005(3)	0.012(3)
C2	0.054(4)	0.046(4)	0.045(3)	0.002(4)	-0.013(3)	0.011(3)
C5	0.043(3)	0.033(3)	0.0040(3)	-0.008(3)	0.000(3)	0.000(3)

a. The form of the anisotropic displacement parameter is: $\exp[-2\pi^2\{h^2a^2U(1,1) + k^2b^2U(2,2) + l^2c^2U(3,3) + 2hkabU(1,2) + 2hlacU(1,3) + 2klbcU(2,3)\}]$ where a, b, and c are reciprocal lattice constants.

Table 3-4. (Continued)

Name	U(1,1)	U(2,2)	U(3,3)	U(1,2)	U(1,3)	U(2,3)
C6	0.058(4)	0.042(4)	0.059(4)	-0.014(3)	-0.006(3)	-0.012(4)
C7	0.062(4)	0.060(4)	0.032(3)	0.006(4)	-0.009(3)	-0.009(4)
C8	0.057(4)	0.080(5)	0.032(3)	0.001(4)	-0.006(4)	-0.000(4)
C9	0.053(4)	0.045(4)	0.066(4)	0.004(3)	0.011(3)	-0.024(4)
C10	0.079(5)	0.053(4)	0.058(4)	0.001(4)	0.007(4)	-0.016(4)
C11	0.040(3)	0.073(5)	0.056(4)	0.008(4)	-0.020(3)	-0.002(4)
C12	0.052(4)	0.162(8)	0.078(5)	0.025(5)	-0.030(4)	-0.042(6)
C13	0.038(3)	0.067(4)	0.057(4)	0.008(4)	0.009(3)	-0.017(4)
C14	0.052(4)	0.068(5)	0.086(5)	0.016(4)	0.005(4)	-0.014(5)
C15	0.045(4)	0.052(4)	0.064(4)	-0.011(3)	-0.005(3)	-0.002(4)
C16	0.071(5)	0.095(6)	0.078(5)	-0.038(5)	0.020(4)	0.003(5)

Table 3-5. Table of selected bond distances in angstroms for $Mo_4(OEt)_{14}(HOEt)_2$

Atom 1	Atom 2	Distance[a]	Atom 1	Atom 2	Distance[a]
Mo1	Mo1'	2.685(1)	Mo1	O5	1.982(4)
Mo1	Mo2	2.6862(7)	Mo2	O1	2.136(4)
Mo1	Mo2'	2.7306(7)	Mo2	O2	2.012(4)
Mo1	O1	2.100(4)	Mo2	O3	2.008(4)
Mo1	O1'	2.131(4)	Mo2	O6	2.106(4)
Mo1	O2	2.044(4)	Mo2	O7	1.910(4)
Mo1	O3	2.053(4)	Mo2	O8	1.984(4)
Mo1	O4	2.106(4)			

a. Numbers in parentheses are estimated standard deviations in the least significant digits.

Table 3-6. Table of selected bond angles in degrees for $Mo_4(OEt)_{14}(HOEt)_2$.

Atom 1	Atom 2	Atom 3	Angle[a]	Atom 1	Atom 2	Atom 3	Angle[a]
Mo1'	Mo1	Mo2	61.11(2)	O1'	Mo1	O5	169.5(2)
Mo2	Mo1	Mo2'	120.58(2)	O2	Mo1	O3'	173.5(2)
Mo1	Mo2	Mo1'	59.42(2)	O2	Mo1	O4'	87.8(2)
Mo1'	Mo1	Mo2'	59.47(2)	O2	Mo1	O5	93.3(2)
Mo1'	Mo1	O1	51.1(1)	O3	Mo1'	O4	90.1(2)
Mo1'	Mo1	O2	95.5(1)	O3'	Mo1	O5	80.6(2)
Mo1	Mo1'	O3	90.6(1)	O4'	Mo1	O5	89.8(2)
Mo1	Mo1'	O4	129.7(1)	Mo1	Mo2	O1	50.0(1)
Mo1'	Mo1	O5	139.8(1)	Mo1	Mo2	O2	49.0(1)
Mo2	Mo1	O1	51.3(1)	Mo1	Mo2	O3	91.6(1)
Mo2	Mo1	O2	48.0(1)	Mo1	MO2	O6	134.5(1)
Mo2'	Mo1'	O3	134.7(1)	Mo1	Mo2	O7	99.0(1)
Mo2'	Mo1'	O4	135.2(1)	Mo1	Mo2	O8	130.7(1)
Mo2	Mo1	O5	98.3(1)	Mo1'	Mo2	O1	50.1(1)
Mo2'	Mo1	O1	89.9(1)	Mo1	Mo2	O2	94.8(1)
Mo2'	Mo1	O2	138.7(1)	Mo1'	Mo2	O3	48.5(1)
Mo2	Mo1'	O3	47.1(1)	Mo1'	Mo2	O6	83.5(1)
Mo2	Mo1'	O4	86.0(1)	Mo1	Mo2	O7	132.7(1)
Mo2	Mo1'	O5	127.4(1)	Mo1'	Mo2	O8	136.0(1)
O1	Mo1	O1'	101.2(1)	O1	Mo2	O2	98.4(2)
O1	Mo1	O2	98.6(2)	O1	Mo2	O3	98.4(2)
O1	Mo1'	O3	83.5(2)	O1	Mo2	O6	86.7(2)

a. Numbers in parentheses are estimated standard deviations in the least significant digits.

Table 3-6. (Continued)

Atom 1	Atom 2	Atom 3	Angle[a]	Atom 1	Atom 2	Atom 3	Angle[a]
O1'	Mo1'	O4	173.5(2)	O1	Mo2	O7	83.2(2)
O1	Mo1	O5	88.7(1)	O1	Mo2	O8	173.9(2)
O1'	Mo1	O2	88.4(2)	O2	Mo2	O3	92.4(2)
O2	Mo2	O6	171.9(2)	O2	Mo2	O7	99.8(2)
O2	Mo2	O8	81.7(2)	O3	Mo2	O6	80.5(2)
O3	Mo2	O7	167.3(2)	O3	Mo2	O8	87.7(2)
O6	Mo2	O7	87.1(2)	O6	Mo2	O8	94.0(2)
O7	Mo2	O8	90.8(1)	Mo1	O1	Mo1'	78.8(2)
Mo1	O1	Mo2	78.7(1)	Mo1'	O1	Mo2	79.6(1)
Mo1	O2	Mo2	82.9(1)				

2.6862(7) and 2.7306(7) Å The difference between the two edge distances is only 0.044(1) Å. The central Mo-Mo distance is nearly equal to the edge distances with a value of 2.685(1) Å. The cluster unit sits on an inversion center such that the center of the Mo(1)-Mo(1)' bond is the inversion point.

There are 2 capping or μ^3- oxygen atoms one each above and below the plane of molybdenum atoms. Each edge of the rhomboid is bridged by one ethoxide ligand, and each molybdenum is terminally coordinated by 2 ethoxide ligands. In addition, the cluster has two ethanol molecules, one coordinated to each of two different molybdenum atoms. This is evidenced by the O(6)-O(4) distance of 2.38 Å. This distance is very short and indicates strong hydrogen bonding occurs between these two atoms. The two oxygen atoms appear to bend toward one another giving an O(4)-Mo(1)'-Mo(2) bond angle of 86.0(1)° and an O(6)-Mo(2)-Mo(1)' bond angle of 83.5(1)°. Furthermore, the Mo(2)-O(6) and Mo(1)'-O(4) distances are identical and equal to 2.106(4) Å. This distance is longer than the other terminal Mo-O distances in the cluster by an average of 0.15 Å. However, it is somewhat shorter than what would be expected for a coordinated ethanol molecule. A typical Mo-O distance that one might expect for a coordinated ethanol molecule is ~2.2 Å. In general, it has been determined that the M-M-O(HOR) bond angle is smaller than the M-M-O(OR^-) bond angle where the HOR and OR^- ligands are hydrogen bonded to one another. This observation indicates that the more weakly bound alcohol molecule bends more toward the oxygen atom of the alkoxide ligand to which it is hydrogen bonded [13]. However, in the case of 4, the Mo-Mo-O bond angles for O6 and O4 are nearly the same, and the Mo-O distances for O(4) and O(6) are identical.

Therefore, it is impossible to determine unequivically which ligand is the ethanol molecule from the structure determination. Furthermore, the equal Mo-O distances may indicate that the H atom is located exactly between O(4) and O(6). A peak in the final electron-density difference map can be detected between O6 and O4 with coordinates of x = 0.3125, y = 0.5273, z = 0.3652 which places it almost equidistance from the two oxygens (1.2 and 1.3 Å from O4 and O6, respectively). This result implies that neither ligand can be considered to be the coordinated ethanol molecule, but rather, each ligand exhibits partial characteristics of a coordinated ethanol and ethoxide group.

The formation of alcohol adducts of metal alkoxide compounds is not uncommon. Other examples include $M_2(OPr^i)_8(HOPr^i)_2$ where M = Zr, or Ce [13]. Other molybdenum alkoxides have also shown this alcohol adduct formation. An example is the $Mo_4(OCH_2\text{-c-Bu})_{12}(HOCH_2\text{-c-Bu})$ compound [2]. This cluster exhibits a nearly planar RO-Mo-Mo-O(H)R unit with an average O-O distance of 2.58 Å (from 2 crystallographically independent clusters). However, the two Mo-O distances are unequal (1.97 and 2.34 Å) suggesting that the H atom (not located in the structure) is positioned asymmetrically between the two oxygen atoms. Thus, in this molecule, it is reasonably easy to distinguish the alkoxide ligand as apposed to the coordinated alcohol ligand based on distance and angle arguments. The Mo-Mo distances in this cluster are an average 2.67 Å.

The total number of electrons available for metal-metal bonding in 4 is ten. This accounts for the essentially regular rhomboidal arrangement of molybdenum atoms with nearly equal Mo-Mo bond distances. There are 5 Mo-Mo interactions possible, and each

interaction has 2 electrons available to form a bond. An analogous eight-electron tungsten cluster, $W_4(OEt)_{16}$, has also been synthesized [3]. This compound exhibits a severe distortion of the rhomboid such that two edges of the rhomboid are 0.30 Å longer than the other two. This distortion of the cluster has been attributed to a second-order Jahn-Teller effect [14]. This phenomenon can occur in a symmetric molecule when a low-lying excited state is coupled to the ground state by one of the normal vibrations of the symmetric molecule. This distortion will then take the formation of the vibration which couples the two states. For $W_4(OEt)_{16}$, it has been determined that an A_g ground state is present with a very low-lying state of B_g symmetry. Coupling of these two states would lead to a second-order Jahn-Teller distortion with a b_g normal vibration. This vibration leads to the type of distortion seen in the cluster. Furthermore, it has been shown by Fenske-Hall calculations completed on the model ten electron cluster, $Mo_4(OH)_{16}^{2-}$, that a selective weakening of the edge bonds of the metal framework takes place in preference to a weakening of the central bond. These calculations suggest that the HOMO is involved primarily in peripheral Mo-Mo bond formation. Thus, removing electrons from this orbital to produce an eight electron cluster would not affect the central Mo-Mo bond. It was proposed that if a ten electron cluster of this type were synthesized it should exhibit a regular arrangement of the metal atoms with nearly equal metal-metal bond distances, and this has been found to be the case with 4.

CONCLUSIONS

The isolation of molybdenum ethoxide has been accomplished through the use of the molybdenum-chloride complex, $Mo_2Cl_4py_4$. The procedure to synthesize this starting material is more convenient than the method to isolate $Mo_2(NMe_2)_6$, which is the starting material to produce $Mo(OEt)_3$ isolated by Chisholm et. al. [5]. However, the Mo(II) starting material does not oxidize completely to form the molybdenum(III) ethoxide. Furthermore, the material isolated may be a mixture of materials rather than a single product. The final product, 3, isolated from a reaction of $Mo_2Cl_4py_4$ and NaOEt at higher temperatures, does appear to form from a single intermediate complex determined to be $Mo_4(OEt)_{10}py$. This intermediate is crystalline and can be isolated from a room temperature reaction of $Mo_2Cl_4py_4$ and NaOEt. The fact that this single intermediate product continues to react and form a complicated mixture of products may be a result of the small steric constraints of the ethoxide ligand i.e. the steric requirements of the ethoxide ligands do not limit possible products. It may be that by using a more sterically hindered alcohol, such as tert-butanol, a single product may be isolated. In addition, it seems reasonable to presume that other alcohols should react in a fashion similar to ethanol to produce possibly new molybdenum alkoxides.

The molybdenum ethoxide material, 3, has been used to isolate a novel molybdenum ethoxide cluster, $Mo_4(OEt)_{14}(HOEt)_2$, 4, from a reaction with the oxidizing agent iodosobenzene. This molecule cannot be isolated from a reaction of molybdenum(III) ethoxide with iodosobenzene. 4 is unique because it is the only known molybdenum alkoxide cluster to exhibit this structure type i.e. a planar rhomboid. All

other molybdenum alkoxides of the M_4 type exhibit a butterfly-type structure. An analogous tungsten cluster, $W_4(OEt)_{16}$, has been synthesized which does exhibit the same structure type as 4. However, in the tungsten compound only eight electrons are available for W-W bonding, and the metal framework distorts from a second-order Jahn-Teller effect.

REFERENCES

1. Bradley, D.C.; Mehrotra, R.C.; Gaur, P. Metal Alkoxides; Wiley, New York, 1978. Bradley, D.C. Nature (London), **1958**, 182, 1211. Bradley, D.C. Coord. Chem. Rev. **1967**, 2, 299.
2. Chisholm, M.H.; Cotton, F.A.; Murillo, C.A.; Reichart, W.W. Inorg. Chem. **1977**, 16, 1801.
3. Chisholm, M.H.; Huffman, J.C.; Kirkpatrick, C.C.; Leonelli, J.; Folting, K. J. Amer. Chem. Soc. **1981**, 103, 6093.
4. McCarley, R.E.; Luly, M.H.; Ryan, T.R.; Torardi, C.C. ACS Symp. Ser. **1981**, 155, 41.
5. Chisholm, M.H.; Haitko, D.A.; Murillo, C.A.; In: Inorganic Synthesis, Volume XXI J.P. Fackler, Jr., Ed; John Wiley and Sons, Inc.: New York, 1982; pp. 51-56.
6. Luly, M.H.; McCarley, R.E. Unpublished results.
7. McCarley, R.E.; Templeton, J.L.; Colburn, T.J.; Katovic, V.; Hoxmier, R.J. Adv. Chem. Serv. **1976**, 150, 318.
8. Sheldrick, G.M. In: Crystallographic Computing 3, G.M. Sheldrick; C. Kruger; R. Goddard, Eds.; Oxford University Press, 1985; pp. 175-189.
9. "SDP Structure Analysis Computer Software Package" B.A. Frenz & Associates, Inc., College Station, Texas, 1985.
10. Elwell, W.R.; Wood, D.F. Analytical Chemistry of Molybdenum and Tungsten; Pergamon Press: New York, 1971.

11. Diehl, H.; Smith, G.F. In: Quantitative Analysis; John Wiley and Sons, Inc.: New York, 1952; pp. 270-275.

12. Banks, C.V.; O'Laughlin, J.W. Anal. Chem. **1956**, 28, 1338.

13. Vaartstra, B.A.; Huffman, J.C.; Gradeff, P.S.; Hubert-Pfalzgraf, L.G.; Dara, J.C.; Parraud, S.; Yunlu, K.; Caulton, K.G. Inorg. Chem. **1990**, 29, 3126.

14. Cotton, F.A.; Fang, A. J. Amer. Chem. Soc. **1982**, 104, 113.

GENERAL SUMMARY

The sol-gel method, which has been used to synthesize high purity metal oxides, has proven to be a viable route to the production of reduced molybdenum compounds. When molybdenum(III) ethoxide was hydrolyzed in hydrocarbon solvent at room temperature, $Mo_2(OH)_5(OEt)$ was quantitatively produced. This precursor can be thermally processed in the presence of flowing hydrogen at 250°C to form the mixed oxide-hydroxide species, MoO(OH). This compound, while it cannot smoothly be converted to the pure oxide, does react with alkali metals to produce reduced ternary molybdenum oxides. Na_xMoO_2, where x = 0.66, and $LiMoO_2$ have been synthesized by starting with MoO(OH) at temperatures less than those used in the past and in much shorter periods of time.

Related to this work is the surprising synthesis of the cluster, $Mo_6O(OEt)_{18}$, which formed when molybdenum(III) ethoxide was hydrolyzed with greater than 14 moles of water per mole of $[Mo(OEt)_3]_4$. The structure of this cluster is novel and has not been identified previously. It consists of an octahedron of molybdenum atoms centered with an oxygen atom. The cluster distorts along the 3-fold axis of the octahedron such that two distinct metal-metal bonded trimers can be detected.

Because this compound forms in such small quantities from the given synthetic route, alternate routes to its formation have been explored. Other oxidizing agents, such as iodosobenzene, antimony pentoxide, nitrous oxide, and trimethylamine-N-oxide, have been employed in reactions with molybdenum(III) ethoxide. However, these reagants have failed to reproduce the oxygen-centered cluster.

From these attempts, however, some other new clusters of molybdenum ethoxide have been isolated. A reaction of antimony pentoxide and molybdenum(III) ethoxide has produced the compound, $Mo_6O_x(OH)_{8-x}(OEt)_{10}$, where x is presumed to be 4. This cluster appears to be a non-centered regular octahedron of molybdenum atoms. This type of molybdenum cluster has not been previously observed in the alkoxide compounds of molybdenum or tungsten. When trimethylamine-N-oxide was used in a reaction with molybdenum(III) ethoxide, another new cluster, $Mo_9O_4(OH)_6(OEt)_{22}$ was formed. This compound consists of two planar tetrameric units connected together through a molybdate-type species. Because both of these clusters contain hydroxide ligands, it is certain that adventitious water must be playing a role in their production.

Finally, because the yield of $Mo_2(NMe_2)_6$, which is used to synthesize molybdenum(III) ethoxide, is low when it is made by the published route, a study of another starting material, $Mo_2Cl_4py_4$, to produce $Mo(OEt)_3$ was explored. When the molybdenum-chloride compound, $Mo_2Cl_4py_4$, was used in a reaction with sodium ethoxide in ethanol at room temperature, $Mo_4(OEt)_{10}py$ was formed. This compound appears to convert to a mixture of homoleptic molybdenum ethoxide compounds upon heating in hydrocarbon solvent. This mixture can, however, be used to produce $Mo_4(OEt)_{14}(HOEt)_2$ from a reaction with iodosobenzene. This cluster species, which exhibits a planar rhomboidal arrangement of molybdenum atoms, is again a novel cluster-type for molybdenum alkoxides.

REFERENCES

1. Mazdiyasni, K.S. Cer. Int. 1982, 8, 42.

2. Vidyasagar, K.; Ganaphthi, L.; Gopalakrishnan, J.; Rao, C.N.R. J. Chem. Soc. Chem. Commun. 1986, 449.

3. Vidyasagar, K.; Gopalakrishnan, J.; Rao, C.N.R. J. Solid State Chem. 1985, 58, 29.

4. Vidyasagar, K. ; Gopalakrishnan, J.; Rao, C.N.R. Inorg. Chem. 1984, 23, 1206.

5. Tyszkiewicz, M.T. M.S. Dissertation, Iowa State University, Ames, IA 1987.

6. Chisholm, M.H.; Cotton, F.A.; Murillom C.A.; Reichart, W.W. Inorg. Chem 1977, 16, 1801.

7. Chisholm, M.H.; Haitko, D.A.; Murillo, C.A. In: Inorganic Synthesis, Volume XXI J.P. Fackler, Jr., Ed; John Wiley and Sons, Inc.: New York, 1982; pp. 51-56.

ACKNOWLEDGEMENTS

I would like to acknowledge those people who have been supportive and helpful throughout my graduate studies. First, I would like to thank Dr. R. E. McCarley for guiding and reguiding my research endeavors over the past 4 1/2 years. I would also like to acknowledge my high school chemistry teacher, Terry Holstien. The enthusiasm for chemistry that he instilled in me at the very beginning has continued to inspire me throughout my career.

I would especially like to thank my husband, Rusty, for standing by me no matter how tough it got, and reminding me "I could always work at McDonalds if I wanted to" and to my Mom and Dad, Connie and Ed Shutek, a huge "thank you!!" for everything (I couldn't possibly list it all here).

This work was performed at Ames Laboratory under contract no. W-7405-ENG-82 with the U.S. Department of Energy. The United States government has assigned the DOE report number IS-T-1610 to this thesis.

APPENDIX

Table A-1. Table of complete crystallographic data for $Mo_6O(OEt)_{18} \bullet 4.8H_2O$

Formula	$Mo_6O_{19}C_{36}H_{90}$
Formula weight	1492.82
Space Group	R$\bar{3}$m
a, Å	18.317(5)
c, Å	15.359(3)
V, Å	4463(3)
Z	3
d_{calc}, g/cm^3	1.666
Crystal size, mm	0.10 x 0.15 x 0.15
μ(Mokα), cm^{-1}	12.638
Data collection instrument	Enraf-Nonius CAD4
Radiation (monochromated in incident beam)	MoKα (λ = 0.71073 Å)
Orientation reflections, number, range (2θ)	25, 17.6 < 2θ < 34.4
Temperature, °C	-75(1)
Scan method	θ - 2θ
Data col. range, 2θ, deg	4 - 55
No. unique data, total:	1245
with $F_o^2 > 4\sigma(F_o^2)$	697
No. of parameters refined	86
R^a	0.0311
$R_w{}^b$	0.0391
Quality-of-fit indicator^c	1.023
Largest peak, e/Å^3	0.7

a. $R = \Sigma||F_o| - |F_c||/\Sigma|F_o|$.

b. $R_w = [\Sigma\omega(|F_o| - |F_c|)^2/\Sigma\omega|F_o|^2]^{1/2}$; $\omega = 1/\sigma^2(|F_o|)$.

c. Quality-of-fit = $[\Sigma\omega(|F_o| - |F_c|)^2/(N_{obs} - N_{parameters})]^{1/2}$.

Table A-2. Table of complete crystallographic data for $Mo_9O_4(OH)_6(OEt)_{22}$

Formula	$Mo_9O_{32}C_{44}H_{116}$
Formula weight	2019.46
Space Group	C2/c
a, Å	23.03(1)
b, Å	11.550(6)
c, Å	38.01(3)
β	111.64(6)°
V, Å	9399(14)
Z	6
d_{calc}, g/cm^3	2.142
Crystal size, mm	0.30 x 0.10 x 0.10
μ(Mokα), cm^{-1}	17.843
Data collection instrument	Rigaku AFC6R
Radiation (monochromated in incident beam)	MoKα (λ = 0.71073 Å)
Orientation reflections, number, range (2θ)	14, 12.9 < 2θ < 15.0
Temperature, °C	25
Scan method	ω - 2θ
Data col. range, 2θ, deg	0 - 50
No. unique data, total:	8772
with $F_o^2 > 4\sigma(F_o^2)$	2640
No. of parameters refined	170
Transmission factors	0.7699 - 1.0000
R[a]	0.164
R_w[b]	0.229
Quality-of-fit indicator[c]	5.10
Largest peak, e/Å^3	1.3

a. $R = \Sigma||F_o| - |F_c||/\Sigma|F_o|$.

b. $R_w = [\Sigma\omega(|F_o| - |F_c|)^2/\Sigma\omega|F_o|^2]^{1/2}$; $\omega = 1/\sigma^2(|F_o|)$.

c. Quality-of-fit = $[\Sigma\omega(|F_o| - |F_c|)^2/(N_{obs} - N_{parameters})]^{1/2}$.

Table A-3. Table of fractional atomic positions, number of positions, occupancy and isotropic thermal parameters for $Mo_9O_4(OH)_6(OEt)_{22}$

Atom	No. of Positions	K[a]	x	y	z	B[b]
Mo1	8 f	1	0.0259(4)	0.8227(7)	0.3430(2)	2.9(4)*
Mo2	8 f	1	-0.0725(4)	0.9686(7)	0.3111(2)	3.5(4)*
Mo3	8 f	1	-0.0643(4)	0.8376(7)	0.3725(2)	3.1(4)*
Mo4	8 f	1	0.0346(4)	0.6930(7)	0.4042(2)	4.0(4)*
Mo5	4 e	1	0.000	0.868(1)	0.2500	3.4(5)*
O1	8 f	1	-0.064(3)	0.790(6)	0.317(2)	8(2)
O2	8 f	1	0.028(2)	0.871(4)	0.392(1)	3(1)
O3	8 f	1	0.116(3)	0.830(5)	0.358(2)	5(1)
O4	8 f	1	-0.061(3)	0.656(5)	0.387(2)	5(2)
O5	8 f	1	0.036(2)	0.646(5)	0.348(1)	4(1)
O6	8 f	1	0.132(3)	0.712(5)	0.416(2)	5(1)
O7	8 f	1	0.033(2)	0.784(5)	0.294(1)	4(1)
O8	8 f	1	-0.151(3)	0.807(5)	0.355(2)	5(2)

a. K is the occupancy number.

b. Starred atoms (*) were not refined.

Table A-3. (Continued)

Atom	No. of Positions	K[a]	x	y	z	B[b]
O9	8 f	1	-0.055(3)	0.942(5)	0.255(2)	5(2)
O10	8 f	1	-0.079(3)	1.019(5)	0.359(2)	5(2)
O11	8 f	1	-0.086(3)	1.146(6)	0.301(2)	7(2)
O12	8 f	1	0.047(2)	0.722(4)	0.457(1)	3(1)
O13	8 f	1	0.026(2)	0.994(5)	0.331(1)	4(1)
O14	8 f	1	-0.065	0.888	0.421(2)	6(2)
O15	8 f	1	0.044(3)	0.516(6)	0.416(2)	6(2)
O16	8 f	1	-0.160(3)	0.937(6)	0.286(2)	7(2)
C1	8 f	1	-0.1146	0.6865	0.2952	4*
C2	8 f	1	-0.1136	0.6745	0.2568	4*
C3	8 f	1	0.051(3)	0.980(6)	0.425(2)	2(2)
C4	8 f	1	0.123(4)	0.991(7)	0.437(2)	4(2)
C5	8 f	1	-0.0981	0.5154	0.3520	4*
C6	8 f	1	-0.102(5)	0.55(1)	0.396(3)	9(4)
C7	8 f	1	-0.093(6)	1.14(1)	0.380(3)	9(4)
C8	8 f	1	-0.152(4)	1.171(8)	0.364(2)	4(2)

Table A-3. (Continued)

Atom	No. of Positions	K[a]	x	y	z	B[b]
C10	8 f	1	-0.0843	1.2177	0.2709	4*
C11	8 f	1	0.1114	1.3393	0.2838	4*
C12	8 f	1	-0.257(7)	0.92(1)	0.225(4)	13(5)
C13	8 f	1	-0.207(6)	0.98(1)	0.245(4)	10(4)
C14	8 f	1	0.159(4)	0.837(8)	0.346(2)	4(2)
C15	8 f	1	0.225(5)	0.88(1)	0.361(3)	8(3)
C18	8 f	1	0.033(4)	0.534(8)	0.325(2)	4(2)
C19	8 f	1	0.088(4)	0.521(8)	0.327(2)	5(2)
C20	8 f	1	-0.207(5)	0.87(1)	0.348(3)	2(2)
C21	8 f	1	-0.266(7)	0.78(1)	0.343(4)	7(4)
C22	8 f	1	0.74(7)	1.09(1)	0.339(4)	7(4)
C24	8 f	1	-0.094(7)	0.84(1)	0.455(5)	14(5)
C25	8 f	1	-0.092	0.91(2)	0.479(5)	16(7)

Table A-4. Table of general anisotropic displacement parameters[a] expressed in U's for $Mo_9O_4(OH)_6(OEt)_{22}$

Name	U(1,1)	U(2,2)	U(3,3)	U(1,2)	U(1,3)	U(2,3)
Mo1	0.049(6)	0.030(5)	0.032(5)	-0.002(5)	0.014(5)	-0.006(5)
Mo2	0.069(7)	0.033(5)	0.031(5)	0.011(5)	0.016(5)	0.004(5)
Mo3	0.060(6)	0.038(6)	0.027(5)	-0.008(5)	0.022(5)	-0.001(6)
Mo4	0.069(7)	0.037(6)	0.041(5)	-0.005(5)	0.016(5)	0.003(5)
Mo5	0.048(8)	0.041(8)	0.036(7)	0	0.013(7)	0

a. The form of the anisotropic displacement parameter is: $\exp[-2\pi^2\{h^2a^2U(1,1) + k^2b^2U(2,2) + l^2c^2U(3,3) + 2hkabU(1,2) + 2hlacU(1,3) + 2klbcU(2,3)\}]$ where a, b, and c are reciprocal lattice constants.

Table A-5. Table of complete bond distances in angstroms for $Mo_9O_4(OH)_6(OEt)_{22}$

Atom 1	Atom 2	Distance[a]	Atom 1	Atom 2	Distance[a]
Mo1	Mo2	2.72(1)	Mo4	O6	2.12(6)
Mo1	Mo3	2.71(1)	Mo4	O12	1.94(5)
Mo1	Mo4	2.71(1)	Mo4	O15	2.09(7)
Mo1	O1	1.98(7)	Mo5	O7	1.85(5)
Mo1	O2	1.92(5)	Mo5	O9	1.61(6)
Mo1	O3	1.94(6)	O1	C1	1.65(7)
Mo1	O5	2.06(5)	O2	C3	1.72(8)
Mo1	O7	1.96(5)	O3	C14	1.23(9)
Mo1	O13	2.03(6)	O4	C6	1.6(1)
Mo2	Mo3	2.73(1)	O5	C18	1.54(9)
Mo2	O1	2.08(7)	O8	C20	1.4(1)
Mo2	O9	2.31(6)	O10	C7	1.7(1)
Mo2	O10	1.96(6)	O11	C10	1.44(7)
Mo2	O11	2.08(7)	O13	C22	1.5(2)
Mo2	O13	1.92(7)	O14	C24	1.7(2)
Mo2	O16	1.92(7)	O16	C13	1.6(1)
Mo3	Mo4	2.72(1)	O14	C24	1.7(2)
Mo3	O1	2.20(7)	O16	C13	1.6(1)
Mo3	O2	2.02(5)	C1	C2	1.4746(9)
Mo3	O4	2.17(6)	C3	C4	1.55(9)
Mo3	O8	1.90(6)	C5	C6	1.8(1)
Mo3	O10	2.15(6)	C7	C8	1.3(1)
Mo3	O14	1.96(6)	C10	C11	1.681(1)

a. Numbers in parentheses are estimated standard deviations in the least significant digits.

Table A-5. (Continued)

Atoms 1	Atoms 2	Distance[a]	Atom 1	Atom 2	Distance[a]
Mo4	O2	2.11(5)	C12	C13	1.4(2)
Mo4	O4	2.10(6)	C14	C15	1.5(1)
Mo4	O5	2.23(5)	C18	C19	1.3(1)
C20	C21	1.6(2)	C24	C25	1.2(2)

Table A-6. Table of complete bond angles in degrees for $Mo_9O_4(OH)_6(OEt)_{22}$

Atom 1	Atom 2	Atom 3	Angle [a]	Atom 1	Atom 2	Atom 3	Angle [a]
MO2	MO1	MO3	60.4(3)	O2	MO1	O3	93(2)
MO2	MO1	MO4	120.7(4)	O2	MO1	O5	104(2)
MO2	MO1	O1	49(2)	O2	MO1	O7	173(2)
MO2	MO1	O2	88(2)	O2	MO1	O13	86(2)
MO2	MO1	O3	137(2)	O3	MO1	O5	87(2)
MO2	MO1	O5	135(1)	O3	MO1	O7	81(2)
MO2	MO1	O7	94(2)	O3	MO1	O13	86(2)
MO2	MO1	O13	51(2)	O5	MO1	O7	79(2)
MO3	MO1	MO4	60.3(3)	O5	MO1	O13	168(2)
MO3	MO1	O1	53(2)	O7	MO1	O13	90(2)
MO3	MO1	O2	48(1)	MO1	MO2	MO3	59.5(3)
MO3	MO1	O3	141(2)	MO1	MO2	O1	46(2)
MO3	MO1	O5	96(1)	MO1	MO2	O9	86(1)
MO3	MO1	O7	138(2)	MO1	MO2	O10	96(2)
MO3	MO1	O13	96(2)	MO1	MO2	O11	137(2)
MO4	MO1	O1	93(2)	MO1	MO2	O13	48(1)
MO4	MO1	O2	51(2	MO1	MO2	O16	131(2)
MO4	MO1	O3	92()	MO3	MO2	O1	52(2)
MO4	MO1	O5	541)	MO3	MO2	O9	137(1)
MO4	MO1	O7	133(2)	MO3	MO2	O10	51(2)
MO4	MO1	O13	137(2)	MO3	MO2	O11	131(2)
O1	MO1	O2	101(2)	MO3	MO2	O13	93(1)
O1	MO1	O3	165(3)	MO3	MO2	O16	93(2)
O1	MO1	O5	85(2)	O1	MO2	O9	85(2)
O1	MO1	O7	85(3)	O1	MO2	O10	104(3)
O1	MO1	O13	99(3)	O1	MO2	O11	176(3)

a. Angles are in degrees. Estimated standard deviations in the least significant figure are given in parentheses.

Table A-6. (Continued)

Atom 1	Atom 2	Atom 3	Angle [a]	Atom 1	Atom 2	Atom 3	Angle [a]
O1	MO2	O13	93(2)	MO2	MO3	O14	129(2)
O1	MO2	O16	84(3)	MO4	MO3	O1	88(2)
O9	MO2	O10	170(2)	MO4	MO3	O2	50(1)
O9	MO2	O11	92(2)	MO4	MO3	O4	49(2)
O9	MO2	O13	80(2)	MO4	MO3	O8	130(2)
O9	MO2	O16	91(2)	MO4	MO3	O10	138(2)
O10	MO2	O11	79(2)	MO4	MO3	O14	94(2)
O10	MO2	O13	94(2)	O1	MO3	O2	91(2)
O10	MO2	O16	95(3)	O1	MO3	O4	89(2)
O11	MO2	O13	90(2)	O1	MO3	O8	89(2)
O11	MO2	O16	92(3)	O1	MO3	O10	94(2)
O13	MO2	O16	171(3)	O1	MO3	O14	177(3)
MO1	MO3	MO2	60.1(3)	O2	MO3	O4	99(2)
MO1	MO3	MO4	60.0(3)	O2	MO3	O8	180(2)
MO1	MO3	O1	46(2)	O2	MO3	O10	87(2)
MO1	MO3	O2	45(1)	O2	MO3	O14	89(2)
MO1	MO3	O4	95(2)	O4	MO3	O8	81(2)
MO1	MO3	O8	135(2)	O4	MO3	O10	173(2)
MO1	MO3	O10	92(2)	O4	MO3	O14	94(2)
MO1	MO3	O14	134(2)	O8	MO3	O10	92(2)
MO2	MO3	MO4	120.1(4)	O8	MO3	O14	91(2)
MO2	MO3	O1	48(2)	O10	MO3	O14	84(2)
MO2	MO3	O2	86(1)	MO1	MO4	MO3	59.8(3)
MO2	MO3	O4	137(2)	MO1	MO4	O2	45(1)
MO2	MO3	O8	94(2)	MO1	MO4	O4	96(2)
MO2	MO3	O10	45(2)	MO1	MO4	O5	48(1)

Table A-6. (Continued)

Atom 1	Atom 2	Atom 3	Angle[a]	Atom 1	Atom 2	Atom 3	Angle[a]
MO1	MO4	O6	82(2)	O7	MO5	O9	108(3)
MO1	MO4	O12	136(2)	O7	MO5	O9	108(3)
MO1	MO4	O15	134(2)	O7	MO5	O9	104(3)
MO3	MO4	O2	47(1)	O9	MO5	O9	116(4)
MO3	MO4	O4	51(2)	MO1	O1	MO2	84(3)
MO3	MO4	O5	92(1)	MO1	O1	MO3	81(2)
MO3	MO4	O6	132(2)	MO1	O1	C1	143(4)
MO3	MO4	O12	97(2)	MO2	O1	MO	79(2)
MO3	MO4	O15	135(2)	MO2	O1	C1	130(4)
O2	MO4	O4	99(2)	MO3	O1	C1	114(4)
O2	MO4	O5	93(2)	MO1	O2	MO3	87(2)
O2	MO4	O6	86(2)	MO1	O2	MO4	85(2)
O2	MO4	O12	92(2)	MO1	O2	C3	145(4)
O2	MO4	O15	178(2)	MO3	O2	MO4	82(2)
O4	MO4	O5	92(2)	MO3	O2	C3	113(4)
O4	MO4	O6	172(2)	MO4	O2	C3	124(4)
O4	MO4	O12	96(2)	MO1	O3	C14	144(6)
O4	MO4	O15	83(2)	MO3	O4	MO4	79(2)
O5	MO4	O6	81(2)	MO3	O4	C6	142(5)
O5	MO4	O12	170(2)	MO4	O4	C6	135(5)
O5	MO4	O15	86(2)	MO1	O5	MO4	78(2)
O6	MO4	O12	91(2)	MO1	O5	C18	144(5)
O6	MO4	O15	92(2)	MO4	O5	C18	137(5)
O12	MO4	O15	89(2)	MO1	O7	MO5	126(3)
O7	MO5	O7	117(3)	MO3	O8	C20	138(6)
O7	MO5	O9	104(3)	MO2	O9	MO1	127(3)

Table A-6. (Continued)

Atom 1	Atom 2	Atom 3	Angle[a]	Atom 1	Atom 2	Atom 3	Angle[a]
MO2	O10	MO3	83(2)				
MO2	O10	C7	140(5)				
MO3	O10	C7	137(5)				
MO2	O11	C10	132(4)				
MO1	O13	MO2	82(2)				
MO1	O13	C22	137(7)				
MO2	O13	C22	140(7)				
MO3	O14	C24	138(7)				
MO2	O16	C13	128(6)				
O1	C1	C2	107(2)				
O2	C3	C4	106(5)				
O4	C6	C5	74(5)				
O10	C7	C8	109(10)				
O11	C10	C11	97(3)				
O16	C13	C12	117(12)				
O3	C14	C15	136(9)				
O5	C18	C19	103(8)				
O8	C20	C21	112(10)				
O14	C24	C25	116(16)				

Table A-7. Table of complete crystallographic data for $Mo_6O_4(OH)_4(OEt)_{10}$

Formula	$Mo_6O_{18}C_{20}H_{54}$
Formula weight	1158.28
Space Group	PT
a, Å	12.215(3)
b, Å	12.215(3)
c, Å	11.572(7)
α	108.4(1)°
β	108.4(1)°
γ	110.5(1)°
V, Å	1346(3)
Z	1
d_{calc}, g/cm^3	1.429
Crystal size, mm	0.10 x 0.20 x 0.15
μ(Mokα), cm^{-1}	13.7
Data collection instrument	Enraf-Nonius CAD4
Radiation (monochromated in incident beam)	MoKα (λ = 0.71073 Å)
Orientation reflections, number, range (2θ)	25, 17.6 < 2θ < 31.4
Temperature, °C	25
Scan method	θ - 2θ
Data col. range, 2θ, deg	4 - 50
No. unique data, total:	4438
with $F_o^2 > 4\sigma(F_o^2)$	2060
No. of parameters refined	190
Correction factors (numerical)	0.702 - 1.142
R[a]	0.0570
R_w[b]	0.0800
Quality-of-fit indicator[c]	2.012
Largest peak, e/Å^3	1.1

a. $R = \Sigma||F_o| - |F_c||/\Sigma|F_o|$.

b. $R_w = [\Sigma\omega(|F_o| - |F_c|)^2/\Sigma\omega|F_o|^2]^{1/2}$; $\omega = 1/\sigma^2(|F_o|)$.

c. Quality-of-fit = $[\Sigma\omega(|F_o| - |F_c|)^2/(N_{obs} - N_{parameters})]^{1/2}$.

Table A-8. Table of fractional atomic positions, number of positions, occupancy and isotropic thermal parameters for $Mo_6O_4(OH)_4(OEt)_{10}$

Atom	No. of Positions	K[a]	x	y	z	B[b]
Mo1	2 i	1	0.0603(1)	0.1590(1)	0.1710(1)	7.14(4)
Mo2	2 i	1	0.1589(1)	0.0987(1)	-0.0121(1)	7.14(4)
Mo3	2 i	1	0.0988(1)	-0.0602(1)	0.1108(1)	7.15(4)
O1	2 i	1	-0.0424(8)	0.2227(7)	0.0610(9)	8.5(3)
O2	2 i	1	0.1617(8)	0.1005(8)	0.2901(8)	8.1(3)
O3	2 i	1	0.2650(7)	0.0418(7)	0.1033(9)	8.3(3)
O4	2 i	1	0.2219(8)	0.2644(8)	0.1615(9)	8.4(3)
O5	2 i	1	-0.1001(7)	0.0621(8)	0.1895(8)	7.8(3)
O6	2 i	1	-0.0606(8)	-0.1621(7)	0.1277(8)	7.9(3)
O7	2 i	1	0.1233(9)	0.3229(9)	0.3438(9)	10.9(4)
O8	2 i	1	0.3230(8)	0.1998(9)	-0.0205(9)	11.4(4)
O9	2 i	1	0.1987(9)	-0.1239(8)	0.220(1)	11.3(4)
C1	2 i	0.5	0.007(3)	0.371(3)	0.113(4)	13(1)*
C2	2 i	0.5	-0.105(3)	0.371(3)	0.113(4)	14(1)*
C3	2 i	0.33	0.292(3)	0.182(3)	0.415(4)	8(1)*

a. K is the occupancy number of the atomic position.

b. Temperature factors were not refined for atoms marked with #. Starred atoms (*) were refined isotropcally.

Table A-8. (Continued)

Atom	No. of Positions	K[a]	x	y	z	B[b]
C3*	2 i	0.32	0.169(4)	0.097(4)	0.419(4)	8(1)*
C4	2 i	0.65	0.287(3)	0.168(3)	0.519(3)	13(1)*
C5	2 i	0.5	0.369(3)	0.0007(3)	0.108(3)	13(1)*
C6	2 i	0.5	0.470(3)	0.099(3)	0.210(4)	13(1)*
C7	2 i	0.5	0.366(3)	0.377(3)	0.266(4)	14(1)*
C8	2 i	0.5	0.361(4)	0.471(4)	0.254(4)	14(1)*
C9	2 i	0.33	-0.106(4)	0.66(4)	0.314(4)	9(1)*
C9*	2 i	0.32	-0.182(3)	0.110(3)	0.233(3)	6.8(9)*
C10	2 i	0.65	-0.168(3)	0.129(3)	0.350(3)	14(1)*
C11	2 i	0.37	-0.106(3)	-0.289(3)	0.127(3)	9(1)*
C11*	2 i	0.28	-0.0663(4)	-0.166(4)	0.254(5)	8(1)*
C12	2 i	0.65	-0.121(2)	-0.285(3)	0.234(3)	12.8(9)*
C13	2 i	0.5	0.207(3)	0.519(3)	0.53693)	10.6(9)*
C14	2 i	0.5	0.517(3)	0.314(3)	-0.017(3)	10.7(9)*
C15	2 i	0.5	0.0309(3)	-0.207(3)	0.332(3)	10.4(9)*
C16	2 i	0.5	0.151(3)	0.400(3)	0.446(3)	10.0#
C17	2 i	0.5	0.250(3)	-0.146(3)	0.297(3)	10.0#
C18	2 i	0.5	0.597(3)	0.750(3)	0.041(3)	10.0#

Table A-9. Table of general anisotropic displacement parameters[a] expressed in U's for $Mo_6O_4(OH)_4(OEt)_{10}$

Name	U(1,1)	U(2,2)	U(3,3)	U(1,2)	U(1,3)	U(2,3)
Mo1	0.0949(5)	0.0842(5)	0.0860(6)	0.0448(4)	0.0430(5)	0.0338(5)
Mo2	0.0844(5)	0.0898(5)	0.0979(6)	0.0392(4)	0.0478(4)	0.0467(4)
Mo3	0.0898(5)	0.0947(5)	0.0914(6)	0.0504(4)	0.0394(5)	0.0485(4)
O1	0.126(4)	0.088(3)	0.127(5)	0.066(3)	0.064(4)	0.055(3)
O2	0.099(4)	0.121(4)	0.081(4)	0.058(3)	0.035(3)	0.047(3)
O3	0.086(3)	0.117(4)	0.127(5)	0.061(3)	0.054(3)	0.059(4)
O4	0.090(4)	0.087(4)	0.107(5)	0.027(4)	0.039(4)	0.035(4)
O5	0.111(4)	0.108(4)	0.096(4)	0.059(3)	0.065(3)	0.047(3)
O6	0.104(4)	0.104(4)	0.107(4)	0.048(3)	0.054(3)	0.067(3)
O7	0.152(6)	0.114(6)	0.095(6)	0.060(4)	0.055(4)	0.006(5)
O8	0.120(4)	0.163(6)	0.200(6)	0.063(4)	0.113(4)	0.113(4)
O9	0.144(6)	0.163(5)	0.137(6)	0.092(4)	0.040(5)	0.097(4)

a. The form of the anisotropic displacement parameter is:
$\exp[-2\pi^2\{h^2a^2U(1,1) + k^2b^2U(2,2) + l^2c^2U(3,3) + 2hkabU(1,2) + 2hlacU(1,3) + 2klbcU(2,3)\}]$ where a,b, and c are reciprocal lattice constants.

Table A-10. Table of complete bond distances in angstroms for $Mo_6O_4(OH)_4(OEt)_{10}$

Atom 1	Atom 2	Distance[a]	Atom 1	Atom 2	Distance[a]
Mo1	Mo2	2.781(1)	O3	C5	1.46(3)
Mo1	Mo2	2.791(1)	O4	C7	1.53(3)
Mo1	Mo3	2.791(1)	O5	C9	1.45(4)
Mo1	Mo3	2.782(1)	O5	C9*	1.46(3)
Mo1	O1	2.025(7)	O6	C11	1.45(3)
Mo1	O2	2.027(7)	O6	C11*	1.48(4)
Mo1	O4	2.003(7)	O7	C16	1.10(3)
Mo1	O5	2.020(7)	O8	C17	1.09(3)
Mo1	O7	2.004(7)	O9	C18	1.09(3)
Mo2	Mo3	2.781(1)	C1	C2	1.27(4)
Mo2	Mo3	2.791(1)	C3	C3*	1.52(4)
Mo2	O3	2.017(7)	C3	C4	1.29(3)
Mo2	O4	2.022(7)	C3*	C4	1.27(4)
Mo2	O5	2.030(7)	C5	C6	1.21(4)
Mo2	O6	2.030(7)	C7	C8	1.21(4)
Mo2	O8	2.003(7)	C9	C9*	1.47(4)
Mo3	O1	2.013(7)	C9	C10	1.26(4)
Mo3	O2	2.028(7)	C9*	C10	1.28(3)
Mo3	O3	2.022(7)	C11	C11*	1.50(5)
Mo3	O6	2.018(6)	C11	C12	1.30(3)
Mo3	O9	1.999(8)	C11*	C12	1.28(4)
O1	C1	1.53(3)	C13	C16	1.25(3)
O2	C3	1.46(3)	C14	C17	1.22(3)
O2	C3*	1.47(4)	C15	C18	1.26(3)

a. Numbers in parentheses are estimated standard deviations in the least significant digits.

Table A-11. Table of complete bond angles in degrees for $Mo_6O_4(OH)_4(OEt)_{10}$

Atom 1	Atom 2	Atom 3	Angle[a]	Atom 1	Atom 2	Atom 3	Angle[a]
Mo2	Mo1	Mo2	89.99(4)	Mo3	Mo1	O7	134.4(3)
Mo2	Mo1	Mo3	59.88(3)	O1	Mo1	O2	176.8(3)
Mo2	Mo1	Mo3	60.22(3)	O1	Mo1	O4	90.2(3)
Mo2	Mo1	O1	91.7(2)	O1	Mo1	O5	89.4(3)
Mo2	Mo1	O2	91.3(2)	O1	Mo1	O7	88.2(3)
Mo2	Mo1	O4	46.6(2)	O2	Mo1	O4	91.3(3)
Mo2	Mo1	O5	136.6(2)	O2	Mo1	O5	89.0(3)
Mo2	Mo1	O7	134.0(2)	O2	Mo1	O7	89.1(3)
Mo2	Mo1	Mo3	60.00(3)	O4	Mo1	O5	176.8(3)
Mo2	Mo1	Mo3	59.88(3)	O4	Mo1	O7	87.4(3)
Mo2	Mo1	O1	90.2(2)	O5	Mo1	O7	89.4(3)
Mo2	Mo1	O2	90.7(2)	Mo1	Mo2	Mo1	90.01(4)
Mo2	Mo1	O4	136.6(2)	Mo1	Mo2	Mo3	60.23(3)
Mo2	Mo1	O5	46.6(2)	Mo1	Mo2	Mo3	59.89(3)
Mo2	Mo1	O7	136.0(2)	Mo1	Mo2	O3	90.8(2)
Mo3	Mo1	Mo3	90.00(4)	Mo1	Mo2	O4	46.0(2)
Mo3	Mo1	O1	136.3(2)	Mo1	Mo2	O5	136.3(2)
Mo3	Mo1	O2	46.5(2)	Mo1	Mo2	O6	90.9(2)
Mo3	Mo1	O4	91.6(2)	Mo1	Mo2	O8	134.3(3)
Mo3	Mo1	O5	90.9(2)	Mo1	Mo2	Mo3	59.90(3)
Mo3	Mo1	O7	135.6(3)	Mo1	Mo2	Mo3	60.01(3)
Mo3	Mo1	O1	46.3(2)	Mo1	Mo2	O3	91.6(2)
Mo3	Mo1	O2	136.5(2)	Mo1	Mo2	O4	136.0(2)
Mo3	Mo1	O4	90.7(2)	Mo1	Mo2	O5	46.3(2)
Mo3	Mo1	O5	91.2(2)	Mo1	Mo2	O6	90.7(2)

a. Numbers in parentheses are estimated standard deviations in the least significant digits.

Table A-11. (Continued)

Atom 1	Atom 2	Atom 3	Angle[a]	Atom 1	Atom 2	Atom 3	Angle[a]
O1	Mo3	O6	91.0(3)	Mo1	O5	C9*	130.(1)
O1	Mo3	O9	87.1(3)	Mo2	O5	C9	128.(1)
O2	Mo3	O3	89.7(2)	Mo2	O5	C9*	128.(1)
O2	Mo3	O6	89.1(2)	C9	O5	C9*	61.(2)
O2	Mo3	O9	89.8(4)	Mo2	O6	Mo3	87.2(2)
O3	Mo3	O6	176.8(3)	Mo2	O6	C11	130.(1)
O3	Mo3	O9	88.2(4)	Mo2	O6	C11*	127.(2)
O6	Mo3	O9	88.8(4)	Mo3	O6	C11	129.(1)
Mo1	O1	Mo3	87.1(2)	Mo3	O6	C11*	128.(2)
Mo1	O1	C1	127.(1)	C11	O6	C11*	62.(2)
Mo3	O1	C1	136.(1)	Mo1	O7	C16	170.(2)
Mo1	O2	Mo3	87.0(3)	Mo2	O8	C17	172.(2)
Mo1	O2	C3	129.(1)	Mo3	O9	C18	167.(2)
Mo1	O2	C3*	131.(1)	O1	C1	C2	103.(3)
Mo3	O2	C3	129.(1)	O2	C3	C3*	59.(2)
Mo3	O2	C3*	125.(1)	O2	C3	C4	112.(3)
C3	O2	C3*	62.(2)	C3*	C3	C4	53.(2)
Mo2	O3	Mo3	87.0(2)	O2	C3*	C3	58.(2)
Mo2	O3	C5	137.(1)	O2	C3*	C4	113.(3)
Mo3	O3	C5	126.(1)	C3	C3*	C4	54.(2)
Mo1	O4	Mo2	87.4(3)	C3	C4	C3*	73.(3)
Mo1	O4	C7	137.(1)	O3	C5	C6	106.(3)
Mo2	O4	C7	128.(1)	O4	C7	C8	101.(3)
Mo1	O5	Mo2	87.1(3)	O5	C9	C9*	60.(2)
Mo1	O5	C9	128.(1)	O5	C9	C10	115.(3)

Table A-11. (Continued)

Atom 1	Atom 2	Atom 3	Angle[a]	Atom 1	Atom 2	Atom 3	Angle[a]
Mo1	Mo2	O8	135.7(3)	Mo1	Mo3	O1	136.6(2)
Mo3	Mo2	Mo3	90.01(4)	Mo1	Mo3	O2	46.5(2)
Mo3	Mo2	O3	46.6(2)	Mo1	Mo3	O3	90.4(2)
Mo3	Mo2	O4	91.5(2)	Mo1	Mo3	O6	90.9(2)
Mo3	Mo2	O5	91.0(2)	Mo1	Mo3	O9	136.2(3)
Mo3	Mo2	O6	136.3(2)	Mo1	Mo3	Mo2	60.22(3)
Mo3	Mo2	O8	133.9(3)	Mo1	Mo3	Mo2	59.88(3)
Mo3	Mo2	O3	136.6(2)	Mo1	Mo3	O1	46.6(2)
Mo3	Mo2	O4	90.1(2)	Mo1	Mo3	O2	136.5(2)
Mo3	Mo2	O5	90.7(2)	Mo1	Mo3	O3	91.7(2)
Mo3	Mo2	O6	46.2(2)	Mo1	Mo3	O6	91.2(2)
Mo3	Mo2	O8	136.1(3)	Mo1	Mo3	O9	133.8(3)
O3	Mo2	O4	90.2(3)	Mo2	Mo3	Mo2	89.99(4)
O3	Mo2	O5	91.0(3)	Mo2	Mo3	O1	90.7(2)
O3	Mo2	O6	177.2(3)	Mo2	Mo3	O2	91.3(2)
O3	Mo2	O8	87.3(3)	Mo2	Mo3	O3	46.4(2)
O4	Mo2	O5	177.3(3)	Mo2	Mo3	O6	136.6(2)
O4	Mo2	O6	89.3(3)	Mo2	Mo3	O9	134.6(3)
O4	Mo2	O8	88.3(3)	Mo2	Mo3	O1	91.7(2)
O5	Mo2	O6	89.3(3)	Mo2	Mo3	O2	90.6(2)
O5	Mo2	O8	89.4(3)	Mo2	Mo3	O3	136.4(2)
O6	Mo2	O8	89.9(3)	Mo2	Mo3	O6	46.6(2)
Mo1	Mo3	Mo1	90.00(4)	Mo2	Mo3	O9	135.4(3)
Mo1	Mo3	Mo2	59.89(3)	O1	Mo3	O2	176.9(3)
Mo1	Mo3	Mo2	59.99(3)	O1	Mo3	O3	90.1(3)

Table A-11. (Continued)

Atom 1	Atom 2	Atom 3	Angle[a]	Atom 1	Atom 2	Atom 3	Angle[a]
C9*	C9	C10	55.(2)	O6	C11*	C11	58.(2)
O5	C9*	C9	59.(2)	O6	C11*	C12	112.(3)
O5	C9*	C10	113.(2)	C11	C11*	C12	55.(2)
C9	C9*	C10	54.(2)	C11	C12	C11*	72.(3)
C9	C10	C9*	71.(3)	O7	C16	C13	152.(3)
O6	C11	C11*	60.(2)	O9	C18	C15	151.(3)
O6	C11	C12	113.(2)	O8	C17	C14	157.(3)
C11*	C11	C12	54.(2)				

Table A-12. Table of complete crystallographic data for $Mo_4(OEt)_{14}(HOEt)_2$

Formula	$Mo_4O_{16}C_{32}H_{82}$
Formula weight	1104.74
Space Group	$P2_1/n$
a, Å	13.084(2)
b, Å	9.712(1)
c, Å	18.213(3)
β	90.44(1)°
V, Å	2314.2
Z	2
d_{calc}, g/cm^3	1.585
Crystal size, mm	0.10 x 0.10 x 0.15
μ(Mokα), cm^{-1}	10.913
Data collection instrument	Enraf-Nonius CAD4
Radiation (monochromated in incident beam)	MoKα (λ = 0.71073 Å)
Orientation reflections, number, range (2θ)	22, 16.7 < 2θ < 31.9
Temperature, °C	-75(1)
Scan method	θ - 2θ
Data col. range, 2θ, deg	4 - 45
No. unique data, total:	3018
with $F_o^2 > 4\sigma(F_o^2)$	1942
No. of parameters refined	233
Transmission factors	0.8787 - 0.9969
R[a]	0.026
R_w[b]	0.033
Quality-of-fit indicator[c]	0.883
Largest peak, e/Å^3	0.46

a. $R = \Sigma||F_o| - |F_c||/\Sigma|F_o|$.

b. $R_w = [\Sigma\omega(|F_o| - |F_c|)^2/\Sigma\omega|F_o|^2]^{1/2}$; $\omega = 1/\sigma^2(|F_o|)$.

c. Quality-of-fit = $[\Sigma\omega(|F_o| - |F_c|)^2/(N_{obs} - N_{parameters})]^{1/2}$.

Table A-13. Table of complete bond distances in angstroms for $Mo_4(OEt)_{14}(HOEt)_2$

Atom 1	Atom 2	Distance[a]	Atom 1	Atom 2	Distance[a]
Mo(1)	Mo'(1)	2.685(1)	O(2)	C(3)'	1.48(2)
Mo(1)	Mo(2)	2.6862(7)	O(3)	C(5)	1.433(7)
Mo(1)	Mo'(2)	2.7306(7)	O(4)	C(7)	1.433(8)
Mo(1)	O(1)	2.100(4)	O(5)	C(9)	1.396(8)
Mo(1)	O'(1)	2.131(4)	O(6)	C(11)	1.426(8)
Mo(1)	O(2)	2.044(4)	O(7)	C(13)	1.423(8)
Mo(1)	O(3)	2.053(4)	O(8)	C(15)	1.380(8)
Mo(1)	O(4)	2.106(4)	C(1)	C(2)	1.505(9)
Mo(1)	O(5)	1.982(4)	C(3)	C(4)	1.53(2)
Mo(2)	O(1)	2.136(4)	C(3)'	C(4)'	1.49(2)
Mo(2)	O(2)	2.012(4)	C(4)	C(4)'	1.49(2)
Mo(2)	O(3)	2.008(4)	C(5)	C(6)	1.505(9)
Mo(2)	O(6)	2.106(4)	C(7)	C(8)	1.52(1)
Mo(2)	O(7)	1.910(4)	C(9)	C(10)	1.48(1)
Mo(2)	O(8)	1.984(4)	C(11)	C(12)	1.47(1)
O(1)	C(1)	1.439(7)	C(13)	C(14)	1.50(1)
O(2)	C(3)	1.43(1)	C(15)	C(16)	1.48(1)

a. Numbers in parentheses are estimated standard deviations in the least significant digits.

Table A-14. Table of complete bond angles in degrees for $Mo_4(OEt)_{14}(HOEt)_4$

Atom 1	Atom 2	Atom 3	Angle[a]	Atom 1	Atom 2	Atom 3	Angle[a]
Mo'(1)	Mo(1)	Mo(2)	61.11(2)	O(1)	Mo(1)	O(5)	88.7(2)
Mo'(1)	Mo(1)	Mo'(2)	59.47(2)	O'(1)	Mo(1)	O(2)	88.4(2)
Mo'(1)	Mo(1)	O(1)	51.1(1)	O'(1)	Mo(1)	O(3)	97.2(2)
Mo'(1)	Mo(1)	O'(1)	50.1(1)	O'(1)	Mo(1)	O(4)	80.0(2)
Mo'(1)	Mo(1)	O(2)	95.5(1)	O'(1)	Mo(1)	O(5)	169.5(2)
Mo'(1)	Mo(1)	O(3)	90.6(1)	O(2)	Mo(1)	O(3)	173.5(2)
Mo'(1)	Mo(1)	O(4)	129.7(1)	O(2)	Mo(1)	O(4)	87.8(2)
Mo'(1)	Mo(1)	O(5)	139.8(1)	O(2)	Mo(1)	O(5)	93.3(2)
Mo(2)	Mo(1)	Mo'(2)	120.58(2)	O(3)	Mo(1)	O(4)	90.1(2)
Mo(2)	Mo(1)	O(1)	51.3(1)	O(3)	Mo(1)	O(5)	80.6(2)
Mo(2)	Mo(1)	O'(1)	90.5(1)	O(4)	Mo(1)	O(5)	89.8(2)
Mo(2)	Mo(1)	O(2)	48.0(1)	Mo(1)	Mo(2)	Mo'(1)	59.42(2)
Mo(2)	Mo(1)	O(3)	134.7(1)	Mo(1)	Mo(2)	O(1)	50.0(1)
Mo(2)	Mo(1)	O(4)	135.2(1)	Mo(1)	Mo(2)	O(2)	49.0(1)
Mo(2)	Mo(1)	O(5)	98.3(1)	Mo(1)	Mo(2)	O(3)	91.6(1)
Mo'(2)	Mo(1)	O(1)	89.9(1)	Mo(1)	Mo(2)	O(6)	134.5(1)
Mo'(2)	Mo(1)	O'(1)	50.3(1)	Mo(1)	Mo(2)	O(7)	99.0(1)
Mo'(2)	Mo(1)	O(2)	138.7(1)	Mo(1)	Mo(2)	O(8)	130.7(1)
Mo'(2)	Mo(1)	O(3)	47.1(1)	Mo'(1)	Mo(2)	O(1)	50.1(1)
Mo'(2)	Mo(1)	O(4)	86.0(1)	Mo'(1)	Mo(2)	O(2)	94.8(1)
Mo'(2)	Mo(1)	O(5)	127.4(1)	Mo'(1)	Mo(2)	O(3)	48.5(1)
O(1)	Mo(1)	O'(1)	101.2(1)	Mo'(1)	Mo(2)	O(6)	83.5(1)
O(1)	Mo(1)	O(2)	98.6(2)	Mo'(1)	Mo(2)	O(7)	132.7(1)
O(1)	Mo(1)	O(3)	83.5(2)	Mo'(1)	Mo(2)	O(8)	136.0(1)
O(1)	Mo(1)	O(4)	173.5(2)	O(1)	Mo(2)	O(2)	98.4(2)

a. Numbers in parentheses are estimated standard deviations in the least significant digits.

Table A-14. (Continued)

Atom 1	Atom 2	Atom 3	Angle[a]	Atom 1	Atom 2	Atom 3	Angle[a]
O(1)	Mo(2)	O(3)	98.4(2)	Mo(2)	O(2)	C(3)	130.6(5)
O(1)	Mo(2)	O(6)	86.7(2)	Mo(2)	O(2)	C(3)'	134.4(6)
O(1)	Mo(2)	O(7)	83.2(2)	C(3)	O(2)	C(3)'	35.4(6)
O(1)	Mo(2)	O(8)	173.9(2)	Mo(1)	O(3)	Mo(2)	84.5(2)
O(2)	Mo(2)	O(3)	92.4(2)	Mo(1)	O(3)	C(5)	135.4(4)
O(2)	Mo(2)	O(6)	171.9(2)	Mo(2)	O(3)	C(5)	139.7(4)
O(2)	Mo(2)	O(7)	99.8(2)	Mo(1)	O(4)	C(7)	127.8(4)
O(2)	Mo(2)	O(8)	81.7(2)	Mo(1)	O(5)	C(9)	134.7(4)
O(3)	Mo(2)	O(6)	80.5(2)	Mo(2)	O(6)	C(11)	130.1(4)
O(3)	Mo(2)	O(7)	167.3(2)	Mo(2)	O(7)	C(13)	128.6(5)
O(3)	Mo(2)	O(8)	87.7(2)	Mo(2)	O(8)	C(15)	132.2(4)
O(6)	Mo(2)	O(7)	87.1(2)	O(1)	C(1)	C(2)	113.7(6)
O(6)	Mo(2)	O(8)	94.0(2)	O(2)	C(3)	C(4)	109.(1)
O(7)	Mo(2)	O(8)	90.8(1)	O(2)	C(3)'	C(4)'	111.(1)
Mo(1)	O(1)	Mo(1)	78.8(2)	C(3)	C(4)	C(4)'	39.3(8)
Mo(1)	O(1)	Mo(2)	78.7(1)	C(3)'	C(4)'	C(4)	37.6(9)
Mo(1)	O(1)	C(1)	122.8(4)	O(3)	C(5)	C(6)	112.3(6)
Mo(1)	O(1)	Mo(2)	79.6(1)	O(4)	C(7)	C(8)	110.1(6)
Mo(1)	O(1)	C(1)	139.0(4)	O(5)	C(9)	C(10)	111.4(6)
Mo(2)	O(1)	C(1)	134.8(4)	O(6)	C(11)	C(12)	111.7(7)
Mo(1)	O(2)	Mo(2)	82.9(1)	O(7)	C(13)	C(14)	109.8(7)
Mo(1)	O(2)	C(3)	137.6(5)	O(8)	C(15)	C(16)	110.6(6)
Mo(1)	O(2)	C(3)'	139.1(7)				

Table A-15. Table of calculated hydrogen atom positions and isotropic temperature factors for $Mo_4(OEt)_{14}(HOEt)_2$

Atom	x	y	z	B(Å²)
H1	-0.0096	0.2704	-0.0939	4
H2	-0.0896	0.3184	-0.0368	4
H3	-0.1526	0.3525	-0.1537	4
H4	-0.1398	0.1969	-0.1705	4
H5	-0.2197	0.2449	-0.1135	4
H6	0.0919	0.3882	0.0007	3
H7	0.1939	0.3477	-0.0363	3
H8	0.2274	0.4735	0.0685	5
H9	0.1683	0.3662	0.1149	5
H10	0.2704	0.3256	0.0778	5
H11	0.0356	0.1742	0.2255	5
H12	0.1506	0.2088	0.2165	5
H13	0.1262	0.0972	0.3283	5
H14	0.0792	-0.0279	0.2873	5
H15	0.1942	0.0067	0.2783	5
H16	-0.1297	0.2568	0.1675	5
H17	-0.1613	0.3488	0.1015	5
H18	-0.1288	0.4830	0.2021	6